EJP SOIL

European Joint Programme

Towards climate-smart sustainable management of agricultural soils

Indicators for successful carbon sequestration and greenhouse gas mitigation by rewetting cultivated peat soils (INSURE)

Deliverable 6

Modelling CO2 emissions of cultivated and

rewetted peat soils with SWAP-ANIMO

Due date of deliverable: July 2024
Actual submission date: 20.08.2024

GENERAL DATA

Grant Agreement: 862695
Project acronym: EJP SOIL
Programme title: Towards climate-smart sustainable management of agricultural soils
Project website: www.ejpsoil.eu
Project title: Indicators for successful carbon sequestration and greenhouse gas mitigation by rewetting cultivated peat soils (INSURE)
Project website:

Start date of the project: February 1st, 2020
Project duration: 60 months
Name of lead contractor: INRAE

Funding source: H2020-SFS-2018-2020 / H2020-SFS-2019-1
Type of action: European Joint Project COFUND

DELIVERABLE NUMBER:	6D-WP4.1
DELIVERABLE TITLE:	Modelling CO2 emissions of cultivated and rewetted peat soils with SWAP-ANIMO
DELIVERABLE TYPE:	Report
WORK PACKAGE N:	WP4
WORK PACKAGE TITLE:	Improving biogeochemical and hydrological modelling for rewetted peat soils
DELIVERABLE LEADER:	Rudi Hessel
AUTHOR:	Daniël van de Craats, Pim Dik, Rudi Hessel, Sonja Paul, Jens Leifeld, Poul Erik Lærke, Rasmus Jes Petersen, Johannes Wilhelmus Maria Pullens
DOI:	10.5281/zenodo.14041243
LICENCE	CC BY 4.0

This project has received funding from the European Union's Horizon 2020 research and innovation programme under grant agreement N° 862695

DISSEMINATION LEVEL: PU

This project has received funding from the European Union's Horizon 2020 research and innovation programme under grant agreement N° 862695

ABSTRACT

Three locations in Europe (wet river valley (Denmark), coastal peatland (The Netherlands) and broad river floodplain (Switzerland)) were selected for which two to three years of measurements of hydrological variables and CO_2 exchange fluxes were available for some period between 2015 and 2023. The hydrology, grass growth and CO_2 fluxes of these sites were modelled with the SWAP-ANIMO model using the available measurement period for model input and calibration. Model simulations were used to improve the understanding of the hydrological drivers of each site and to obtain estimates of the different pools contributing to the measured CO_2 fluxes using a period of 10 years (2014-2023). Rewetting was considered either by calibration on direct measurements of an actual rewetting measure (Denmark, The Netherlands) or extrapolation of the reference simulation (Switzerland). Also, the potential impact of climate change on the rate of peat oxidation was modelled for these sites for both the reference and rewetting measure.

The relation between the yearly averaged groundwater level and the CO_2 emission related to peat oxidation was remarkably similar for the three sites. In all cases, deeper yearly-averaged groundwater levels resulted in higher peat oxidation and CO_2 emissions. The relation was, however, affected by the type of rewetting measure, which was partly related to the existence of a correlation between yearly averaged soil temperatures and yearly averaged groundwater levels (i.e. a higher soil temperature tends to coincide with deeper groundwater levels) and partly related to the nature of the rewetting measure (limiting only drainage, or also promoting infiltration). Also, the steepness of the relation between groundwater levels and peat oxidation was found to increase with increasing temperatures for each of the sites due to the relation between temperature and peat oxidation rates.

This project has received funding from the European Union's Horizon 2020 research and innovation programme under grant agreement N° 862695

Table of Contents

This project has received funding from the European Union's Horizon 2020 research and innovation programme under grant agreement N° 862695

This project has received funding from the European Union's Horizon 2020 research and innovation programme under grant agreement N° 862695

List of acronyms and abbreviations

AC	Automated chambers
C	Carbon
CO_2	Carbon dioxide
CH_4	Methane
EC	Eddy covariance
GHG	Greenhouse gas
GPP	Gross primary production (photosynthesis)
NECB	Net ecosystem carbon balance
NEE	Net ecosystem exchange
N_2O	Nitrous oxide
Reco	Respiration from the ecosystem (plants and soil)
SL	Surface level

This project has received funding from the European Union's Horizon 2020 research and innovation programme under grant agreement N° 862695

1. Introduction

Peatlands can be found in many places and in a broad range of climates across the globe. Peatlands consist to a large degree of organic materials and are formed under wet conditions when the soil is completely saturated or flooded, such that decay of organic material is hampered due to a lack of oxygen. Plant residues accumulate and gradually form a layer of peat that increases in thickness over the course of thousands of years. Peatlands represent a major carbon (C) stock, and therefore potentially also form a significant source of greenhouse gasses (GHG) (Leifeld and Menichetti, 2018). When the soil is drained to allow for e.g. agricultural land use, buildup of organic material halts and peat is exposed to oxygen, leading to decomposition of peat. During decomposition the stored C is released to the atmosphere as carbon dioxide (CO_2). Thus, upon drainage of peatlands, these lands are transformed from a sink to a source of C.

Approximately 10% of the worlds peatlands is actively drained, leading to a significant return of the stored C to the atmosphere (Leifeld and Menichetti, 2018). As decay of organic material is dependent on temperature, rising temperatures due to climate change may speed up the release of C even further, providing a positive feedback loop between peat oxidation, GHG emission and global warming (Hopple et al. 2020).

An intuitive measure to mitigate GHG emission by peat oxidation is by rewetting drained peat soils to limit or even stop GHG emissions. Depending on the degree of rewetting, this allows for some extensive agriculture or paludiculture to continue (Leifeld and Menichetti, 2018). Rewetting is, however, not straightforward to do. Flooding the formerly drained lands may, in the short term, result in large emissions of methane (CH_4) or nitrous oxide (N_2O), depending on e.g. the land use history. Both CH_4 and N_2O are stronger GHGs than CO_2. To be able to evaluate the combined effect of all three gasses, emissions are often expressed as CO_2-equivalents. Research suggests that an optimum groundwater level, in terms of actual emissions of GHG in CO_2 equivalents, is around 20 cm-sl (surface level) (Evans et al. 2021). At shallower water table depths, an increasing release of CH_4 may exceed the decreasing emission of CO_2.

In this report, we examined the effects of both rewetting and climate change on groundwater levels and CO_2 emissions in three distinctly different locations in Europe, situated in Denmark, The Netherlands and Switzerland, by modelling these sites with SWAP-ANIMO (Kroes et al. 2017, Groenendijk et al. 2005). These sites represent a part of the range of peatlands which can be found in Europe, including a wet river valley (Denmark), coastal peatland (Netherlands) and broad river floodplain (Switzerland) with varying land-use and drainage histories. We used measurements of CO_2 emissions (by eddy covariance (EC) or automated chamber (AC) measurements), hydrology and various soil parameters to represent the current field situation as well as possible. In both Denmark and The Netherlands, the effect of rewetting was included in the measurements and therefore included in the calibration, whereas in Switzerland a hypothetical rewetting case was considered. Based on the calibration, we extended the analyses to obtain estimates of the effects of both rewetting and climate change on CO_2 emissions.

In this report, we first briefly describe the models and methods used (chapter 3). Then, we present for each of the three sites (chapters 4, 5 and 6 for Switzerland, Denmark and The Netherlands, respectively) the characteristics and measurements of the site, the model setup, model outcomes for the calibration period and the results of the scenario analyses. Finally, we combine the results to draw conclusions on the potential of rewetting on GHG mitigation in the current and future climates (chapter 7).

This project has received funding from the European Union's Horizon 2020 research and innovation programme under grant agreement N° 862695

2. Executive summary

Three locations in Europe (wet river valley (Denmark), coastal peatland (The Netherlands) and broad river floodplain (Switzerland)) were selected in this study. For each site, two to three years of measurements of hydrological variables and CO_2 exchange fluxes were available, for some period between 2015 and 2023. The hydrology, grass growth and CO_2 fluxes of these sites were modelled with the SWAP-ANIMO model (Kroes et al. 2017, Groenendijk et al. 2005) using the available measurement period for model input and calibration. Model simulations were used to improve the understanding of the hydrological drivers of each site and to obtain estimates of the different pools contributing to the measured CO_2 fluxes using a period of 10 years (2014-2023). Rewetting was considered either by calibration on direct measurements of an actual rewetting measure (Denmark, The Netherlands) or extrapolation of the reference simulation (Switzerland).

The potential impact of climate change on the rate of peat oxidation was modelled for these sites for both the reference and rewetting measure. For each country, we selected a number of climate models for which simulated daily weather data was available for a reference period (i.e. 1980-2010 or 1990-2020) and two future periods (mid-century and end of century) in the SSP1-2.6 and SSP5-8.5 socioeconomic pathways or RCP2.6 and RCP8.5 emission scenarios. The climate models were chosen based on the data availability for each national meteorological institute to adhere to the national climate scenarios as much as possible. The impact of climate change on expected groundwater levels and peat oxidation was assessed for each of these periods.

Cressier, Switzerland
For the Swiss site (Paul, 2021) measurements were available for the years 2015 and 2016, of which 2015 was exceptionally warm and dry. The site included a reference field without rewetting measures in a broad river floodplain with a relatively thin layer (60 cm) of heavily degraded peat on top of mineral sediments. Grass was grown and mowed three times a year, without any application of fertilizer. The field was actively drained when groundwater levels were shallower than 60 (2015) or 50 (2016) cm below soil surface, such that groundwater levels were relatively deep and occasionally fell to 1 m below soil surface. The local hydrology was influenced by the presence of a canal, yet the most relevant feature was the artificial drainage of water at shallow groundwater levels, which lead to a rather fast decrease in groundwater levels. Flooding of the site in spring of 2015 also had an impact on the hydrology, as well as on grass growth and carbon fluxes.

The measured and modelled net ecosystem carbon balances (NECBs) were 17.5 and 21.9 t CO_2 ha^{-1} for 2015, respectively, and 15.9 and 16.5 t CO_2 ha^{-1} for 2016, respectively. The overestimation in 2015 by the model could be attributed to an overestimation of grass yield following the period of flooding. For the years 2015 and 2016, the (modelled) contribution of peat oxidation was 20.0 and 16.7 t CO_2 ha^{-1} in the years 2015 and 2016, respectively. The average peat oxidation for the period 2014-2023 was 17.1 t CO_2 ha^{-1} yr^{-1}.

A hypothetical situation was considered where drainage of water would occur only if groundwater levels would be shallower than 25 cm below soil surface, rather than 50 cm below soil surface, which we consider to be the rewetted case in contrast to the reference case. For the reference climate period (1990-2020), rewetting resulted in a shallower yearly-averaged groundwater level (27 cm-sl as opposed to 45cm-sl for the reference) and reduced oxidation of peat (9.1 as opposed to 14.2 t CO_2 ha^{-1} yr^{-1}). Groundwater levels were only affected by climate change in the end-century period for high global GHG emissions, with 4 cm deeper yearly-averaged groundwater levels. Oxidation of peat was also most strongly affected in this scenario, resulting in an increase to 20.2 t CO_2 ha^{-1} yr^{-1} for the reference situation and 14.4 t CO_2 ha^{-1} yr^{-1} for the rewetted scenario. The low global GHG emission

This project has received funding from the European Union's Horizon 2020 research and innovation programme under grant agreement N° 862695

scenarios lead to a slight increase in modelled CO_2 emissions, with the most prominent increase already occurring mid-century.

Vejrumbro, Denmark
The Danish site (Nielsen et al. 2024) was monitored in 2021-2023 for a consecutive period of 2 years (June – June). The site was situated in a narrow river valley and consists of a relatively pristine peat layer of approximately 2 m in thickness. Grass was grown on the site, but harvest was limited to only one harvest event during the measurement period. The site was wet compared to the other sites in this report, with a maximum groundwater table depth of 40 cm below soil surface and flooded conditions during winter. The local hydrology was strongly influenced by local exchange at the soil surface through precipitation and evapotranspiration as well as surface runoff. Some drainage of water occurred by means of a ditch. In 2022, the ditch was blocked to limit drainage from the field. As such, the measurement period can be split in a reference period and a rewetted period.

The measured and modelled NECBs were 8.6 and 9.8 t CO_2 ha^{-1} for 2021-2022, respectively, and 4.8 and 5.5 t CO_2 ha^{-1} for 2022-2023, respectively. The modelled contribution of peat oxidation to the carbon fluxes was 4.0 and 5.1 t CO_2 ha^{-1} in the periods 2021-2022 and 2022-2023, respectively. The majority of the peat oxidation in the period 2022-2023 occurred during a dry period in 2022, with groundwater tables falling to 40 cm below soil surface. The average peat oxidation for the period 2014-2023 was 4.6 t CO_2 ha^{-1} yr^{-1} with modelled yearly averaged groundwater levels of approximately 15 cm below soil surface.

In the rewetting scenario we considered the situation in which the ditch was blocked, as opposed to a reference scenario resembling the period prior to 2022. For the reference climate period (1980-2010), rewetting resulted in an even shallower yearly-averaged groundwater level (7.9 as opposed to 16.0 cm below soil surface for the reference scenario) and reduced oxidation of peat (3.1 as opposed to 5.2 t CO_2 ha^{-1} yr^{-1}). Groundwater levels were hardly affected by climate change, with a very minor tendency to become shallower. Oxidation of peat was most strongly affected in the end-century period in the high global GHG emission scenario, resulting in a limited increase to 5.7 t CO_2 ha^{-1} yr^{-1} for the reference scenario and 3.2 t CO_2 ha^{-1} yr^{-1} for the rewetted scenario. As the increase in emission is higher for the reference scenario, the effect of rewetting becomes increasingly important as climate change progresses.

Zegveld, The Netherlands
The Dutch site (van den Akker et al. 2021; Aben et al. 2024) was monitored from 2016 onwards, while CO_2 flux measurements were conducted in the period 2021-2023. The site was situated in an extensive coastal peatland area and consisted of a degraded peat layer on top of pristine peat of 6 to 7 m thick. The peatland area is intersected by a dense network of ditches of which the water levels are managed. The site consists of intensively managed grasslands that are fertilized to maintain a high productivity. The site had three treatments, a reference (drained by the surrounding ditches) and two rewetted treatments in which target groundwater levels of 50 and 20 cm-sl were set. These were maintained by a system of subsurface drains which could both drain and infiltrate water. In this system, the drains were connected to a reservoir and the pressure in the drains could be controlled by varying the water level in the reservoir. As such, the local hydrology was strongly determined by the exchange with the drains and ditches. Groundwater levels dropped to 1 m below soil surface in the reference field, whereas groundwater levels in the rewetted plots did not fall below 60 and 35 cm-sl, respectively.

The average modelled and measured NECBs for the years 2022 and 2023 were 15.8 and 19.3 for the reference plot, 9.0 and 11.4 for the rewetted plot with a target level of 50 cm-sl and 6.5 and 6.5 t CO_2

This project has received funding from the European Union's Horizon 2020 research and innovation programme under grant agreement N° 862695

ha^{-1} yr^{-1} for the rewetted plot with a target level of 20 cm-sl, respectively. The modelled contribution of peat oxidation was 17.6, 10.3 and 5.5 t CO_2 ha^{-1} yr^{-1} for these fields over the two-year period.

For the reference climate period (1990-2020) the average modelled groundwater level in the three fields was 37, 30 and 15 cm-sl, respectively, with a modelled peat oxidation of 14.5, 8.4 and 5.6 t CO_2 ha^{-1} yr^{-1}. Groundwater levels were impacted by climate change, with decreases of up to 3 and 7 cm at the end of the century for the low and high global GHG emission scenarios in the reference field, respectively. The impact of climate change on groundwater levels was less pronounced in the other fields (maximum up to 3 cm), due to the possibility to infiltrate water during dry periods. As with the other sites, peat oxidation increased in all future scenarios, with the most prominent increase at the end of the century in the high GHG emission scenario. The emissions increased to 25.3, 13.8 and 10.3 t CO_2 ha^{-1} yr^{-1} for the reference and two rewetted fields, respectively.

General findings

The relation between the yearly averaged groundwater level and the CO_2 emission related to peat oxidation was remarkably similar for the three sites. In all cases, deeper yearly-averaged groundwater levels resulted in higher peat oxidation and CO_2 emissions. The relation was, however, affected by the rewetting measure, which was partly related to the correlation between yearly averaged soil temperatures and yearly averaged groundwater levels (i.e. a higher soil temperature tends to coincide with deeper groundwater levels) and partly related to the nature of the rewetting measure (limiting only drainage, or also promoting infiltration). Also, the steepness of the relation between groundwater levels and peat oxidation was found to increase with increasing temperatures for each of the sites due to the relation between temperature and peat oxidation rates.

This project has received funding from the European Union's Horizon 2020 research and innovation programme under grant agreement N° 862695

3. SWAP-ANIMO model

3.1. Overview

The SWAP-ANIMO model (Kroes et al. 2017, Groenendijk et al. 2005) is a 1D model combination which simulates hydrology and temperature (SWAP) and organic matter decay and nutrient transport (ANIMO) in the soil. Also crop growth is modelled, which in the context of this report is done using the grass growth module (WOFOST based; Boogaard et al., 2014, Kroes and Supit, 2011). The model combination considers a domain from the top of the canopy down to some depth below soil surface, where the soil surface is divided into an arbitrary number of compartments. Each compartment (e.g. a 1 cm thick layer at the top soil, or a 20 cm thick layer at a few meters below the soil surface) is part of a soil horizon, a layer with distinctly different properties compared to the layer above or below. In SWAP-ANIMO, many soil properties (e.g. soil hydraulic functions, bulk density) are defined on the scale of soil horizons.

The core of the SWAP model (Kroes et al. 2017) solves the Richards equation to model vertical water flow within the soil (Heinen et al. 2024). The model makes use of the Mualem-van Genuchten parameters (Mualem, 1976; van Genuchten, 1980) to describe the relation between water content, water pressure and hydraulic conductivity. To determine the inflow and outflow of water at the top, sides and bottom of the 1D column, the model includes processes as interception, evaporation, transpiration, ponding and surface runoff, driving the water exchange at the top of the soil, drainage and infiltration of water through drains or open water, driving water exchange at the sides, and exchange with the underlying aquifer through the bottom of the soil column considered (Figure 3.1).

To solve the set of model equations, hydrological boundary conditions are required, including meteorological data at the top of the soil, a (time dependent) water level in the surrounding surface water for any of the defined drainage or infiltration means, and a water level in the underlying aquifer. Both drainage and infiltration through the sides, and seepage through the bottom of the soil column are calculated from a head difference between the groundwater and e.g. surface water, divided over a resistance, of which the latter are calibrated based on groundwater level observations.

Transpiration in SWAP is determined by the meteorological parameters and the crop. Crop growth (in the context of this report: grass) is modelled with a WOFOST-based module in SWAP. This module uses solar radiation and air temperature to calculate the biomass development over time. Also the atmospheric CO_2 concentrations play a role. Crop development may be hampered by sub-optimal temperatures (i.e. low night-time temperatures or high maximum temperatures) or water availability (i.e. too dry (water stress) and too wet (oxygen stress) conditions). This results in a potential as well as actual crop development. In the case of grassland, grasses may be harvested several times during the growing season, which affects crop development and transpiration as well. The root zone thickness is kept constant, but root density may vary dynamically based on root water extraction.

Important output data of the SWAP model which are further used by ANIMO include the water content and temperature in each model compartment, the fluxes between model compartments and the exchange fluxes with the surrounding area. ANIMO (Groenendijk et al. 2005) uses this information to calculate the transport of dissolved organic matter (DOM), nitrogen (N; in a mineral form (ammonium; NH_4, nitrate; NO_3) and organic form (DON)), the diffusion of oxygen (O) into the soil and to calculate the breakdown of organic matter (OM) in the soil. Any OM in the soil may be broken down aerobically (by oxygen) or anaerobically (by nitrate). We do not consider anaerobic decomposition by other means (i.e. methanogenesis). Several adaptations to the ANIMO model were introduced for enhancing GHG simulations in peatland soils (Hendriks et al. 2024).

This project has received funding from the European Union's Horizon 2020 research and innovation programme under grant agreement N° 862695

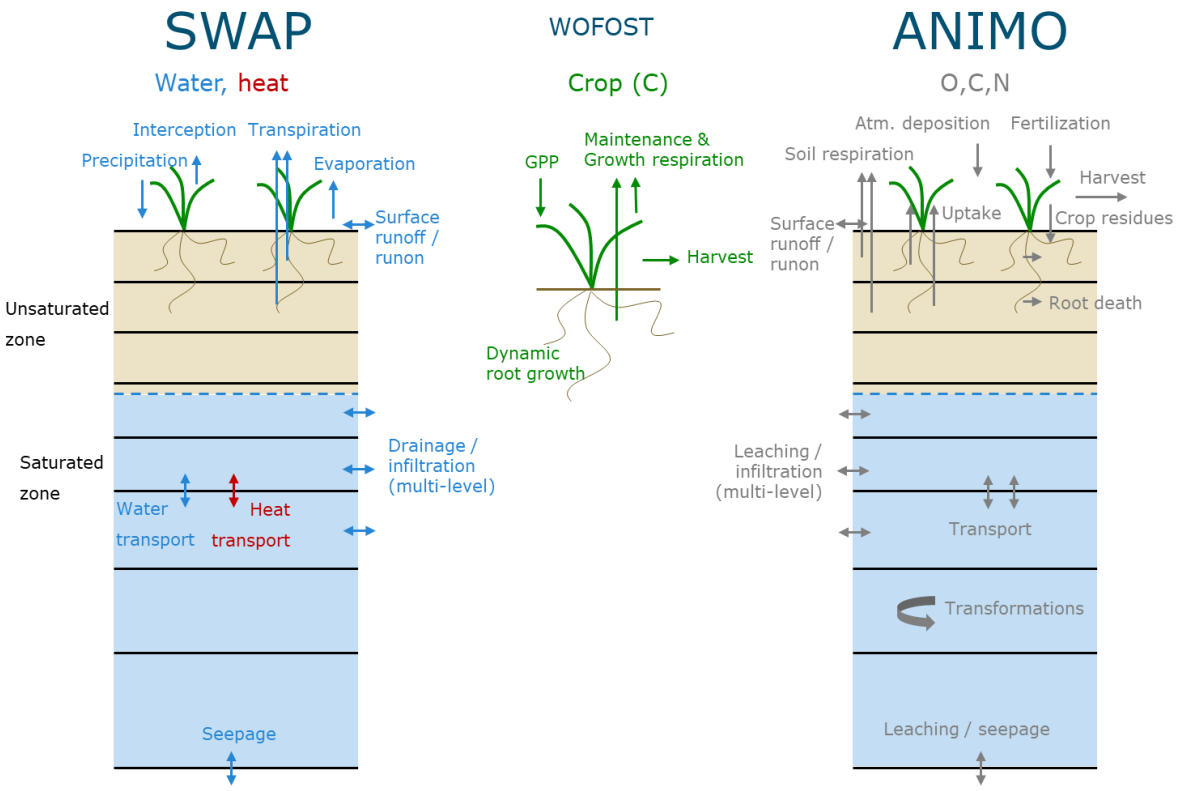

Figure 3.1 Overview of the coupled SWAP-ANIMO model, including the WOFOST-based crop growth model incorporated in SWAP. SWAP is used to simulated transport of water and heat, for which WOFOST supplies information regarding crop conditions which determine e.g. transpiration. WOFOST also supplies information regarding the CO_2 uptake and emission through photosynthesis (GPP) and respiration. ANIMO uses the conditions provided by SWAP to model soil respiration, based on oxygen (O), carbon (C) and nitrate (N) availability. Note that, for readability, transport arrows are only indicated between two of the compartments, even though these occur between each compartment.

3.2. Carbon modelling

The main aim of the modelling in this report is to quantify the net CO_2 flux from the soil to the atmosphere (or vice versa). To do so, we set up the net ecosystem carbon balance as

$$NECB = GPP + R_{eco} + Cout + Cin \quad (1)$$

where GPP is the gross primary production, Reco is the ecosystem respiration, Cout is the sum of the carbon which is removed from the plant-soil system via processes other than respiration (e.g. harvest, outflow of DOM), Cin is the sum of the carbon fluxes which is added to the soil via processes other than photosynthesis (e.g. inflow of DOM, manure application). All fluxes are defined in t CO_2 ha^{-1} yr^{-1} and are positive into the atmosphere. In contrast to the original definition of the NECB (Chapin et al. 2006), we ignore the contribution of methane and alternative forms of C in this balance. Each of the terms on the right hand side of (1) is further detailed in the following paragraphs.

This project has received funding from the European Union's Horizon 2020 research and innovation programme under grant agreement N° 862695

GPP

In the model, photosynthesis, assimilation or gross primary production (GPP) – which are all terms for the same process – is determined by the amount of radiation, the available leaf area, leaf characteristics and the atmospheric temperature and - CO_2 concentration. GPP is obtained as the potential GPP on a given day given the actual amount of biomass, without any reduction due to non-optimal soil water conditions. We provide a brief overview of the mechanisms involved in obtaining GPP; a detailed description of the equations used is provided in Kroes et al. (2017).

Of the daily global radiation, which is input to the model, it is assumed that half of it is photosynthetically active radiation (PAR), and thus can be used by the plant for photosynthesis. In addition, the available PAR depends on the solar elevation (Spitters 1986; Spitters et al. 1986). Part of the radiation is direct and part of it is diffuse, the partitioning between them depending on the time of year, the location on earth and the amount of measured radiation. Radiation reaching the top of the canopy is distributed through the leaf layers and is partly absorbed, partly scattered and partly reflected, depending on the leaf area index (LAI). Light extinction due to absorption of light and scattering differs between the direct and diffuse radiation and the parameters describing this are (standardized) input to the model.

The assimilation rate of a leaf in the canopy is determined by the light response curve (Peat, 1970), which describes the relation between PAR (which differs with position in the canopy) and CO_2 uptake. In the light response curve both the maximum CO_2 assimilation rate (A_{max}) and the light-use efficiency (ε_{PAR}) are prescribed parameters, where A_{max} varies throughout the year. For any day, A_{max} may be reduced by sub-optimal average – and minimum day temperatures. The relation between temperature and reduction is standardized model input as well.

The atmospheric CO_2 concentration influences the parameters A_{max} and ε_{PAR}, and also impacts the relation between assimilation and transpiration through an increased stomatal resistance. Parameterizations of these relations are obtained from Droppers et al. (2022).

Reco

Ecosystem respiration is determined by various processes, and can be separated into autotrophic and heterotrophic respiration. Direct plant respiration (autotrophic respiration) is modelled with SWAP, and involves, in order of calculation, respiration due to growth reduction, maintenance respiration and growth respiration. We do not account explicitly for any root exudates; they are part of the direct plant respiration due to their short residence times in the soil.

Respiration due to growth reduction involves the influence of soil moisture conditions on crop growth. A reduced growth due to non-optimal conditions is reflected in the factor Ta/Tp, where Ta is the actual transpiration, and Tp the potential transpiration. If this factor is below one, the potential GPP is reduced to the actual GPP following this factor. The difference between the two is respired as CO_2.

The remaining carbohydrates (i.e. the actual GPP) are used for maintenance respiration. It is dependent on the available biomass and temperature. We use a (fixed) Q_{10} factor for crop respiration of 2.0 (as commonly used; see e.g. Wythers et al. 2005 and references therein), meaning a doubling of the maintenance respiration rate for an increase in temperature of 10°C. Other factors are standardized in the input.

This project has received funding from the European Union's Horizon 2020 research and innovation programme under grant agreement N° 862695

Finally, if any carbohydrates remain, they are used for crop growth. During the formation of biomass, a fraction of the carbohydrates is transformed into CO_2 and lost to the atmosphere. We use standardized input for these fractions.

In addition to direct plant respiration, ecosystem respiration is determined by the breakdown of organic matter in the soil (heterotrophic respiration) as calculated with ANIMO. This organic matter may stem from recently deceased plant material (dying roots or shoots), from organic manure, inflowing DOM or from the decomposition of peat (old plant material). Organic matter is broken down into humus or DOM, and part of the organic matter is lost to the atmosphere as CO_2. Also humus and DOM can be broken down into CO_2. Each form of organic material has its own decomposition rate and the carbon – and nitrogen content of each material may vary as well. Furthermore, the assimilation efficiency and partitioning of the remaining organic material between humus and dissolved organic matter may vary between the materials. Parameterization of these factors is either standardized input, or based on lab measurements, calibration and additional information such as C/N ratios.

Apart from the availability and characteristics of organic matter at a certain depth in the soil, breakdown of organic matter in the soil is further determined by the oxygen and nitrate availability, soil water content, pH and soil temperature. Oxygen availability is modelled explicitly, by considering a balance between the supply of oxygen, through diffusion, and the consumption of oxygen for breakdown of organic matter. In case no oxygen is available, nitrate may be used as alternative electron acceptor for the decomposition of organic matter. No other anaerobic processes are considered. At low soil water contents, decomposition may be limited due to drought stress for the microbial community. At pH values below 4, decomposition is severely hampered, whereas at pH values exceeding 6, decomposition is hardly impacted by the pH. Finally, at increasing soil temperatures also the breakdown of organic material accelerates. The factor driving this increase may be differentiated per soil horizon.

Cin
Input of organic material into the system other than GPP may stem from inflow of DOM through infiltrating water or from the application of manure. The inflow of DOM is given by the DOM concentration in the source of water, which in the model is constant over time, multiplied by the volume. Manure application is given as input to the model.

Cout
Organic material moving out of the system other than Reco may occur due to harvest of plant material and the outflow of DOM through draining water. Harvest of plant material which is not left on the field is counted as an immediate source of CO_2, as it is assumed to – eventually – be respired back into the atmosphere. The outflow of DOM is dependent on the DOM concentration and the drainage of water from different soil layers.

3.3. Model implementation

For each site, a SWAP model was set up using the available measurements at the site, such as soil properties and measured or estimated surface water levels. In case information was lacking, estimates of certain properties were made based on alternative descriptions or expert judgement. The SWAP model was calibrated mostly based on groundwater level measurements. Wherever available, we also used soil moisture measurements. The calibrated parameters are related to the drainage – and infiltration resistance of the drainage measures in the fields. Measurements of

This project has received funding from the European Union's Horizon 2020 research and innovation programme under grant agreement N° 862695

harvest and GPP were used to calibrate a limited set of crop growth parameters. A detailed description is given for each site individually.

Similarly, the ANIMO model was set up using available measurements wherever possible. This was based on e.g. measurements of the current carbon and organic matter availability and quality and, whenever available, measurements of the decomposition rate with depth. The ANIMO model was calibrated based on measured Reco and NEE. Furthermore, calibration was based on pore water concentrations or concentrations in groundwater wells of e.g. nitrate and organic carbon, whenever available. Calibrated parameters include the oxygen diffusion parameters in each soil layer as well as some properties of the organic material in case no relevant measurements were available.

In contrast to the SWAP model, initialization in ANIMO is important to obtain a correct estimate of the different organic matter pools in the model. Therefore, we modelled a 50 year period prior to the start date of the period considered. Input for this period was either a repetition of the input for the period considered, or actual (weather) measurements obtained close to the field site. The 50 year period was cut into individual 10 year periods. As during the 10 year period organic matter may disappear due to oxidation, after each 10 year period, the organic matter content of each layer was reset to its initial value (as based on the current measurements) by moving a fraction of the peat from the layer below to the given layer. By doing so, we mimic the process of soil subsidence over this period. In case a mineral layer below the peat layer was modelled as well, any oxidized peat was added to the lowest compartment which contained peat, as the goal is to mimic the current status of the peat as measured in the soil. Initialization results in a relatively degraded top soil, while maintaining a pristine subsoil, as generally found in peat soils.

Despite the fact that SWAP and ANIMO are coupled, they do have a different crop growth model which must be run for both models; it is currently not possible to include modelled crop growth by the SWAP model directly into ANIMO, as both crop growth models have different processes involved. In SWAP, we make use of the WOFOST based grass module in which we explicitly model the uptake and distribution of CO_2 and limit this based on water availability, ANIMO has its own grass growth module where uptake of nitrogen is modelled explicitly. With this information, also a reduction in grass growth due to nitrogen deficits can be modelled, a process which is not present in SWAP. The reduction in growth due to water or oxygen stress is accounted for in the ANIMO growth model by using SWAP output on the difference in modelled potential and actual transpiration, but detailed information on CO_2 fluxes is not given and the measured solar radiation is not used in ANIMO. ANIMO therefore models an ‘average grassland’ rather than the year to year variation. In SWAP, the ‘management factor’ can account for an average nitrogen limitation (and other average growth reduction mechanisms). In this study, we use the management factor to match observed and modelled yields as well as observed and modelled GPP. We adjust the ANIMO model input to match the average crop growth as modelled in SWAP as closely as possible. This does, however, lead to minor year-to-year imbalances between the two models.

3.4.Scenario analysis

In addition to modelling the current situation, we extent the analysis to future conditions. Rising temperatures and changes in precipitation and evapotranspiration may lead to changes in the carbon cycle. On the one hand, increased temperatures and atmospheric CO_2 concentrations may result in increased crop productivity, while on the other hand the increased soil temperature may result in more breakdown of organic matter. Also changes in the hydrological cycle may result in increasing or decreasing groundwater tables and soil moisture content during summer times, which may affect the exposure of peat to intruding oxygen. To this end, we obtained climate scenarios from the respective

This project has received funding from the European Union’s Horizon 2020 research and innovation programme under grant agreement N° 862695

national weather institutes, and, depending on the availability of ready-to-use data, ran a selection of climate scenarios for each study site. The details of the scenario analyses differs per country, depending on the availability of data. Generally, we compared three 30-year periods (around the years 2000, 2050 and 2100) and two global greenhouse gas emission scenarios (RCP2.6 and RCP8.5) for a selection of climate models. In all cases, we used the same initial conditions as used for modelling the current situation, meaning that we did not consider the effects of time on e.g. the availability of peat. In addition, no changes in boundary conditions other than weather and atmospheric CO_2 concentrations were considered, i.e. changes in long-term recharge, sea level rise or meltwater supply on the aquifer heads or stream discharges are not taken into account.

This project has received funding from the European Union's Horizon 2020 research and innovation programme under grant agreement N° 862695

4. Cressier, Switzerland

4.1. Site overview

The Swiss field site (47.04N; 7.05 E) is located close to the town Cressier in the province Seeland. It is situated in a north-east, south-west oriented valley which was formed by the Rhône glacier. The valley has a characteristic u-shape, with a rather flat bottom of several kilometers in width. After the retreat of the glacier, fens developed on alluvial or lake sediments in the early post-glacial period. The study site is situated between two lakes, the Bielersee to the east, and Lac de Neuchatel to the west. These two lakes are interconnected by a canal, of which the flow may reverse depending on the water levels in the two lakes and wind direction.

The area was first drained in 1864 and agricultural use started in 1920 (Paul et al. 2021) with the installation of a drainage system. This system was renewed in 1970. It is quite deeply drained, with groundwater levels extending into the mineral soil which starts at a depth of approximately 60 to 70 cm below soil surface. The field itself was under crop rotation until 2008, after which it was converted into an extensively used meadow, which was maintained by two farmers (dividing the field in a southwestern and northeastern part). The field has an elevation of 429.6 m above sea level (with a gentle slope from east to west, the western part being +- 20 cm higher than the eastern part), which is only slightly above the yearly average level in the two lakes. Occasional flooding may therefore occur. Measurements were conducted in the years 2015 and 2016, which therefore form the major focus period for this site.

Figure 4.1 The Swiss field site close to the town Cressier (47.04N, 7.05E). The field site is indicated by the dotted square. The canal (Canal de la Thielle) is situated towards the south-east of the field. The approximate location of the EC tower is indicated by the orange dot, approximate locations of additional measurements are indicated by the white dots.

This project has received funding from the European Union's Horizon 2020 research and innovation programme under grant agreement N° 862695

4.2. Measurements

Soil description

Soil cores (n=25; Paul et al. 2021) were obtained in a south-west-north-east transect in proximity of the EC tower (Figure 4.1). The general soil buildup is 30 to 40 cm of highly degraded peat, followed by a 20-30 cm thick layer of less degraded peat, underlain by mineral sediments of which no further information is available. The thickness of the peat layer varies between 60 and 70 cm. Measurements of soil bulk density and carbon – and nitrogen content were available, of which the mean values are shown in Table 4.1. Highest bulk densities (excluding the mineral layer) were found for the top soil, with values of 0.6 g cm^{-3}. Bulk density was lower in the less-degraded peat layer, with densities of around 0.4 g cm^{-3}, which is still rather high compared to the other sites in this report. There is no information available on the layer below the peat, other than that it is of mineral origin and consists of lake bed sediments or alluvial material.

Table 4.1 Overview of measured soil properties in Cressier, as averages over 25 measurements along a transect (Paul et al. 2021). Von Post gives an estimate of the degradation state of the peat on a scale from 1 to 10 (10 being highly degraded).

Depth cm-sl	BD g cm^{-3}	TOC %	N %	C/N	pH	Composition	Soil horizon	von Post (estimated)
0.0-12.5	0.57	22.33	1.59	14.1	7.91	peat	highly earthified	10
12.5-25.0	0.65	22.19	1.57	14.12	7.67	peat	highly earthified	10
25.0-37.5	0.47	26.32	1.74	15.16	7.69	peat	highly earthified	9
37.5-50.0	0.40	30.52	1.85	16.23	7.38	peat	sapric peat	8
50.0-62.5	0.38	21.00	1.31	15.00	6.88	peat or mineral		8
62.5-75.0	0.76	7.86	0.60	12.61	NA	mineral		

In addition to the values given by Paul et al. (2021), Bader et al. (2017) and Bader et al. (2018) provide soil information on the same field (their grassland site in Cressier), although the sampling points do not exactly match the sampling points in Paul et al. (2021). They do, however, present information on the soil respiration, and, in particular, on the effect of increasing temperatures on the soil respiration rate (Q_{10} values). As such, we used data of both sampling campaigns to initialize the SWAP-ANIMO model. No measurements of LOI, porosity, saturated hydraulic conductivity and soil hydraulic functions were available. We used a C-fraction of the organic matter of 50%, which is close to the average of 49.3% reported for this site based on 28 measurements at different depths (Leifield et al. 2020; site CGL). An overview of the available measurements is given in Figure 4.3, including the SWAP-ANIMO model initialization.

Hydrology

The field was drained using a system of drains (with a spacing of 18 m) from which water was actively pumped if the groundwater levels were shallower than 60 cm (prior to 24th of March, 2016) or 50 cm (March 2016 onwards). No inlet of water (subirrigation) was considered.

South of the field, a canal was present connecting the two major lakes in the valley. The level of Lac du Neuchatel was monitored continuously. The average water levels of these lakes are 429.15 m above sea level in winter, and 429.43 m above sea level in summer (FOEN, 2024) (which corresponds to 45 cm below field surface in winter, and 17 cm below field surface in summer). An overview of the water levels throughout the years is given in Figure 4.2. In May 2015, flooding of the eastern part of the field occurred (Paul et al. 2021), following some major precipitation events in that month. This is also clearly reflected in the water levels of the lake for that year (Figure 4.2).

This project has received funding from the European Union's Horizon 2020 research and innovation programme under grant agreement N° 862695

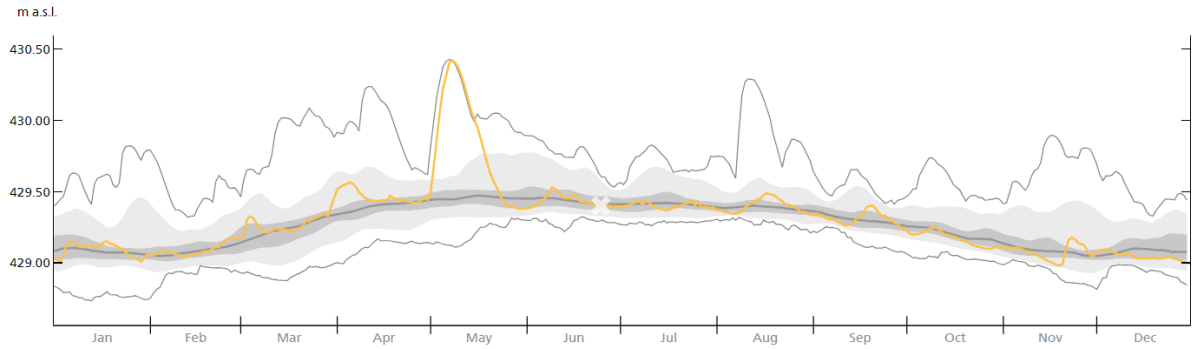

Figure 4.2 Water level in the Lac de Neuchatel. The grey line bounded by the grey dashed area gives the average and 25-75 percentile, respectively. The yellow line denotes the year 2015, with a peak and flooding in that year. Graph obtained from FOEN (2024).

Phreatic groundwater levels in the field were monitored continuously between August 2015 and November 2016 in two locations west and east of the EC tower (Figure 4.1). There was a rather constant difference between the two of approximately 20 cm, corresponding to slightly higher surface levels in the western part compared to the eastern part. We used the average of the two measuring wells to calibrate the model. During the measurement period, an average groundwater level of 40-60 cm was seen, with the winter groundwater levels close to soil surface, and summer groundwater levels falling to 1 m below soil surface. No measurements of any deeper soil layers were available.

Continuous soil moisture measurements were available from March 2015 to December 2016 in proximity of the EC tower as well as in the western – and eastern parts in proximity of the groundwater wells, measured at depths of 5, 10, 20 and 40 cm below soil surface. Measurements were performed using uncalibrated GS3 sensors (Decagon). The sensor uses an electromagnetic field to measure the dielectric permissiveness of the surrounding medium. In principle, the permissivity only provides insight into the relative moisture contents, i.e. wetter and drier. The measurement is then scaled based on soil type to a soil moisture content. As a result, the soil moisture content has a certain uncertainty. To perform a site-specific calibration, samples can be taken to determine the moisture content. This is quite laborious and has not been carried out in this study. Given these uncertainties in soil moisture contents, soil moisture levels can also be adjusted or rescaled at a later date for calibration purposes, which we did for analysis of the model results.

Several scaling formulas are available. The following scaling formula was used in this study:

$$\theta_{o,scaled} = \frac{perc90(\theta_m) - perc10(\theta_m)}{perc90(\theta_o) - perc10(\theta_o)} . \left(\theta_o - perc10(\theta_o)\right) + perc10(\theta_m)$$

with θ_m: moisture content of the simulation (model)
θ_o: moisture content of the measurement (observation)
perc90 and *perc10*: respectively the 90% and 10% percentile.

A method with scaling based on two percentile values has the advantage that 1) outliers (which occur less than 10%) are not included and 2) the scaling of higher and lower values is also well taken into account with skewed distributions (and for soil moisture, a skewed distribution is often a reality because the maximum value is often reached in winter).

This project has received funding from the European Union's Horizon 2020 research and innovation programme under grant agreement N° 862695

NEE and meteorology

NEE (net ecosystem exchange) was determined with an EC tower on the site (see Paul et al. (2021) for details on their methodology). Its position is shown in Figure 4.1. NEE was partitioned in GPP (gross primary production; photosynthesis) and Reco (ecosystem respiration) using ReddyProc (Wutzler et al. 2018) with the night-time partitioning approach as outlined in Paul et al. (2021). The accompanying meteorological variables were measured on-site as well. Data gaps in the meteorological values were filled with data from the nearby meteorological station Cressier (1 km distance, same altitude) of the Swiss national observation network (MeteoSwiss).

Field management

The Cressier site had been under crop rotation before it was converted into an extensively used meadow in 2009. The meadow received no fertilizer and was cut three times a year, with the first cut after June 15th due to nature conservation regulation.

Dominant grass species were Phleum pratensis, Festuca pratensis, Poa pratensis and Dactylus glomerata. The grassland was managed by two farmers (eastern and western part) with similar management strategies: in general, grass mowing events occurred on average within one week of each other, except for the last mowing event (Table 4.2). For model implementation, we used the average mow date for each cut.

Table 4.2 Overview of mowing dates in the eastern and western parts of the fields for the years 2015 and 2016.

Year	Cut	Mow date east	Mow date west	Mow date mean	Difference
2015	1	2015-06-19	2015-06-23	2015-06-21	4
	2	2015-08-12	2015-08-07	2015-08-09	-5
	3	2015-10-09	2015-10-22	2015-10-15	13
2016	1	2016-06-26	2016-07-01	2016-06-28	5
	2	2016-08-22	2016-08-24	2016-08-23	2
	3	2016-10-03	2016-10-29	2016-10-16	26

4.3. Simulation setup

SWAP model setup

A SWAP model simulation was set up based on the described data. Meteorological data on temperatures, rainfall, solar radiation, humidity and wind speed was obtained from the weather station at Cressier (1 km from the field site) for the period 1990-2023. For this report, we considered the ten-year period between 2014 and 2024. Calibration of the model was based on the measurements in the period February 2015 to December 2016, which forms the main focus of the analysis.

For the measurement period the meteorological data obtained at the site itself was used in the modelling, for the remaining period information from the weather station Cressier (1 km from the field site) was used. Any missing data was filled with data from the meteorological station at Neuchatel (a few km away, relatively close to the lake). These data were adapted to represent the data of the Cressier site using a simple linear model of the relation between variables of the two weather stations. Model initialization was done by repeating the time series of 1990 to 2020 for a period of 50 years.

This project has received funding from the European Union's Horizon 2020 research and innovation programme under grant agreement N° 862695

Grass growth, gross primary production (GPP) and plant respiration were modelled in SWAP using the WOFOST-based grass module. This module is specifically designed for intensively managed grasslands covered with ryegrass. As the grass species and mowing and fertilization regime are different in this site, we applied some parameter adjustments based on a calibration with the 'measured' GPP:

- The relative management factor, which lumps several effects of e.g. a shortage of fertilizer, and the presence of pests, diseases and sub-optimal growth conditions, was set at 0.72.
- The root zone thickness was estimated to be 40 cm.
- Partitioning of the carbohydrates was adjusted, such that 50% of the available carbohydrates were used below ground, rather than the standard percentage of 30%. This way, the observed yield could be approximated, while also approximating the observed GPP and adhering to the observations of Bader et al. (2017) that at least 20% of the carbon in the top soil originated from recent plant material.
- Transpiration was slightly increased by decreasing the minimum canopy resistance to 80 s m^{-1} (instead of 94 s m^{-1}).
- Based on a comparison between GPP for the hot summer of 2015, the maximum daily average temperature above which photosynthesis is reduced was set to 20°C instead of 25°C.
- The maximum relative death rates of leaves due to water stress was increased to 0.15, based on a comparison between measured and modelled yield reduction following the prolonged flooding period in 2015.

As no measurements of the soil water retention curve were available, we estimated the Mualem-Van Genuchten parameters from the Dutch Staring set (Heinen, 2020). This set is based on 999 soil samples taken across the Netherlands for which several parameters were determined in the lab. These samples were grouped into 36 classes based on characteristics as sand size, loam, clay and organic matter content, and position in the soil (topsoil (B) or subsoil (O)).

For the entire top soil (0-65 cm-sl) we chose the parameterization for B16 (sandy peat), followed by a mineral subsoil (65-600 cm-sl) given by O10 (sandy loam) as a combination of these best represented the soil profile found in the study site. An overview of the schematization and parameters used is given in Table 4.3. We did not differentiate any parameters for the top soil, as the degree of degradation within the entire peat layer was high.

Table 4.3 Soil profile description as used in the SWAP-ANIMO model for Cressier. Parameters listed include (in order of appearance) the residual water content ϑ_r, saturated water content ϑ_s, shape parameters (α, n, λ) and fitted saturated hydraulic conductivity based on the evaporation method, multiplied by 5 to include the effects of small macropores.

Depth	Staring nr.	Formal description	θ_r	θ_s	α	n	λ	Ksat
cm-sl	-	-	$cm^3\ cm^{-3}$	$cm^3\ cm^{-3}$	cm^{-1}	-	-	$cm\ d^{-1}$
0-65	B16	(Sandy) peat	0.01	0.786	0.021	1.28	-1.22	123.6
65-600	O10	Sandy loam	0.01	0.472	0.010	1.25	-0.79	11.5

Hydrological boundary conditions on the sides and bottom of the SWAP column were described by three drainage systems (sides) and an aquifer head (bottom). Several combinations of drainage system - and bottom flux parameters were explored, based on the available information. However, as this information is, in some aspects, rather limited, multiple options yielded comparable calibration results.

This project has received funding from the European Union's Horizon 2020 research and innovation programme under grant agreement N° 862695

No measurements of the hydraulic head of deeper layers was available. As any aquifer is likely heavily influenced by the presence of the two lakes, it is assumed that the aquifer follows a very similar pattern as the lakes in terms of head. Following Figure 4.2, we use a sine function to describe the aquifer head, with an average water level of 30 cm below soil surface and an amplitude of 20 cm, with its maximum occurring the first of July. Based on model calibration with observed groundwater levels and soil moisture conditions, a resistance of 1250 days was applied (excluding any flow resistance in the soil column itself).

The drainage systems were defined by three levels: the first level represents the canal, the second level represents the drains and the third level represents a shallow superficial drainage system (representing a depression or gentle slope), which accounts for some rapid shallow interflow processes. Surface runoff may occur as well. The characteristics as based on the calibration of the drainage systems are given in Table 4.4.

The water level in the canal was described by prescribing the multi-year monthly mean value (Figure 4.2) for each month at the 15th of the month, corrected for the average field surface level. Drains were allowed to drain water when the groundwater level exceeded 60 (prior to March 2016) or 50 (after March 2016) cm-sl, but infiltration of water was not considered. The superficial drainage system was also only able to drain water.

During the first three weeks of May, 2015, a flooding event occurred which was included explicitly in the model. For this, we prescribed a runon amount of 3 mm d^{-1} for 20 subsequent days, we assumed the drains were unable to drain water and the river water level was set to 5 cm+sl.

Table 4.4 Drainage system characteristics used in modelling of the Cressier site.

	Drainage resistance (d)	Infiltration resistance (d)	Depth (cm-sl)	Spacing (m)
Canal	1500	1500	-150	50
Drains	90	-	-70	18
Superficial	80	-	-5	4

This project has received funding from the European Union's Horizon 2020 research and innovation programme under grant agreement N° 862695

ANIMO model setup

An overview of the soil composition as measured and as used for model input is given in Figure 4.3. There are some clear differences between the reported values by Paul et al. (2021) and Bader et al. (2017), which can likely be attributed to the fact that samples were not taken at the exact same position in the field. Note that the values by Paul et al. (2021) are the averages of 25 samples per depth. Based on a model calibration, we initialized the model using a sort of average of the two measurements, while using the properties related to decomposition as given in Bader et al. (2018) (see also Figure 4.4).

An overview of the partitioning of the sources of organic matter at the start of the simulation period following the initialization runs is shown in Figure 4.4. Fresh organic material is present in the root zone, which is the resultant of added shoot and root material. Despite the increased partitioning of fresh material to roots, its nearly constant exposure to oxygen due to low groundwater tables results in only a limited buildup of fresh material to the soil after model initialization. It is lower than the reported fraction of 20% of the soil organic carbon, as stated in Bader et al. 2018. Also the humus pool remains rather small after initialization.

The measured average dissimilation rate per layer (excluding DOM) under optimal conditions at a soil temperature of 10 °C (Figure 4.4 B) shows no trend from the upper soil layer downward within the root zone. As one would assume that roots have a larger effect on the dissimilation rate in the upper layers of the soil due to a larger root density, this is rather surprising. However, the measurements were performed over a long period of time, and may therefore reflect the dissimilation of peat, rather than recent root tissue which may have been dissimilated already. The peat decomposition rate in ANIMO was therefore calibrated based on the measurements, for the decomposition of recent materials we used standard decomposition rates (which were also used for the other sites in this report). Q_{10} values showed a slightly decreasing trend with depth. We used the measured Q_{10} values in the model input, as indicated in Figure 4.4 C.

This project has received funding from the European Union's Horizon 2020 research and innovation programme under grant agreement N° 862695

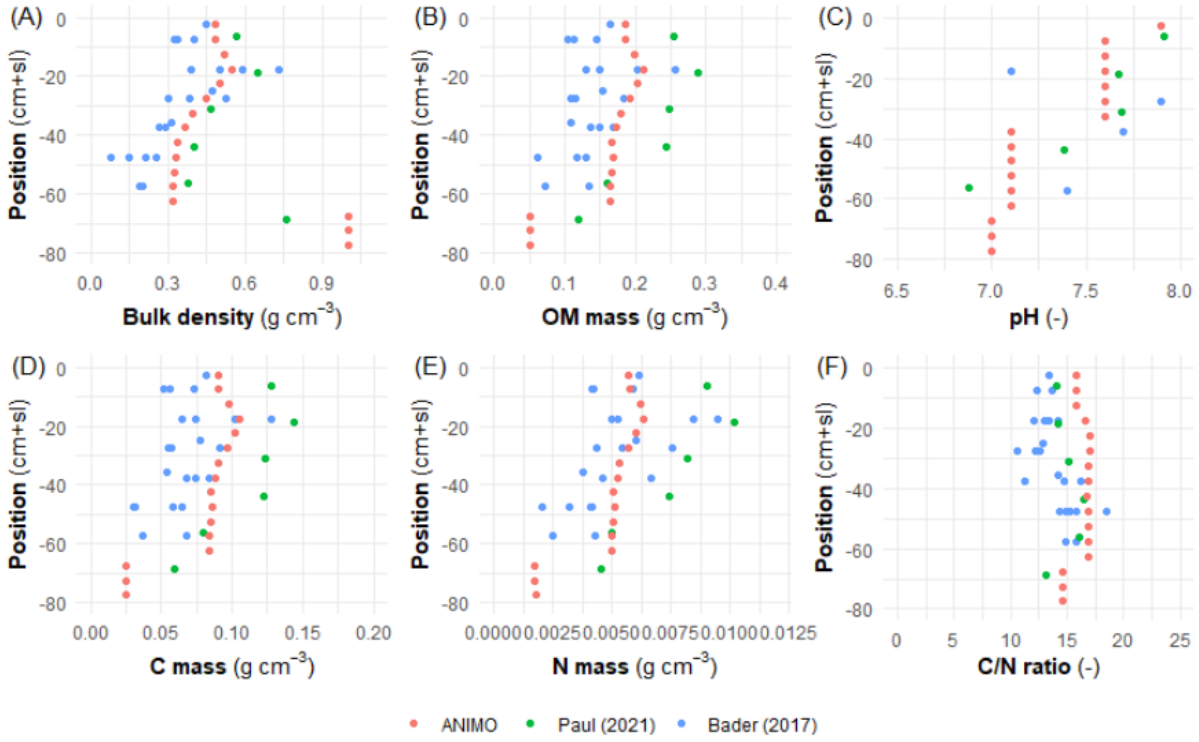

Figure 4.3 Measurements (blue: Bader et al. (2017) and Bader et al. (2018), green: Paul et al. (2021)) and model input after initialization runs (red) for the site Cressier. Shown are dry bulk density (A), OM mass (assuming a carbon fraction of 50% (B), pH (C), carbon mass (D), nitrogen mass (based on reported C/N ratios) (E) and C/N ratio (F), as function of depth.

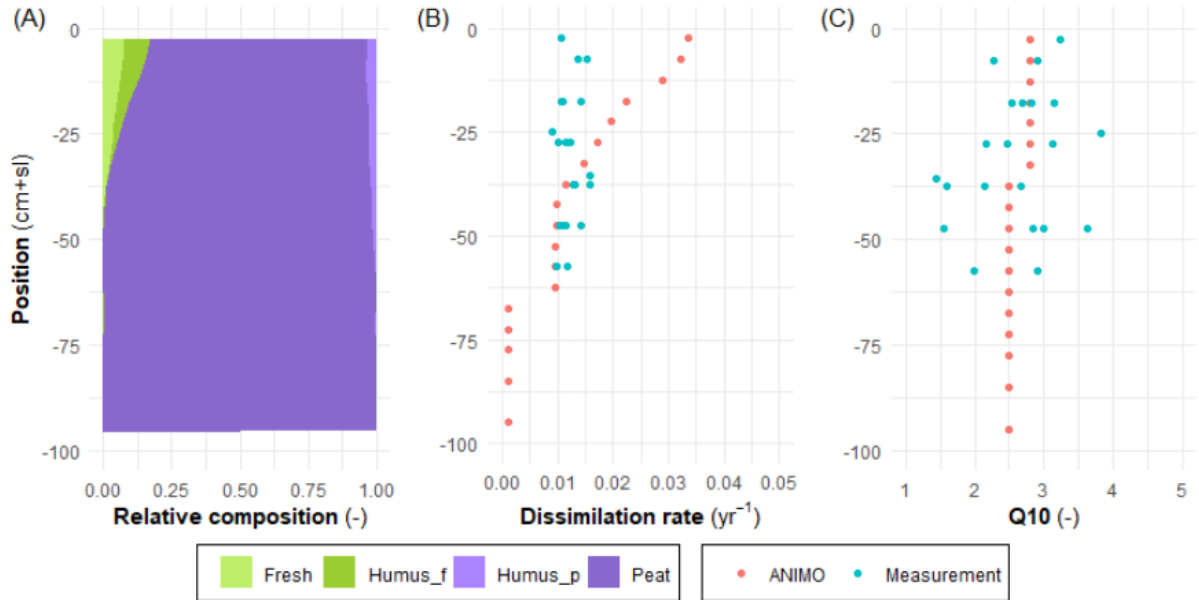

Figure 4.4 (A) Partitioning between fresh and peat (derived) materials at the start of the actual simulation in Cressier, resulting from the initialization runs, (B) corresponding dissimilation rate (excluding DOM) at optimal conditions and 10 °C as function of depth in the soil and (C) Q_{10} values. Measurements are obtained from Bader et al. 2018. The measured dissimilation rate is corrected based on an assumed assimilation factor of 0.15 (i.e. 15% of the peat is transferred to humus, rather than CO_2).

This project has received funding from the European Union's Horizon 2020 research and innovation programme under grant agreement N° 862695

4.4. Scenario definitions

For this site we consider a combination of scenarios based on water level management and climate projections. For the water level management, we consider the reference case, which is the current situation assuming that the threshold groundwater level above which pumps start to drain is at 50 cm-sl, and a hypothetical rewetting scenario in which pumps start to drain only when groundwater levels are shallower than 25 cm-sl. We refer to these water management scenarios for Cressier as reference and rewetted.

We also explored the effects of climate change by considering the CH2018 climate scenarios of the Swiss National Centre for Climate Services (CH2018 Project Team (2018); CH2018 (2018)). Based on the availability of the parameters (radiation, temperature, humidity, rainfall, wind) on a daily basis for both a historical period and two future periods in both the RCP2.6 and RCP8.5 global GHG emission scenarios, we selected 8 climate models (Appendix I) for which we obtained daily weather data for the city Neuchatel, in proximity of Cressier. No further adjustments to these data were required, as the dataset was already downscaled and bias-corrected.

We split each model realization for a given period into three 10-year periods for which we ran the SWAP-ANIMO model for both the reference and rewetted scenario, each time using the same initial conditions as defined by the prerun of the base simulation. We do, therefore, not account for any changes in e.g. peat composition over the period considered.

4.5. Base simulation results

Hydrology

Groundwater levels simulated by the SWAP-ANIMO model were generally well comparable with the observed groundwater levels (Figure 4.5). The trends are well-reflected by the model, although some discrepancies can be seen. The root mean squared error (RMSE) and mean absolute error (MAE) are 11.9 and 9.0 cm, respectively, for the period between August 2015 and November 2016. Peaks in groundwater level and fast drainage of water following those peaks are modelled correctly. A decrease in water level in July 2016 is modelled to be slightly faster compared to the measurements, whereas an increase in groundwater level is modelled to be slightly faster than measured in the late summer of 2015. These differences may be attributed to the absence of measurements of e.g. the soil water retention characteristics. The flooding event in May 2015 is clearly visible in modelled groundwater levels, as the groundwater level reaches the soil surface during this period.

In general, the trends in soil moisture content (when scaled) are reflected quite well by the model, especially at a depth of 40 cm below soil surface. This position most resembles the groundwater level, and is therefore also an indicator of the correctness of the groundwater level for the period beyond which groundwater level measurements were available. Measurements at depths of 5 and 10 cm below soil surface show distinctly less fluctuations in the dry summer of 2015 compared to the model results, which may be related to the extremely dry conditions during this period. Dry conditions in a shrinking soil (which is commonly found to be the case in peat soils, especially close to the soil surface) may affect the water flow and measurements in several ways. The top soil may become water repellent and macropores may form due to soil shrinkage, such that water entering the soil at the top is redirected to the lower layers without wetting the top layers. Also, soil shrinkage may result in a loss of contact of the soil moisture sensor with the soil, resulting in sub-optimal measurements.

This project has received funding from the European Union's Horizon 2020 research and innovation programme under grant agreement N° 862695

The absence of measured soil water retention characteristics or calibrated soil water content measurements makes it impossible to determine the correctness of the modelled soil water content. The minimum modelled soil water content of about 50% at depths of 5 and 10 cm, even during the dry summer of 2015, seems to be too high. The effects on modelled peat oxidation may be two-fold. First, a reduction in oxidation at low water contents may be underestimated. Second, a reduction in oxidation at high water contents may be overestimated due to a reduced oxygen penetration. The latter does not seem to have a profound influence, as modelled oxygen penetration depths regularly exceed the bottom of the peat layer.

An overview of the monthly modelled water balance terms is given in Figure 4.7. For the net balance over the period shown (2015 – 2016), most of the inflowing water originates from precipitation (86%; 888 mm yr^{-1}). Inflow of water from the canal and via the bottom boundary (assumed to be related to the water level in the canal and lakes) accounts for 12% of the inflow (121 mm), especially during summer when the surface water levels are relatively high, and groundwater levels are relatively low. The remaining inflow stems from runon, which is the flooding event in May 2015. Outflow of water is modelled to be mostly due to evapotranspiration (59%; 619 mm yr^{-1}). Drainage through the subsurface drains also accounts for a substantial removal of 30% (322 mm yr^{-1}), especially during winter. Surface runoff and shallow drainage account for the remaining 10% (102 mm yr^{-1}), which is mostly limited to two periods: one period during the flooding event, and another period in January 2016. Both these periods correspond to high peak precipitation events combined with relatively shallow groundwater levels.

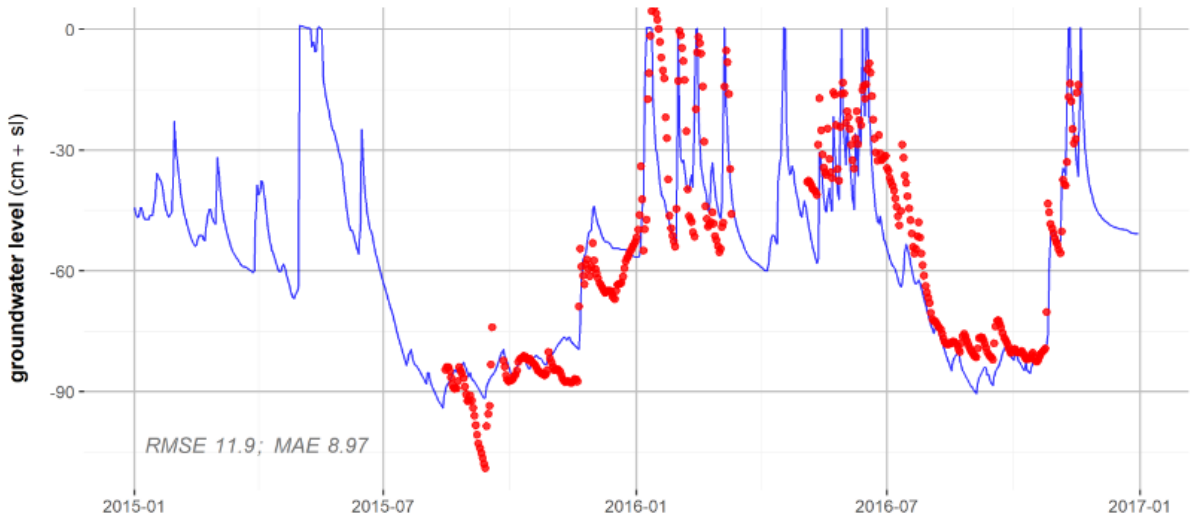

Figure 4.5 Measured (red dots) and modelled (blue line) phreatic groundwater levels in Cressier.

This project has received funding from the European Union's Horizon 2020 research and innovation programme under grant agreement N° 862695

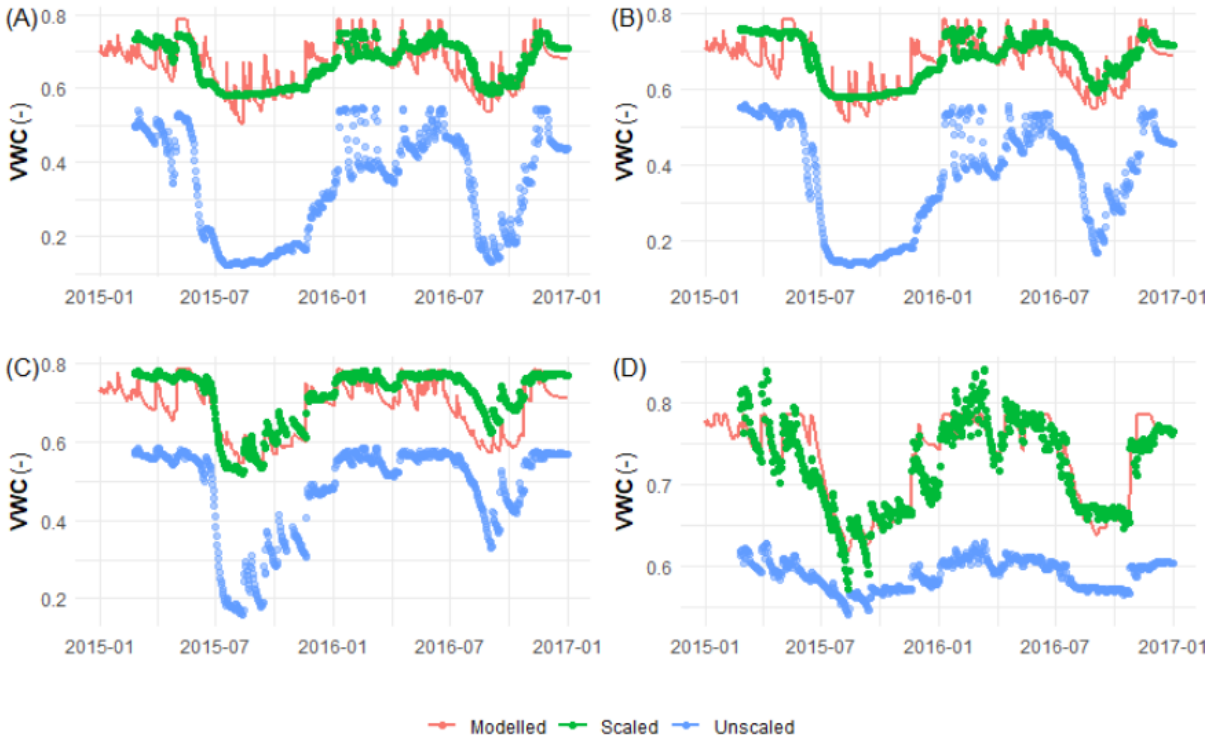

Figure 4.6 Overview of measured and modelled volumetric water contents (VWC) at four depths (5, 10, 20 and 40 cm-sl) in (A) to (D), respectively. The uncalibrated measurements were scaled to the modelled VWC to improve the comparison of measured and modelled trends.

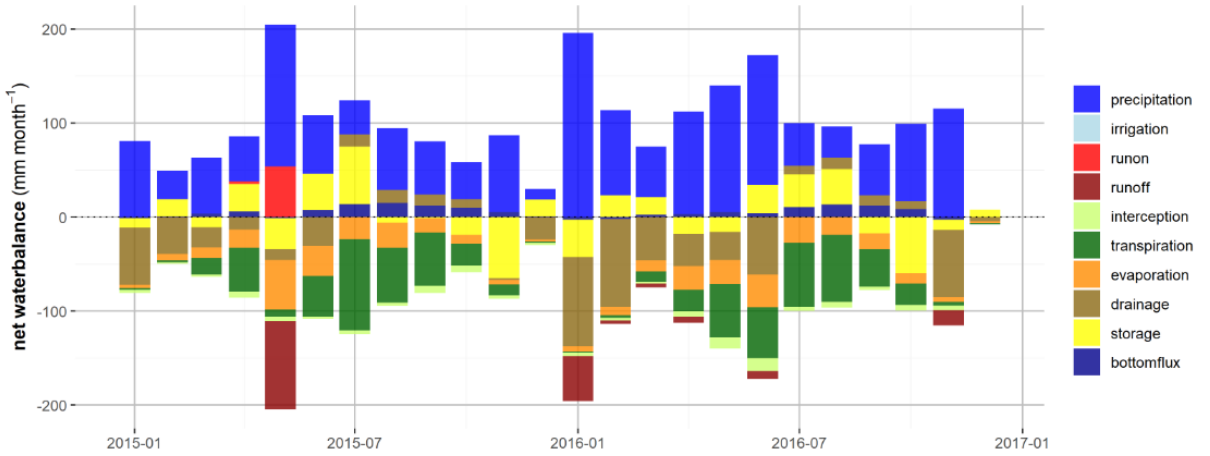

Figure 4.7 Modelled monthly water balance terms in 2015 and 2016 in Cressier. Positive terms describe water supply towards the soil and canopy, negative terms describe removal from the soil and canopy.

This project has received funding from the European Union's Horizon 2020 research and innovation programme under grant agreement N° 862695

CO_2 fluxes

An overview of the cumulative modelled net ecosystem exchange (NEE), gross primary production (GPP) and ecosystem respiration (Reco) is given in Figure 4.8 for the years 2015 and 2016 for which (partially gapfilled) EC measurements were available. The general pattern in NEE is very well captured by the model. In 2015, the modelled NEE is very well comparable to the measured NEE and has a very similar pattern. In contrast, modelled GPP and Reco exceed measured GPP and Reco significantly. This occurs especially during the period of flooding, as the modelled GPP depends on the biomass availability while the true GPP was affected by the standing water. Do note that the modelled GPP is respired immediately and is not allocated to crop growth (which is halted during flooding), and as such does not contribute to the net balance. In 2016, the net uptake during spring is higher in the measurements compared to the model due to an underestimation of GPP in the model. No clear reason for this discrepancy could be found.

Plotting the modelled against the measured daily GPP and Reco rates (Figure 4.9) shows, generally, a good fit for both GPP and Reco. The periods May and June 2015, however, clearly stands out as the model overestimates both GPP and Reco during this period during and just after which the field was flooded. We use Lin's Concordance Correlation Coefficient (CCC) as a measure to determine both the accuracy and precision of all the datapoints with respect to the 1:1 line. A perfect fit yields a value of 1, whereas no relation at all yields a value of 0, similar to Pearsons correlation coefficient. The obtained CCC for the modelled GPP and Reco are 0.783 and 0.725, respectively.

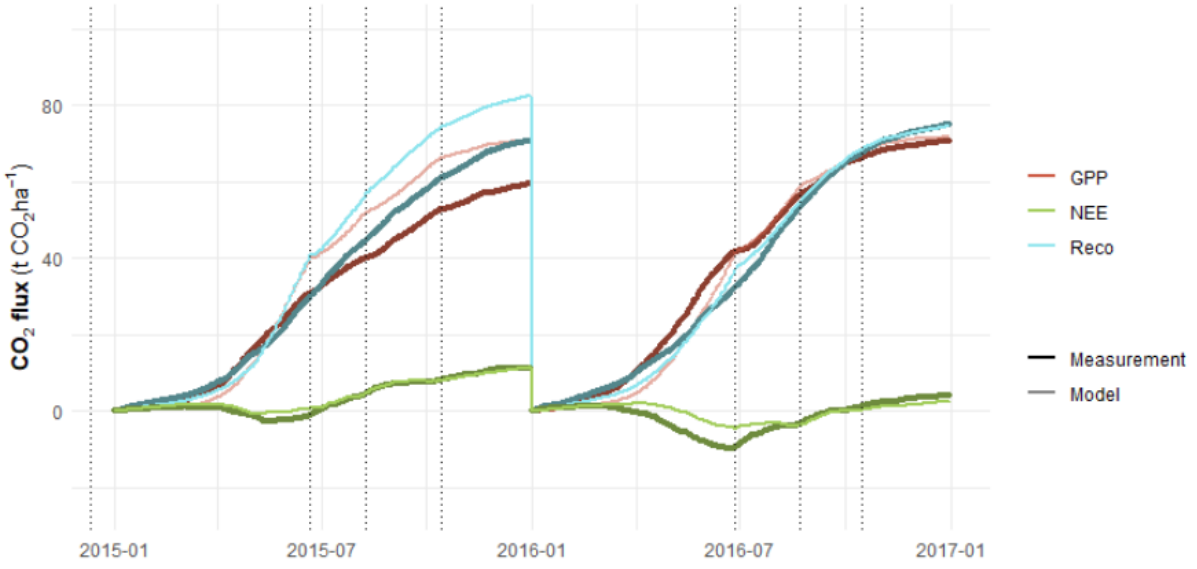

Figure 4.8 Cumulative measured and modelled NEE, GPP and Reco. NEE was measured by EC and gapfilled, GPP and Reco 'measurements' were obtained by partitioning half-hourly gap-filled EC fluxes. Modelled lines were obtained with SWAP-ANIMO. The dotted vertical line indicates a harvest event on September 8th, 2022. As measurements started only in June 2021, the starting point of the cumulative measurement line in 2021 was set at the cumulative amount of that date in 2022.

This project has received funding from the European Union's Horizon 2020 research and innovation programme under grant agreement N° 862695

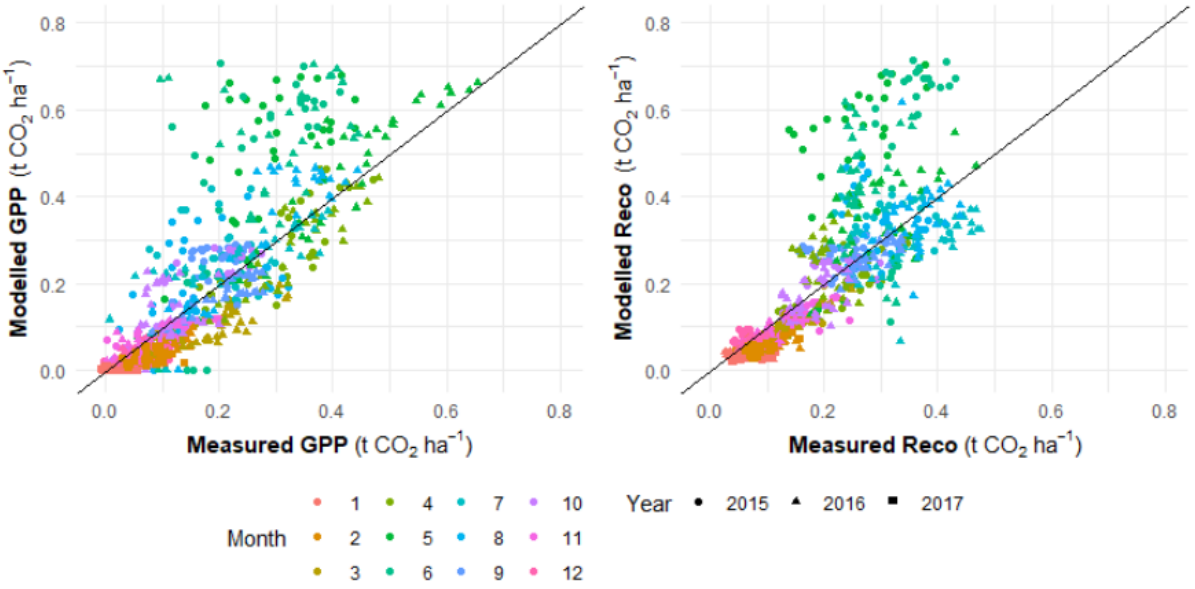

Figure 4.9 Relation between daily modelled and daily measured GPP (left side) and daily modelled and daily measured Reco (right side). Colors indicate the month of the year, symbol shapes denote the year. The line indicates a 1 :1 relation.

*Table 4.5 Measured and modelled yearly average groundwater level (GWL; in cm+sl) and cumulative CO_2 flux terms (all in t CO_2 ha^{-1}; positive to the atmosphere) in Cressier, if available. Harvest was calculated as dry matter yield * carbon fraction * 44/12, with an assumed fraction of 0.45. DOM considers net transport to surface water via runoff and drainage, excluding net transport via the bottom boundary of the model. The column 'peat' denotes the modelled decomposition of peat and its derived products, including the net transport via DOM. A '-' indicates the value was not measured.*

Year	Dataset	GWL	GPP	Reco	NEE	Harvest	DOM	NECB	Peat
2015	Measured	-	59.4	70.7	11.3	6.2	-	17.5	-
	Modelled	59.6	71.0	82.6	11.5	10.4	0.0	21.9	20.0
2016	Measured	-	70.8	75.0	4.3	11.6	-	15.9	-
	Modelled	51.1	71.8	74.6	2.8	13.1	0.6	16.5	16.7

We obtained two year budgets over the measured period from January 2015 to December 2016 (Table 4.5) . Again, it can be seen that both GPP and Reco are strongly overestimated in 2015 due to the flooding event. Over the two year period, NEE is slightly underestimated by the model. As the modelled harvest is slightly higher than the measured harvest, this results in a well-comparable NECB for 2016, and a slightly overestimated NECB for 2015. The general pattern, in terms of which of the two years has highest NEE, yield or NECB, is the same for the measurements and model.

Peat oxidation, which is modelled in ANIMO but cannot be measured directly, was estimated at 20.0 t CO_2 ha^{-1} in 2015, and 16.7 ton CO_2 ha^{-1} in 2016, which is lower than the modelled NECB for 2015, and slightly higher than the modelled NECB in 2016. This indicates the effects of imbalances on a year to year basis in short-term carbon sources (i.e. plant residues).

This project has received funding from the European Union's Horizon 2020 research and innovation programme under grant agreement N° 862695

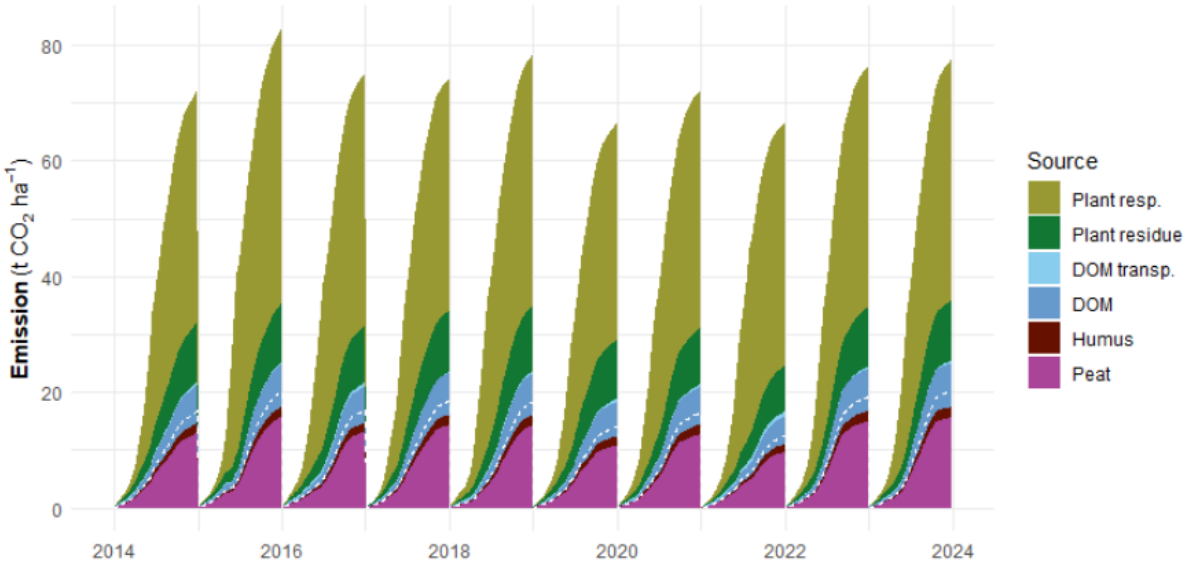

Figure 4.10 Contribution of the different terms to the yearly cumulative CO_2 emission from 2014 to the end of 2023, excluding emission due to harvest and uptake due to photosynthesis. The terms displayed involve plant respiration (direct plant respiration due to growth, maintenance and suboptimal conditions), plant residue (breakdown of recently died off plant material), dissolved organic matter (DOM) transport (net transport of DOM to surface water via runoff and drainage), DOM (breakdown of DOM within the soil), humus (breakdown of humus within the soil) and peat (breakdown of peat within the soil). The white dashed line indicates the sum of the direct and indirect contribution of peat to the CO_2 emission, which involves the entire term of peat, and a part of the humus, DOM and DOM transport terms.

An overview of the contributions of the different terms to the yearly cumulative CO_2 emission over the 10-year modelling period from 2014-2023 is given in Figure 4.10. The largest contributor to the CO_2 emission is direct plant respiration, accounting for approximately 50% of the total emissions. The majority of the emission originating from the soil itself is due to the oxidation of peat (and its derived products, indicated by the white dashed line), accounting for about 50 to 60% of the respiration originating from the soil. Oxidation of peat and its derived products accounts for 17.1 [2.6] t CO_2 ha^{-1} yr^{-1}, the value between brackets denoting the standard deviation over this 10 year period. The remaining part of the CO_2 emission from the soil is due to the respiration of short-lived carbon in the soil, such as root residues. The contribution of peat to the total ecosystem respiration is therefore quite substantial. The modelled year to year variation in total carbon emission is up to 15 t CO_2 ha^{-1} yr^{-1} (varying between 70 and 85 t CO_2 ha^{-1} yr^{-1}) which is 15 to 20% of the maximum modelled emission. Fluctuations in peat oxidation are limited to a 5 to 6 t CO_2 ha^{-1} yr^{-1}, which is about 30% of the maximum modelled emission due to peat loss.

This project has received funding from the European Union's Horizon 2020 research and innovation programme under grant agreement N° 862695

4.6. Scenario simulation results

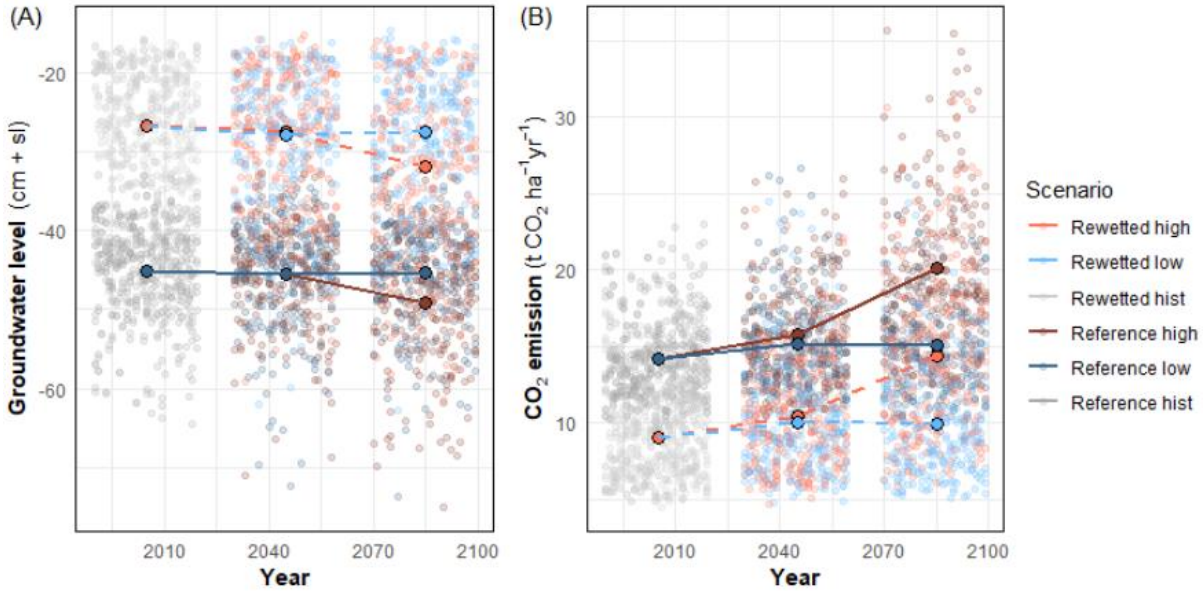

Figure 4.11 Overview of modelled groundwater level (A) and CO_2 emission from peat oxidation (including its derived products) (B) as function of time for the different scenarios. 'Reference' and 'rewetted' refer to the standard situation and the situation with adjusted drain management, respectively, and 'high' and 'low' refer to the RCP2.6 and RCP8.5 climate scenarios, respectively. Large dots and lines represent the mean of all individual model years (small dots) in each group.

The yearly averaged groundwater level is significantly shallower when the management of the drains is adapted to only drain when groundwater levels are shallower than 25 cm (i.e. rewetting scenario), rather than the currently used practice of 50 cm (Figure 4.11 A). The modelled average groundwater level in the reference period than changed from 45.2 [6.0] to 26.7 [7.4] cm below soil surface. This coincides with a reduction in CO_2 emission from peat oxidation of 5.1 t CO_2 ha^{-1} yr^{-1}, which is about 35% of the modelled emission in the reference period (14.2 [2.7] t CO_2 ha^{-1} yr^{-1}). In correspondence with the increased groundwater table, grass growth is reduced due to an increase in water stress, which may impact the potential of the grassland and may alter the storage of carbon in the soil related to grass growth. We did not consider this aspect any further, as also a change in grassland species may occur over this time span and we are specifically interested in the fate of the peat layer. The yearly-averaged groundwater levels in the low global GHG emission scenario seem to be rather constant, but in a high global GHG emission scenario the groundwater levels drop with about 4 cm compared to the reference period, related to a combination of decreased (summer) precipitation and increased evapotranspiration. This holds for both drain management scenarios.

Considering the current drain management practice, yearly-averaged CO_2 emission from peat oxidation increases slightly in the low global GHG emission scenario from the reference period to the period around 2045 (7%; +1.0 t CO_2 ha^{-1} yr^{-1}), but stabilizes moving from 2045 to 2085 as the atmospheric GHG concentrations no longer increase and atmospheric temperatures stabilize. However, for the high GHG emission scenario, an increase in peat oxidation may be expected of 42% (+6.0 t CO_2 ha^{-1} yr^{-1}) for the reference drain management scenario.

For the scenarios with adjusted drain management, the effect of increasing CO_2 emissions due to climate change in the high global GHG emission scenario is completely offset by the decrease in CO_2 emission due to wetter conditions. The modelled emission in 2085 for the high emission scenario under the rewetting scenario (14.4 t CO_2 ha^{-1} yr^{-1}) is well comparable to the modelled emission for the reference year when the current drain management is applied (14.2 t CO_2 ha^{-1} yr^{-1}).

This project has received funding from the European Union's Horizon 2020 research and innovation programme under grant agreement N° 862695

Comparing the modelled 10 year period of the base simulation (2014-2023) with the reference period shows that the modelled groundwater level (52.1 [5.1] cm-sl) and CO_2 emission (17.1 [2.6] t CO_2 ha^{-1} yr^{-1}) for this period are relatively deep and high, respectively, although they fall within the range of 1 standard deviation of each other. This may be explained by the fact that the base model is at the end of the reference model period (1990-2020); with an increasing trend in especially CO_2 emission, one may expect somewhat higher emissions over this period. Also, the years 2015, 2022 and 2023 all show an exceptionally deep yearly averaged groundwater level compared to the simulation based on climate models, even under future scenarios. This may indicate that either this period (2014-2023) showed a large number of remarkable and relatively rare meteorological conditions, or that the frequency of such conditions is underrepresented in the model.

A relation between modelled CO_2 emissions and groundwater level under low and high global GHG emission scenarios is shown in Figure 4.12. The steepness of the relation between emission and groundwater level increases with time, especially for the high emission scenario, which seems to be related to the correlation of groundwater level with temperature (not shown). In general, deeper yearly-averaged groundwater levels coincide with higher temperatures, as is also demonstrated in Figure 4.13. As the relation between temperature and peat oxidation is exponentially shaped, this may lead to the increasing slope. This increase in slope is not seen between 2045 and 2085 in the low global emission scenario, as may also be expected from Figure 4.11.

The relation between temperature and groundwater level in Figure 4.13 may also explain another important observation from Figure 4.12, that at a given groundwater level the emission from the rewetted scenario is higher than the emission from the reference drain management scenario. Yearly averaged groundwater levels of e.g. 40 cm-sl are shallower than the mean of the reference drain management, whereas these water levels are much deeper than the mean of the rewetted simulations. As such, when a groundwater level of 40 cm-sl is modelled in the rewetted scenario, the (soil) temperatures are higher than when this groundwater level is modelled for the reference drain management scenario, leading to an enhanced emission in the unsaturated zone of the rewetted case solely due to the higher soil temperature. It is therefore important to not only consider the relation between groundwater level and emission, but also account for differences in temperatures.

This project has received funding from the European Union's Horizon 2020 research and innovation programme under grant agreement N° 862695

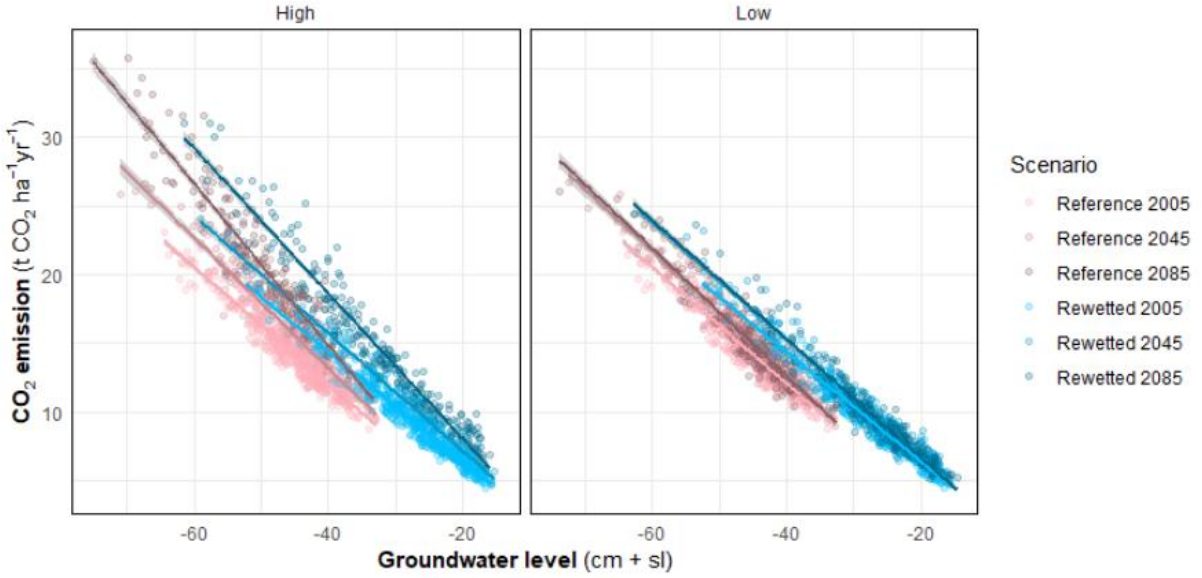

Figure 4.12 CO_2 emission from peat oxidation as function of groundwater level for the high (left panel) and low (right panel) global GHG emission scenarios. Colors indicate a combination of drain management (reference: red, rewetted: blue) and outlook period. Lines indicate a linear model fit for each combination, whereas individual points indicate individual model years.

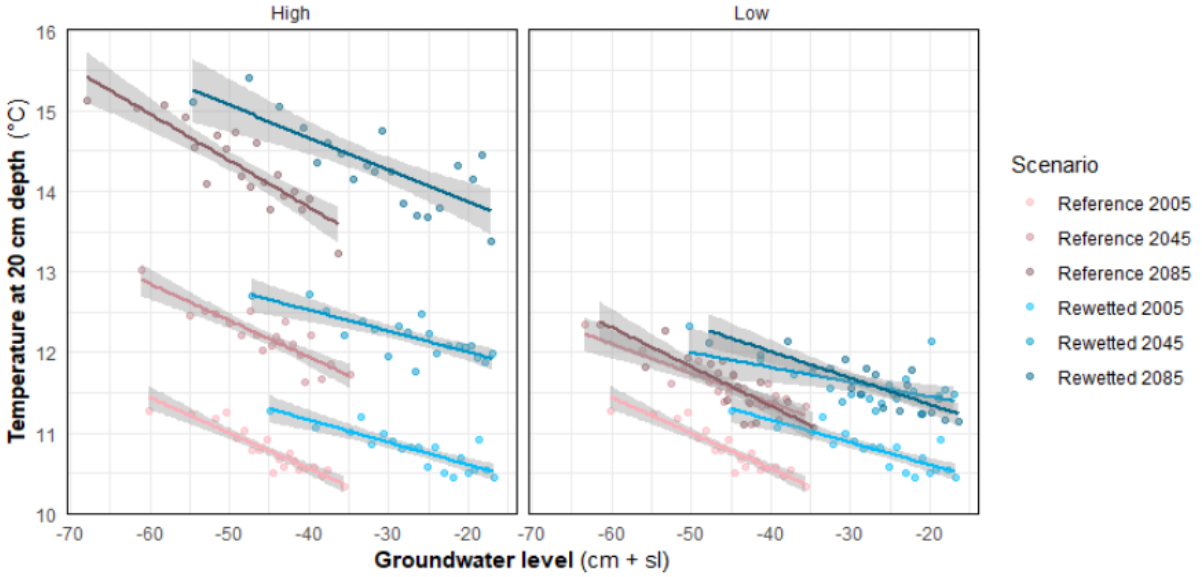

Figure 4.13 Average soil temperature at 20 cm depth as function of groundwater level for the high (left panel) and low (right panel) global GHG emission scenarios. Colors indicate a combination of drain management (reference: red, rewetted: blue) and outlook period. Lines indicate a linear model fit for each combination, whereas individual points indicate the averages of soil temperature and groundwater level after binning the data into 20 equally sized bins based on the annual average groundwater level.

This project has received funding from the European Union's Horizon 2020 research and innovation programme under grant agreement N° 862695

5. Vejrumbro, Denmark

5.1. Site overview

The Danish field site (Figure 5.1; 56.44 N, 9.55 E) is located close to the town Vejrumbro in the central part of Jutland, in the middle of a river valley of approximately 35 km in length. The valley, with a width ranging between 500 and 800 m, is west-east oriented with hills to the north and south extending up to 20 or 30 m above the valley itself. The river Nørreå flows through the valley in an easterly direction, and is, at the field location, approximately 15 m wide. Occasional flooding of the floodplains occurs (Malinowski et al. 2016). The river valley is build-up of (marine) sediments (gyttja) on top of sandy deposits, which form a confined aquifer. A peat cover of approximately 2 m thick is situated on top of the gyttja layer in the floodplain of the river (Mashhadi et al. 2024). The valley can be considered quite representative for peat-covered river valley systems in this part of Denmark (Nielsen et al. 2023).

The peat-covered area in proximity of the river was drained with ditches and cultivated since the early 20th century. The fields have been in agricultural use (pasture) as perennial grassland since then. Due to oxidation and compaction following the drainage of the peat, gradual land subsidence has occurred. This led to a gradually decreasing water table depth with respect to soil surface over time, causing a gradual rewetting of the peat soil (Pullens et al. 2024). The degradation of the top of the peat soil is reflected in measurements of peat decomposition and bulk density on the Vejrumbro field site (Mashhadi et al. 2024). As the river floodplains flood occasionally, also some mineral material may be deposited on the field surface.

Figure 5.1 Field site southwest of Vejrumbro, Denmark (56.44 N, 9.55 E). The EC tower is indicated by the orange dot, the flux footprint considered is indicated by the orange square, which is therefore the field considered. Small dots indicate the locations of the groundwater level measurements considered. The river Nørreå runs from west to east and the river stage was monitored at the blue dot next to the bridge.

This project has received funding from the European Union's Horizon 2020 research and innovation programme under grant agreement N° 862695

Monitoring on the field site was established in 2018. In 2019, a mean annual groundwater table depth of 13 cm was observed (Nielsen et al. 2021). In an attempt to rewet the site beyond the naturally occurring gradual rewetting, the ditches in proximity of the field were blocked in March 2022 to measure the effect of rewetting on the emission of greenhouse gasses (CH4, CO2, N20) (Pullens et al. 2024).

5.2. Measurements

Continuous measurements used for model calibration were available from June 2021 till June 2023. In addition, measurements of e.g. soil properties were used for the setup of the model. This data was obtained prior to the measurement period considered.

Soil description

Borehole descriptions of the first 2 to 10 meters have been made at 35 locations across the field. The general soil buildup is about 2 meters of peat, followed by 6 to 8 meters gyttja, below which a confined aquifer of 25 to 30 m of sand is found (Mashhadi et al, 2024). The gyttja has a relatively low LOI (loss of ignition), 12% on average, and occasionally shows the presence of shell beds. The peat has an average LOI of 76%. The soil bulk density in the peat layer shows the highest values for the top part of the soil from 0 till -20 cm+sl (0.20 g cm^{-3}) and lower values from -80 till -100 cm+sl (0.11 g cm^{-3}). Within the gyttja, the soil bulk density is about 0.5 g cm^{-3}. Porosity was high in both the peat and gyttja layers, with values of 0.7 to 0.9 cm^3 cm^{-3} (Mashhadi et al, 2024). Highest values were generally found in the peat layers. No measurements of the soil water retention curve were available.

The saturated hydraulic conductivity has been measured by slug tests on two different screen depths (we only have data available for the peat soil layers). In Table 5.1 the mean, minimum, maximum and standard deviation of the measured permeability are given. Reported measurements of horizontal permeability in gyttja layers on the same site show a wide variation (10^{-3} to 10^{2} m d^{-1}) in the gyttja layer, as this deposit includes layers consisting almost entirely of shells (Mashhadi et al, 2024). Given the general horizontal layering in gyttja deposits, the presence of poorly permeable layers implies a relatively high resistance to vertical groundwater flow.

Table 5.1 Permeabilty on two depths (mean and other characteristics).

Depth	K gem	K min	K max	K stdev
m-sl	m d^{-1}	m d^{-1}	m d^{-1}	m d^{-1}
0-1	0.696	0.012	5.152	1.802
1-2	0.172	0.006	1.038	0.292

In addition to the aforementioned parameters, also measurements of pH, total carbon content and total nitrogen content were available for several depths in each of the boreholes. These measurements were used to parameterize the SWAP-ANIMO model and are shown in Figure 5.4.

Hydrology

The river Nørreå flows through the valley and acts as the main drainage system of the valley. Continuous river level measurements were available from 2019 onwards, and show a typical seasonal trend with highest levels in late summer and autumn, and lowest levels in early spring, owing to the growth of weeds during summer (Figure 5.2). This trend is well-captured by a sine function, although it misses the peaks due to severe precipitation or melting events.

This project has received funding from the European Union's Horizon 2020 research and innovation programme under grant agreement N° 862695

There are some ditches in the fields which are connected to the river, which are separated by a distance of approximately 150 meters in the field considered. These act as secondary drainage system. The ditches surrounding the considered field were blocked in March 2022. Occasional manual measurements of the ditch water level were available from 2018 onwards. From summer 2022, also continuous measurements were available (Figure 5.2). The measurements indicate that the level in the ditch was raised significantly following the blockage, limiting drainage of water from the field via the ditches. Ditch water levels were relatively high due to the inflow of seepage water from upstream regions.

Phreatic groundwater levels in the field were monitored continuously and were reported once every half hour. Groundwater levels obtained from three measuring wells approximately 30 m from the ditch (their position indicated in Figure 5.1) were averaged and aggregated on a daily basis for model calibration. During the measurement period, the average groundwater level was 11 cm below soil surface, with a lowest reported groundwater table depth of 43 cm below soil surface, and highest groundwater table depth of 7 cm above soil surface, following the blockage of ditches in 2022.

Manual measurements of the aquifer were available both to the east and west of the field, indicating aquifer heads of 0.3 (west) to 0.6 (east) m above field surface (3.55 to 3.85 m above sea level). In Figure 5.3 the isohypses for the first (sandy) aquifer are given (Olsen, 2005). The map clearly shows the higher areas to the north and south of the river. Likely, most of the rainfall excess of these higher parts flows through the aquifer towards the lower parts in the river valley. Due to the low vertical permeability of the gyttja however, seepage is limited to locations where the gyttja layer is relatively thin.

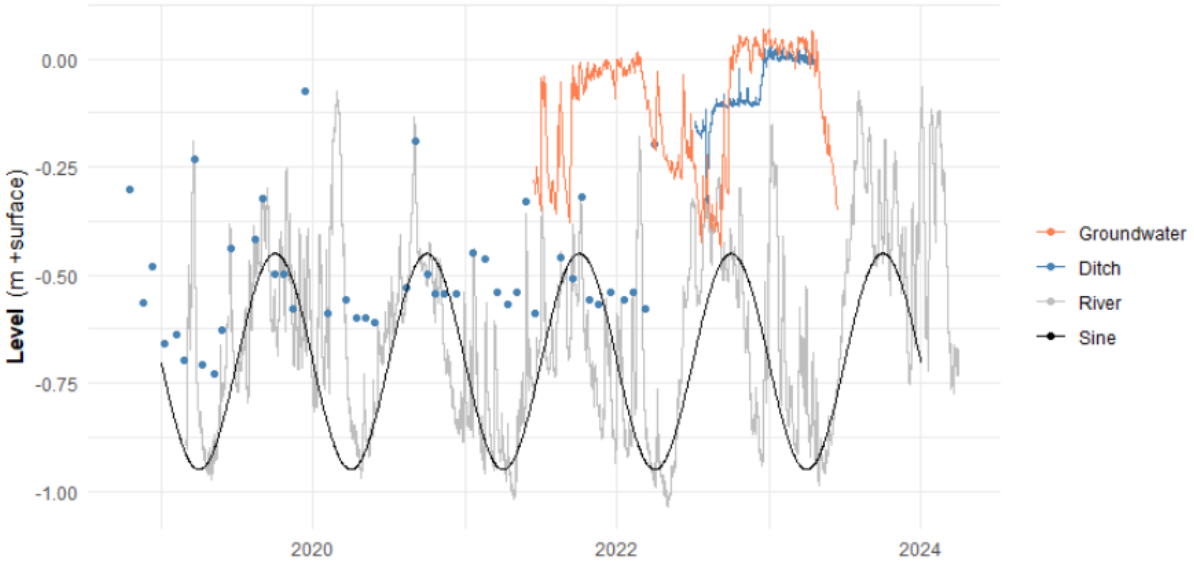

Figure 5.2 Measured groundwater levels as the average of three monitoring wells, and ditch and river stage as measured close to the EC tower and next to the bridge in the proximity of the field location, respectively (see also Figure 5.1). Ditch levels were measured manually prior to the summer of 2022, and continuously since. The effect of the ditch blocking in March 2022 is clearly visible in the ditch water levels. The sine function shown is used to extrapolate river stages beyond the measurement period.

This project has received funding from the European Union's Horizon 2020 research and innovation programme under grant agreement N° 862695

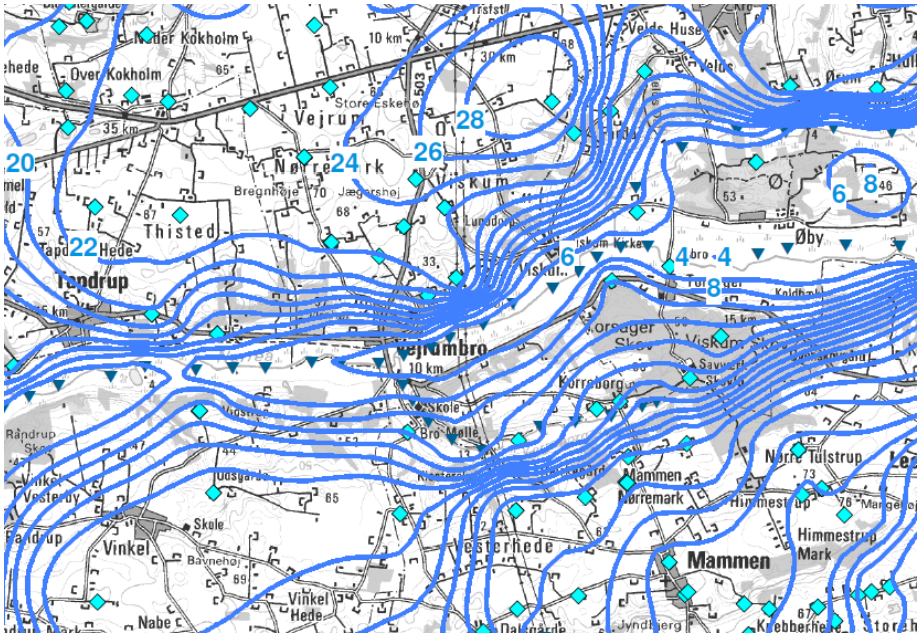

Figure 5.3 Groundwater isohypses in the first aquifer (mean for the year 2005, Olsen (2005)).

NEE and meteorology

NEE (net ecosystem exchange) was measured with an EC tower on the site. Its position is shown in Figure 5.1. Also the accompanying meteorological variables (air temperature, wind speed, relative humidity, global radiation, precipitation and soil temperature) were measured and evapotranspiration and CO_2 fluxes were determined. Flux data was gapfilled using REddyProc based on global radiation, relative humidity and soil temperature according to the methodology outlined in Wutzler et al (2018). NEE was further partitioned in GPP (gross primary production; photosynthesis) and Reco (ecosystem respiration) using the Lloyd-Taylor approach in combination with a rectangular hyperbolic light response curve, as outlined in Aben et al. 2024.

In addition to the on-site meteorological data, meteorological data was available from the Foulum measurement location, which is approximately 6 km away from the field site. This data was used for calculations with SWAP-ANIMO, rather than the on-site data, as there was some missing data in the on-site data, and the data only spanned a two-year period.

It should be noted that the field consists of several sub-plots (a raster which is also observable in Figure 5.1) which receive a specific treatment (e.g. Nielsen et al. 2024). On these sub-plots, measurements of the CO_2 exchange fluxes were performed with manual chambers on a bi-weekly basis in 2020-2021 (Nielsen et al. 2024). The reported fluxes of these sub-plots are considerably higher than the fluxes reported by the EC measurements. We did not include this information in further modelling.

Field management

On the site a (semi)natural grass vegetation grows, consisting of quite water-tolerant grass species. During the measurement period from 2021 to 2023, the field was harvested only once, on September 8th, 2022, with an average yield of +- 5 t dry matter (DM) ha^{-1}. Small patches within the EC footprint have been harvested more frequently for specific plot experiments, but this is not further considered. During the field experiment, no fertilization was applied on the majority of the field, and cattle were absent.

This project has received funding from the European Union's Horizon 2020 research and innovation programme under grant agreement N° 862695

5.3. Simulation setup

SWAP model setup

A SWAP model simulation was set up based on the described data. We considered a soil column extending to 6 m below the soil surface. Even though this column ends within the gyttja layer, missing 2 to 4 m of this layer does not affect simulation results, as the bottom boundary condition and saturated hydraulic conductivity are uncertain.

Meteorological data on temperatures, rainfall, solar radiation, humidity and wind speed was obtained from the weather station at Foulum (6 km from the Vejrumbro site) for the period 2014-2023. This was also the simulation period applied for this site. Calibration of the model was based on measurements in the period June 2021 to June 2023. Any meteorological data obtained at the site itself was not used in the modelling, as these data only covered part of the simulation period. Model initialization was done by repeating these time series for a period of 50 years. Actual evapotranspiration was based on the reported reference Makkink transpiration fluxes, rather than Penman Monteith which was used for the other two sites. This choice was made based on data availability for the climate scenario analyses. As for the Foulum weather station itself both the Makkink and the Penman Monteith input variables were available, we assessed the influence of this choice. It was found to be of minor influence, especially in light of other uncertainties.

Grass growth, gross primary production (GPP) and plant respiration were modelled in SWAP using the WOFOST-based grass module. This module is specifically designed for intensively managed grasslands covered with ryegrass. As the grass species and mowing and fertilization regime are different in this site, we applied some adjustments based on a calibration with the 'measured' GPP:

- The maximum assimilation rate over time was reduced: productivity of the grassland was less compared to frequently fertilized and cut ryegrass.
- The crop coefficient, determining the transpiration rate, was reduced to 0.4 at the start of the growing season and linearly increasing to 0.9 towards the end of the growing season to limit transpiration fluxes, based on calibration with observed groundwater levels.
- Relative death rates of roots and stems during the growing season were increased: as the grasses were not (frequently) harvested, grasses go into senescence and start to decay, which is not modelled properly by the grass module.
- No oxygen stress due to wet conditions was considered: as the grasses were tolerant to temporary waterlogged conditions, it was assumed that prolonged periods of wet conditions in the root zone did not affect growth.
- Drought stress parameters (using the Feddes function) were adjusted as the grass species were adapted to wet conditions, such that some drought stress occurred in dry situations.
- The relative management factor, which lumps several effects of e.g. a shortage of fertilizer, and the presence of pests, diseases and sub-optimal growth conditions, was set at 0.55.
- The root zone thickness was estimated to be 30 cm.
- In ANIMO, it was assumed that 80% of the biomass growth was added to the soil, whereas the 20% remaining biomass was left on the surface each year to gradually be oxidized. The latter process was estimated by adding an above ground biomass degradation flux to the modelled ecosystem respiration. The above ground biomass pool was initialized halfway the year based on the modelled biomass growth during that year, and was dissipated entirely in the following 365 days, distributed over these days based on a cosine function. The harvested biomass was not added to the soil or above ground biomass pool. For the year 2022, biomass was harvested and removed from the field. Hence, for this year the above ground biomass was not added to the soil or above ground biomass pool.

This project has received funding from the European Union's Horizon 2020 research and innovation programme under grant agreement N° 862695

As no measurements of the soil water retention curve were available, we estimated the Mualem-Van Genuchten parameters from the Dutch Staring set (Heinen, 2020). This set is based on 999 soil samples taken across the Netherlands for which several parameters were determined in the lab. These samples were grouped into 36 classes based on characteristics as sand size, loam, clay and organic matter content, and position in the soil (topsoil (B) or subsoil (O)). The most appropriate top soil parameterization is B16 (0-25 cm-sl), followed by a subsoil O16 (25-200 cm-sl) for the more pristine peat layer below (Table 5.2). No parameterization of a gyttja layer (200-600 cm-sl) is present in the Dutch Staring set, as these deposits are not commonly found in the Netherlands. However, due to its position this layer is always saturated, and only the saturated porosity and hydraulic conductivity are of relevance. We therefore chose to parameterize this layer as O17. Based on the model calibration, however, the pF curves of the upper soil layers were found to be inadequate to reproduce the observed groundwater levels. Therefore, the value of the alpha parameter was raised to resemble less dense peat, in accordance with Liu & Lennartz (2019). Also the saturated hydraulic conductivity of the gyttja layer was reduced. An overview of the schematization and parameters used is given in Table 5.2. The saturated hydraulic conductivity and porosity is in range with values reported in Table 5.1 and Mashhadi et al. 2024 for the same site.

Table 5.2 Soil profile description as used in the SWAP-ANIMO model, using slightly modified Staring parameters. Parameters listed include (in order of appearance) the residual water content ϑr, saturated water content ϑs, shape parameters (α, n, λ) and fitted saturated hydraulic conductivity based on the evaporation method, multiplied by 10 to include the effects of small macropores.

Depth	Staring nr.	Formal description	θ_r	θ_s	α	n	λ	Ksat
cm-SL	-	-	$cm^3\ cm^{-3}$	$cm^3\ cm^{-3}$	cm^{-1}	-	-	$cm\ d^{-1}$
0-25	B16 (adj)	(Sandy) peat	0.01	0.786	0.045	1.28	-1.22	123.6
25-200	O16 (adj)	Oligotrophic peat	0.0	0.889	0.050	1.36	-0.66	14.6
200-600	O17 (adj)	Eutrophic peat	0.01	0.849	0.012	1.27	-1.25	5.0

Hydrological boundary conditions on the sides and bottom of the SWAP column were described by three drainage systems (sides) and an aquifer head (bottom). Several combinations of drainage system - and bottom flux parameters were explored, based on the information described in section 5.2. However, as this information is, in some aspects, rather limited, multiple options yielded comparable calibration results.

The bottom boundary condition was given by a constant aquifer head at the bottom of the SWAP column, which was set at 0.4 m above soil surface level, based on measurements of the aquifer head. A resistance of 3000 days was applied (excluding flow resistance in the soil column itself) based on calibration with observed groundwater levels.

The drainage systems were defined by three levels: the first level represents the river, the second level represents the ditches and the third level represents a shallow superficial drainage system ('trench'), which accounts for some shallow (interflow) processes towards the ditch. Prior to rewetting, this third level was activated once groundwater levels reached soil surface. After rewetting, this system was effectively removed from the model and replaced by surface runoff. Surface runoff occurred only when ponding exceeded a threshold of 1.5 cm+sl. The characteristics of the drainage systems as based on model calibration are given in Table 5.3. Water levels were prescribed using the observations given in Figure 5.2 for the period available, and interpolated linearly if applicable. For the remaining modelling period beyond the measurement range, the sine function in Figure 5.2 was used to describe the river stage, whereas for the ditch a constant level of 55 cm below soil surface was used prior to 2022, and a level at soil surface for 2022 and later.

This project has received funding from the European Union's Horizon 2020 research and innovation programme under grant agreement N° 862695

Table 5.3 Drainage system characteristics used in modelling of the Vejrumbro site.

	Drainage resistance (d)	Infiltration resistance (d)	Depth (cm-sl)	Spacing (m)
River	50000	50000	-150	500
Ditches	1500	1500	-50	150
Trench	2	-	-2	4

ANIMO model setup

An overview of the soil composition as measured and as used for model input is given in Figure 5.4. A clear shift in characteristics of the soil is apparent at a depth of 2 m-sl, where the gyttja deposit starts. A more gradual change is visible in the upper +- 50 cm of the soil, where the bulk density gradually decreases from the soil surface downward. As the organic mass only partially shows the same decrease, it appears that the upper soil is slightly enriched with mineral parts. This may be the results of peat oxidation, leaving mineral parts behind in the soil, as well as due to occasional flooding of the site. The pH is generally quite high in the soil, indicative of upward seeping groundwater through the gyttja layer which contains CaCO3-rich shells. Only the upper part of the soil shows a lower pH. The C/N ratio is slightly increasing with depth in the peat layer and is somewhat higher than in the other sites, reflecting its more pristine conditions.

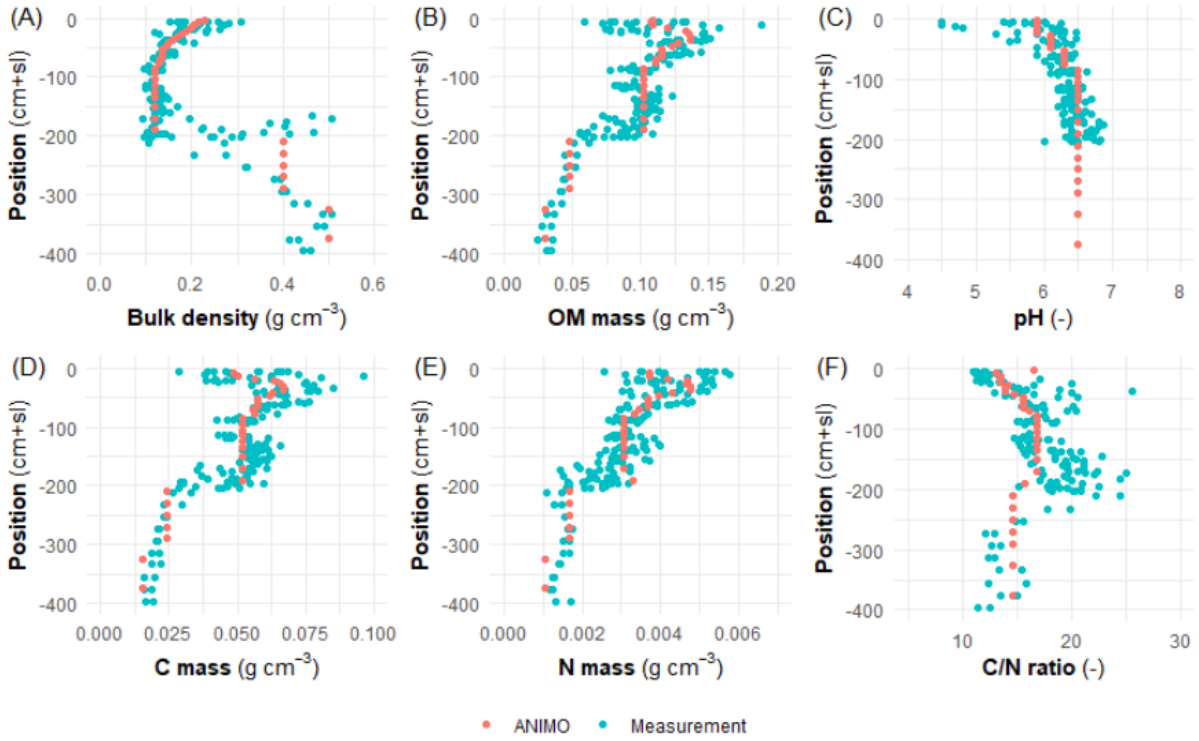

Figure 5.4 Measurements (blue) and model input after initialization runs (red) for Vejrumbro of dry bulk density (A), OM mass (B), pH (C), carbon mass (D), nitrogen mass (E) and C/N ratio (F), as function of depth. For the upper 2 m of soil, a selection of measurements in vicinity of the EC tower was made. For the deeper measurements, all available measurements are plotted.

An overview of the partitioning of the sources of organic matter at the start of the simulation period following the initialization runs is shown in Figure 5.5. Fresh organic material is present in the root zone, which is the resultant of added shoot and root material. Also humus, remaining from the decomposition of fresh organic material, is present. It appears that in the upper 10 cm of the soil more than half of the soil organic matter originates from (recent) plant material, whereas in the rest

This project has received funding from the European Union's Horizon 2020 research and innovation programme under grant agreement N° 862695

of the soil, most organic matter is present in the form of peat or peat-derived humus, with some remnants of roots within the rootzone.

As measurements of the soil respiration rate (with depth) were not available, we used the same rates as in the other sites to parameterize the breakdown rate of organic matter. It was therefore not possible to check whether the initial conditions or parameterization of the respiration rates of the different soil organic matter pools was adequate.

The modelled average respiration rate per layer (excluding DOM) under optimal conditions at a soil temperature of 10 °C (Figure 5.5) shows a strongly decreasing trend from the upper soil layer downward within the root zone. The average respiration rate follows directly from the parameter input and the partitioning of organic matter sources after the initialization runs. The strongly decreasing trend with depth is mainly related to the changing contribution of fresh organic matter to the total organic matter content in a soil layer.

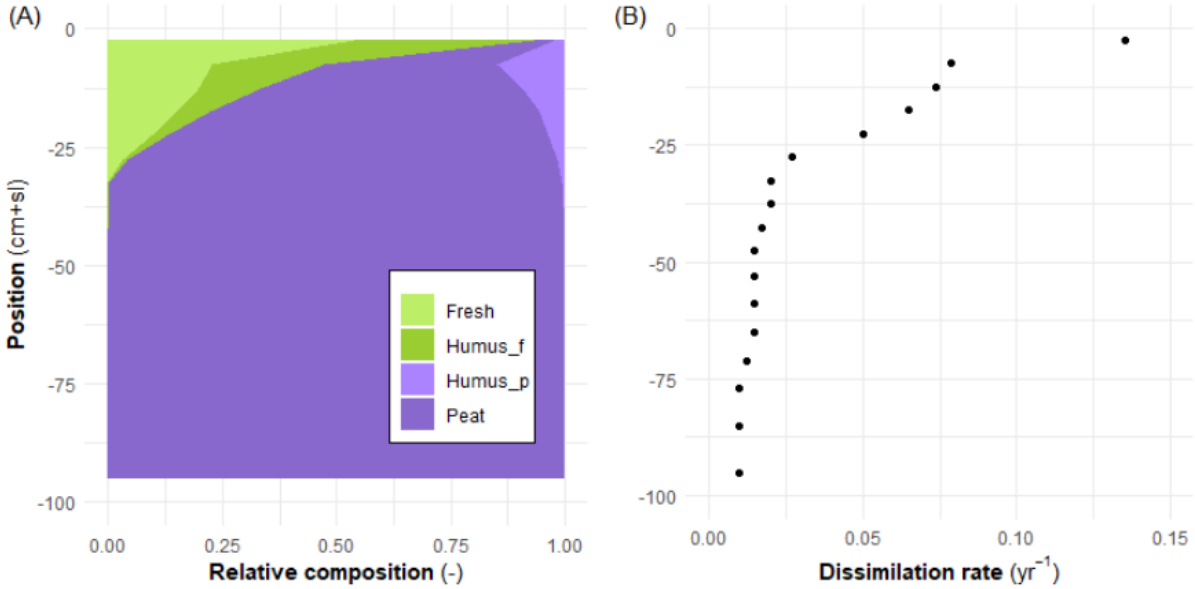

Figure 5.5 (A) Partitioning between fresh and peat (derived) materials at the start of the simulation in Vejrumbro, resulting from the initialization runs and (B) corresponding dissimilation rate (excluding DOM) at optimal conditions and 10 °C as function of depth in the soil.

5.4. Scenario definitions

For this site we consider a combination of scenarios based on water level management and climate projections. For the water level management, we consider the reference case, in which the ditches are not blocked and for which we assume a constant surface water level of 55 cm below soil surface, and the rewetted case in which we assume the ditches are blocked, resulting in a constant surface water level of 10 cm below soil surface. We refer to these water management scenarios for Vejrumbro as reference and rewetted.

We also explored the effects of climate change by considering the DMI Climate Atlas data of the Danish Meteorological Institute (DMI, 2024a; DMI, 2024b), using the daily bias-corrected data on an 12 km (rotated) grid and interpolated to the specific location. Note that the interpolation of gridded data may result in an underestimation of especially (peak) precipitation events on a point scale. We did not analyse these effects in this study. The daily bias-corrected data includes information on the

This project has received funding from the European Union's Horizon 2020 research and innovation programme under grant agreement N° 862695

Makkink reference evapotranspiration rather than all the required input variables for the Penman-Monteith formulation. As this option is also available in SWAP, we used this information as model input.

Based on the availability of data for both the RCP2.6 and RCP8.5 global GHG emission scenarios, in total 27 climate models were available for use. To limit the amount of simulations, we selected 8 climate models (Appendix I; the number of models used is the same as for Cressier) for our simulations. The selection of models was based on the model availability for Cressier, such that, whenever possible, the same models were used. We did not assess the full range in predicted conditions for the specific location in Denmark for all 27 models, and as such the model selection may lead to a bias in SWAP-ANIMO model predictions. However, as the modelled soil temperature increase is in agreement with the other sites (Figure 7.2) and the climate change effect on the hydrology of this site seems to be rather limited (Figure 5.11), a bias is unlikely to have a significant impact.
We considered a reference period (1980 to 2010) and two outlook periods (2040-2070; 2070-2100), in correspondence with the outlook periods described by the DMI (DMI, 2024a). Note that the period 2010-2040, despite its availability, is not modelled, as for the other sites we also considered only two outlook periods in the middle and end of the century.

We split each model realization for a given period into three 10-year periods for which we ran the SWAP-ANIMO model for both the reference and rewetted scenario, each time using the same initial conditions as defined by the prerun of the base simulation. We do, therefore, not account for any changes in e.g. peat composition over the period considered.

5.5. Base simulation results

Hydrology

Groundwater levels simulated by SWAP-ANIMO show the general trends in measured groundwater levels quite well (Figure 5.6). The root mean squared error (RMSE) and mean absolute error (MAE) are 4.9 and 3.6 cm, respectively, for the period between June 2021 and June 2023. In the winter of 2022/2023, the soil is permanently flooded, corresponding to ditch water levels reaching the soil surface level. These extremely wet winter conditions are also simulated by the model following the blockage of the ditch, due to the ponding threshold of 1.5 cm+sl.

An overview of the monthly modelled water balance terms is given in Figure 5.7. For the net balance over the period shown (2021 – 2023), most of the inflowing water originates from precipitation (93%; 794 mm yr^{-1}). A small fraction was simulated to originate from upward seepage through the gyttja layer (7%; 58 mm yr^{-1}). The lower boundary condition therefore has a limited influence on the model results.

Over the 2021-2023 period considered, water is removed from the field primarily by evapotranspiration, removing 473 mm yr^{-1} (56%). This is 125-175 mm yr^{-1} below the reference Makkink evapotranspiration rate. Evapotranspiration was also estimated based on EC measurements, and was on average 545 mm yr^{-1}. For the year 2022, the total evapotranspiration in the model and the measurements was nearly identical, with 448 and 449 mm, respectively. Water removal due to evapotranspiration is mostly restricted to the period from spring to the end of summer. Surface runoff (or runoff via the shallow superficial drainage system) amounts to 335 mm yr^{-1} (39%) and occurs mainly during winter and early spring, or in case of intense precipitation events. The remainder of water removal was through net sub-surface flow to the ditch (32 mm yr^{-1}; 4%). Flow to the river was very small due to the high resistance implemented in the model (as based on

This project has received funding from the European Union's Horizon 2020 research and innovation programme under grant agreement N° 862695

model calibration) and amounted to only 4 mm yr^{-1} (0.5 %). The latter seems rather small, but may be appropriate if there is a large resistance to horizontal flow. This is also suggested by the relatively high resistance calibrated for exchange with the ditch, such that the main processes involved are related to water exchange at the soil surface.

During the period considered, a rewetting of the site occurred in 2022 leading to a shift in contributions of especially the drainage pathways. Following rewetting of the site, some infiltration of water from the ditch into the field occurred, with on average 16.4 mm yr^{-1} in 2022 and 2023. The gross drainage rate in this period was 18.3 mm yr^{-1}, resulting in a net drainage rate of only 1.9 mm yr^{-1} through the soil. Obviously, total drainage of the ditch, including also the contributions of surface runoff, was higher. No infiltration of water was modelled prior to rewetting of the site except for a limited amount in the dry year 2018, and the average net drainage rate of water through the soil towards the ditch was 78 mm yr^{-1}. Following rewetting, the reduction in drainage through the soil was compensated mostly by an increase in surface runoff.

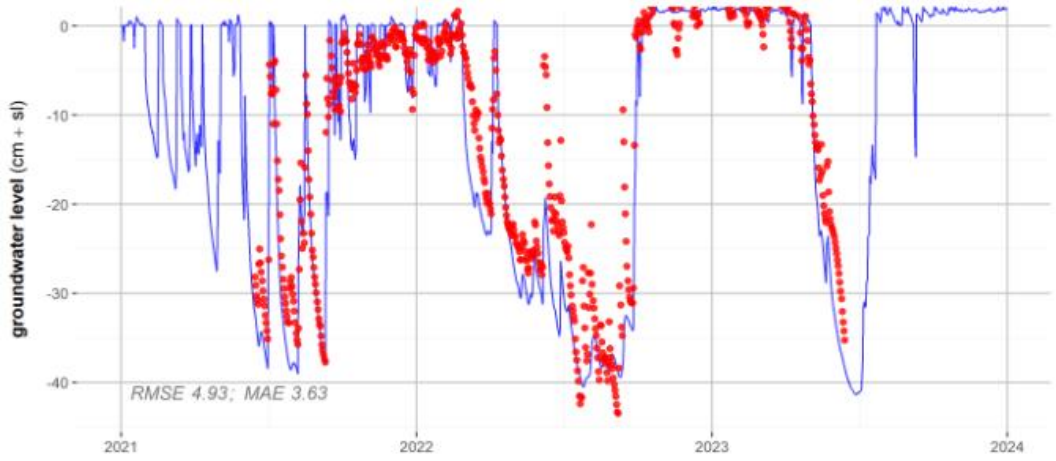

Figure 5.6 Measured (red dots) and modelled (blue line) phreatic groundwater levels in Vejrumbro.

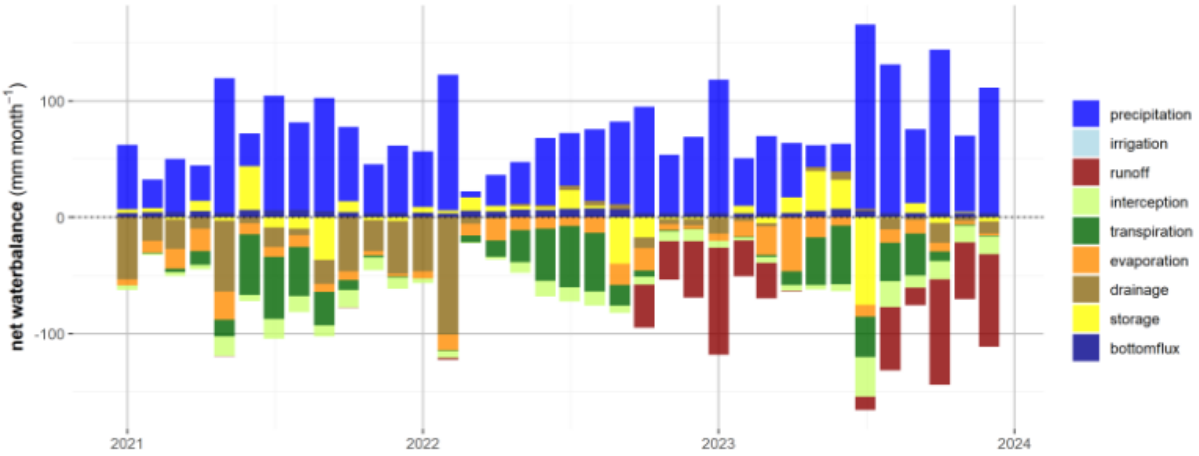

Figure 5.7 Modelled monthly water balance terms from 2021 to 2024 in Vejrumbro. Positive terms describe water supply towards the soil and canopy, negative terms describe removal from the soil and canopy. A sudden change in contribution of runoff and drainage is seen, which is caused by the rewetting. In practice, however, most of the drainage prior to 2022 was due to superficial drainage through the 'trench', which was essentially the same process as runoff.

This project has received funding from the European Union's Horizon 2020 research and innovation programme under grant agreement N° 862695

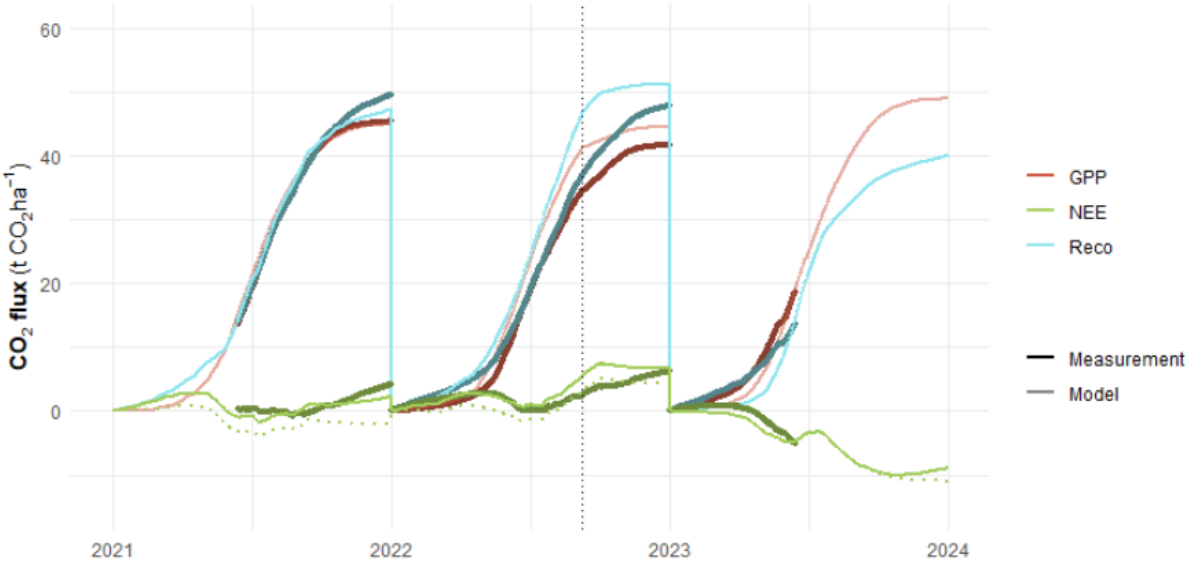

Figure 5.8 Cumulative measured and modelled NEE, GPP and Reco. NEE was measured by EC and gapfilled, GPP and Reco 'measurements' were obtained by partitioning half-hourly gap-filled EC fluxes. Modelled lines were obtained with SWAP-ANIMO. The dotted NEE line represents the modelled NEE without the contribution of the decay of above ground biomass. The dotted vertical line indicates a harvest event on September 8th, 2022. As measurements started only in June 2021, the starting point of the cumulative measurement line in 2021 was set at the cumulative amount of that date in 2022.

CO_2 fluxes

The yearly cumulative modelled net ecosystem exchange (NEE), gross primary production (GPP) and ecosystem respiration (Reco) are shown in Figure 5.8. Cumulative fluxes are displayed in calendar years, as during winter months fluxes are generally low and standing biomass is minimal. As a consequence, the cutoff point is not so much dependent on the year-to-year variation in e.g. weather conditions. Unfortunately, the EC measurements for this site start and end in the middle of the growing season, such that the starting position of the EC measurements in 2021 had to be estimated in this Figure.

In terms of seasonal patterns, both the model and measurements show a slight net uptake of CO_2 during the spring season, and a net emission of CO_2 during the remainder of the season for the years 2021 and 2022. There seems to be a higher net uptake of CO_2 in 2023 in both the model and measurements, although the measurements only last until June of that year. In the model, the net emission is more concentrated in the summer season compared to the measurements, where a net emission seems to be ongoing in the winter period. Given the high groundwater levels during winter, hardly any peat decomposition is modelled during the winter period, but, judging by the EC measurements, some emission still occurs. Standing biomass will be present above the flooded soil surface which may be subject to decomposition during the winter months as well, which is not represented this way in the model as all decaying organic material is, per definition, below the soil surface. We partly compensated for this missing effect by adding the groundwater-independent breakdown of 20% of the organic matter as indicated in section 5.3. Even though this was a rather crude approach, it does improve the model performance during winter periods (compare the green dashed line with the continuous green line in Figure 5.8).

A comparison of modelled and measured daily GPP and Reco rates shows a good relation for GPP with only minor scatter around the 1:1 line (Figure 5.9). On the other hand, Reco appears to be somewhat overestimated during the growing season and underestimated in the winter months by the model, corresponding to the observations from the cumulative plot. We use Lin's Concordance

This project has received funding from the European Union's Horizon 2020 research and innovation programme under grant agreement N° 862695

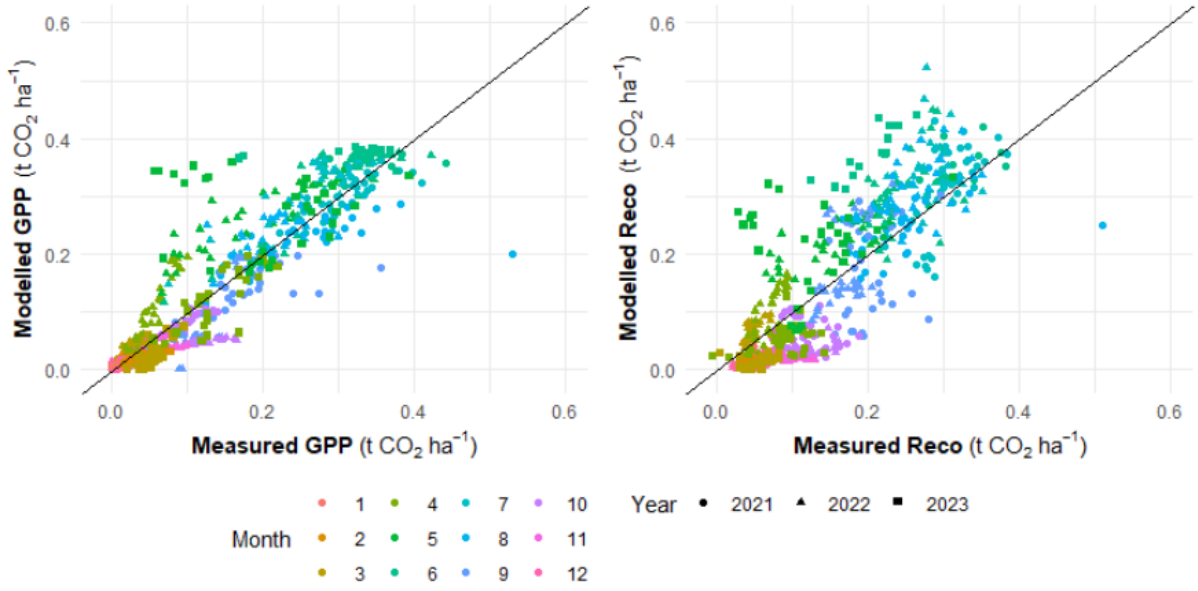

Figure 5.9 Relation between daily modelled and daily measured GPP (left side) and daily modelled and daily measured Reco (right side). Colors indicate the month of the year, symbol shapes denote the year. The line indicates a 1 :1 relation.

Correlation Coefficient (CCC) as a measure to determine both the accuracy and precision of all the datapoints with respect to the 1:1 line. A perfect fit yields a value of 1, whereas no relation at all yields a value of 0, similar to Pearsons correlation coefficient. The obtained CCC for the modelled GPP and Reco are 0.915 and 0.825, respectively. This indeed indicates the very good fit for GPP, and the somewhat poorer fit for Reco.

We obtained two year budgets over the measured period from June 2021 to June 2023 (Table 5.4), despite the argument that it may be more appropriate to use the winter season as cutoff point. The modelled and measured carbon fluxes (GPP, Reco and NEE) are well comparable, although not identical. The modelled and measured NEE are both lower in 2022-2023 compared to 2021-2022. This coincides with a higher yearly-averaged groundwater level, which may be influenced by the blockage of the ditch early 2022.

Summation of the GPP, Reco, harvest and net DOM export to surface water yields an estimate of the net ecosystem carbon balance (NECB; excluding the contribution of methane to this balance and distributing the harvest of 2022 over the two budgets equally). As the DOM export was not measured, this term is only accounted for in the model outcomes. This results in a higher modelled NECB compared to the measured NECB.

Peat oxidation, which is modelled in ANIMO but cannot be measured directly, was 4.0 t CO_2 ha^{-1} in the period 2021-2022, and 5.1 t CO_2 ha^{-1} in 2022-2023. The majority of peat oxidation occurred in the second half of the summer of 2022, when groundwater tables were relatively low. The remainder of the 2022-2023 period hardly any peat oxidation occurred. In both cases peat oxidation was slightly higher than the modelled NEE, but lower than the modelled NECB.

This project has received funding from the European Union's Horizon 2020 research and innovation programme under grant agreement N° 862695

*Table 5.4 Measured and modelled yearly average groundwater level (GWL; in cm+sl) and cumulative CO_2 flux terms (all in t CO_2 ha^{-1}; positive to the atmosphere). The period considered lasts from June 15th of the year mentioned, to June 14th of the following year. To obtain the yearly average groundwater level, daily groundwater levels exceeding soil surface were set to 0 cm+sl. Harvest was calculated as dry matter yield * carbon fraction * 44/12, with an assumed fraction of 0.45. Harvest in 2022 was distributed evenly over both years. DOM considers net transport to surface water via runoff and drainage, excluding net transport via the bottom boundary of the model. DOM was not measured. The column 'peat' denotes the modelled decomposition of peat and its derived products, including the net transport via DOM.*

Year	Dataset	GWL	GPP	Reco	NEE	Harvest	DOM	NECB	Peat
2021 -	Measured	-12.6	-44.9	49.4	4.5	4.1	-	8.6	-
2022	Modelled	-14.3	-46.7	50.9	-4.3	4.3	+1.2	9.8	4.0
2022 -	Measured	-11.4	-46.3	47.0	0.7	4.1	-	4.8	-
2023	Modelled	-12.7	-45.9	46.9	1.0	4.3	+0.2	5.5	5.1

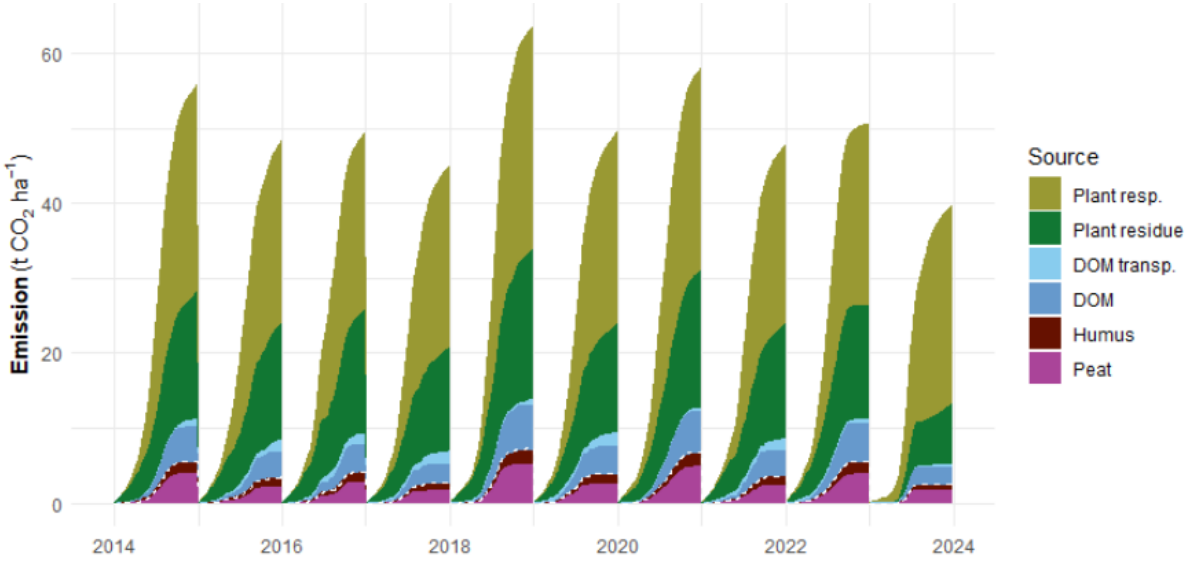

Figure 5.10 Contribution of the different terms to the yearly cumulative CO_2 emission from 2014 to the end of 2023, excluding emission due to harvest and uptake due to photosynthesis. The terms displayed involve plant respiration (direct plant respiration due to growth, maintenance and suboptimal conditions), plant residue (breakdown of recently died off plant material), dissolved organic matter (DOM) transport (net transport of DOM to surface water via runoff and drainage), DOM (breakdown of DOM within the soil), humus (breakdown of humus within the soil) and peat (breakdown of peat within the soil). The white dashed line indicates the sum of the direct and indirect contribution of peat to the CO_2 emission, which involves the entire term of peat, and a part of the humus, DOM and DOM transport terms.

An overview of the contributions of the different terms to the yearly cumulative CO_2 emission over the 10-year modelling period from 2014-2023 is given in Figure 5.10. Clearly, the largest contributor to the CO_2 emission is direct plant respiration, accounting for roughly 40-60 % of the total emissions. The majority of the emission originating from the soil itself is due to the decay of young plant material, and only a minor part is due to the breakdown of peat or peat-derived products, the latter indicated by the white dashed line. The magnitude of the breakdown of peat-derived products is in line with the measured NEE and NECBs presented in Table 5.4. The modelled year to year variation in carbon emission is up to 15 t CO_2 ha^{-1} yr^{-1}, which is 25% of the maximum modelled emission. Fluctuations in peat oxidation are however up to 65% of the maximum modelled emission due to peat loss (compare 2018 with 2017). The average modelled emission due to peat oxidation amounts to 4.60 [1.66] t CO_2 ha^{-1} yr^{-1} over this 10-year period, the value between brackets denoting the standard deviation.

This project has received funding from the European Union's Horizon 2020 research and innovation programme under grant agreement N° 862695

5.6. Scenario simulation results

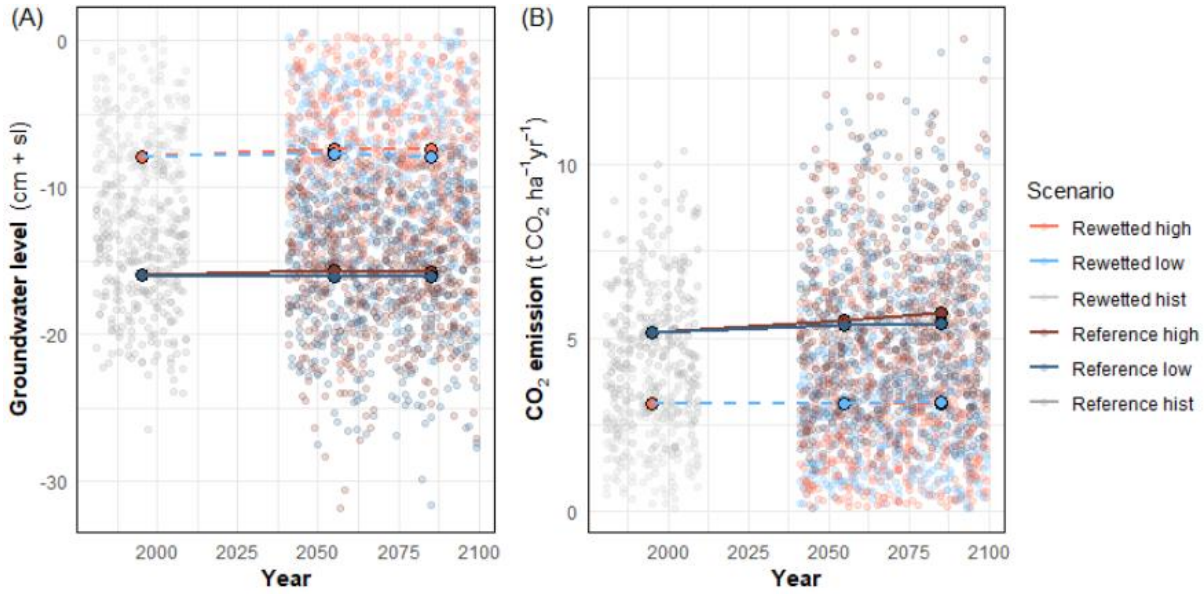

Figure 5.11 Overview of modelled groundwater level (A) and CO_2 emission from peat oxidation (including its derived products) (B) as function of time for the different scenarios. 'Reference' and 'rewetted' refer to the standard situation and the situation with a blocked ditch, respectively, and 'high' and 'low' refer to the RCP2.6 and RCP8.5 climate scenarios, respectively. Large dots and lines represent the mean of all individual model years (small dots) in each group.

Modelled groundwater depth in the rewetted situation is considerably shallower compared to the situation without rewetting, with a decrease in average depth of 8 cm (~50%) for the reference period. The CO_2 emission is lower for the rewetted situation as well, showing a decrease of 40% owing to the wetter conditions. The modelled groundwater depth shows a minimal decrease over time for both the high global GHG emission scenario, and remains the same for the low emission scenario. The CO_2 emission, in contrast, shows a slight upward trend, which is slightly more pronounced for the high global GHG scenario compared to the low GHG scenario. The modelled emission for the reference situation increases from 5.17 [1.89] t CO_2 ha^{-1} yr^{-1} for the reference period (1980-2010) to 5.72 [2.37] t CO_2 ha^{-1} yr^{-1} for the most extreme scenario (high GHG emission, 2085), whereas the increase is negligible for the rewetted situation (3.09 [1.72] to 3.17 [2.21] t CO_2 ha^{-1} yr^{-1}. Therefore, the beneficial effect of rewetting on peat conservation will increase under future climatic conditions. Also note that for both the modelled groundwater level and CO_2 emission, the year to year variation increases as demonstrated by an increase in standard deviation for both parameters.

This project has received funding from the European Union's Horizon 2020 research and innovation programme under grant agreement N° 862695

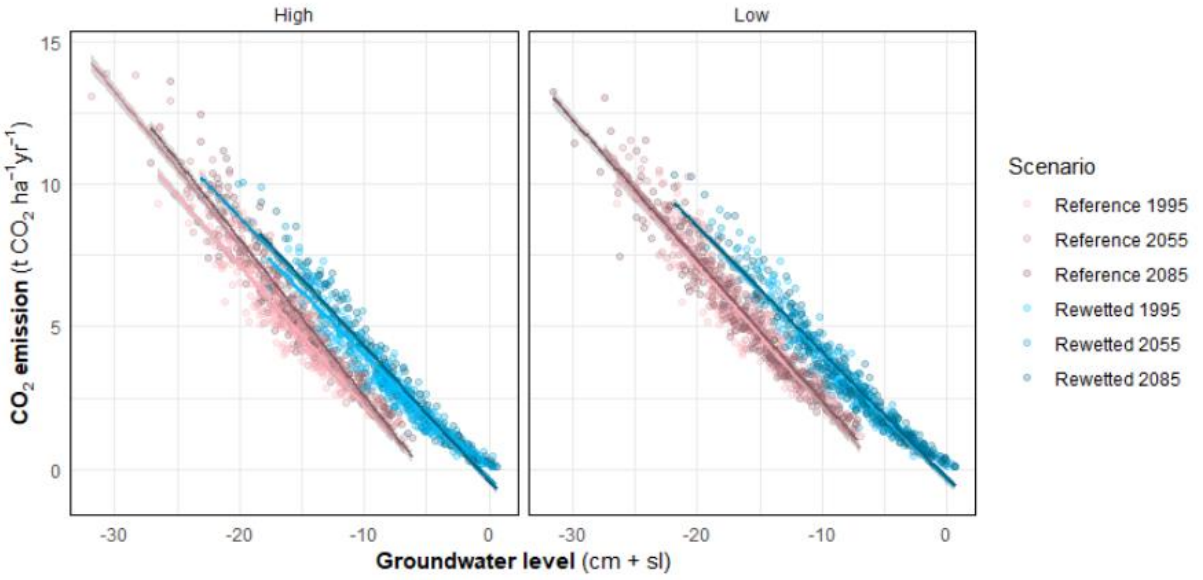

Figure 5.12 CO_2 emission from peat oxidation as function of groundwater level for the high (left panel) and low (right panel) global GHG emission scenarios. Colors indicate a combination of drain management (reference: red, rewetted: blue) and outlook period. Lines indicate a linear model fit for each combination, whereas individual points indicate individual model years.

The relation between groundwater level and CO_2 emission is affected by rewetting (Figure 5.12). This relation appears to be non-linear, especially at very shallow groundwater table depths, but becomes more or less linear at depths larger than 10 cm-sl. At a given groundwater level, the emission in the rewetted situation is higher compared to the emission in the reference situation. In this particular case, this may be related to two conditions. First, in the rewetted case ponding frequently occurs, resulting in situations with groundwater levels above surface level. This may impact the average yearly groundwater level slightly, but does not have any effect on the CO_2 emission, as for decomposition in the model, it is irrelevant whether groundwater levels are at some height above soil surface, or at soil surface itself. Second, as there is generally a correlation between groundwater table depth and (soil) temperature, with deeper groundwater levels coinciding with higher soil temperatures, the average soil temperature at a given groundwater table depth is likely higher in the rewetted case compared to the reference. This is also demonstrated for the Cressier site (Figure 4.13).

This project has received funding from the European Union's Horizon 2020 research and innovation programme under grant agreement N° 862695

6. Zegveld, The Netherlands

6.1. Site overview

The Dutch field site (Figure 6.1; 52.14 N, 4.84 E) is located close to the town Zegveld in the western, peat covered part of the Netherlands. It is situated in the middle of a vast coastal peatland area which formed in the Holocene. The peat cover currently has a thickness of 6 to 7 meters and overlays a sandy Pleistocene deposit. During its formation, it was situated slightly above the average sea level, keeping up with a gradual rise in sea level (Erkens et al. 2016). Following the drainage of the area in the Middle Ages, during which ditches were excavated to drain the land, land subsidence and ongoing drainage have resulted in the disappearance of several meters of peat in the area, and a gradual increase in soil bulk density and mineral content in the top layer. After initial drainage of the area, land use has been arable for some time, until conditions became too wet to sustain large scale arable farms and the area was turned into pasture. Improved opportunities for drainage (i.e. windmills, mechanization) led to a further decrease in drainage base, followed by an increase in land subsidence. The area is currently 2 to 3 meters below sea surface level, and subsidence is ongoing.

In the area considered, fields are typically 50 m wide and 300 m long, and surrounded by ditches of which the water level is managed continuously. As such, ditch water levels are relatively constant, although winter and summer levels may differ. A typical problem in these sites is that, even though ditch water levels may be at e.g. 40 cm below the soil surface, groundwater levels in the middle of the parcels may drop to more than 1 m below soil surface during dry summer months, leaving a large part of the soil available for decomposition.

The field site considered is part of a long-term experimental site, at which measurements started already 50 years ago. A long-term experiment was set up in 1966 (van den Akker et al. 2021), consisting of a part with high ditch water levels (20 to 25 cm below soil surface) and a part with low ditch water levels (55 to 60 cm below soil surface). Soil subsidence has been monitored since then, showing initial subsidence rates of as much as 15 mm yr^{-1} in the parcels with low ditch water levels. Parcels with high ditch water levels had substantially lower subsidence rates. Subsidence rates have been decreasing over time, as the ditch water levels were not fully adapted to field surface lowering.

In 2016, subsurface drains were installed in some of the parcels to shorten travel pathways for water towards the middle of the parcel in order to maintain a more constant groundwater level throughout the field. During dry summer periods, these drains may infiltrate water to increase groundwater levels, whereas during wet winter periods these drains may drain water from the parcels, leading to a decrease in groundwater level. In this report, we describe and model the parcel shown in Figure 6.1 by the dashed line. The particular parcel has a reference part (RF), in which no drains were installed, and a part in which drains were installed (MP) using a drain spacing of 6 m, for which a target groundwater level of 50 cm below soil surface was prescribed. If groundwater levels fell below this target level, water was pumped into the drains via a reservoir to increase the gradient between the soil and drain and improve the infiltration of water.

Groundwater levels were monitored bi-weekly at 9 to 18 wells throughout the field from 2016 onwards (Figure 6.2). For both the reference and rewetted part, a small plot was fenced off for more intensive measurements starting in 2020, including CO_2 flux measurements with transparent automated chambers (Aben et al. 2024).

This project has received funding from the European Union's Horizon 2020 research and innovation programme under grant agreement N° 862695

Figure 6.1 Field site in proximity of Zegveld, The Netherlands (52.14 N, 4.84 E). The reference field (RF) and field with a target level of 50 cm below soil surface (MP) are situated on the same parcel (indicated by the dotted square). The field with a target level of 20 cm below soil surface (HW) is situated towards the east. Fenced-off areas can be seen in each of the parcels, with a size of approximately 10x20 m.

In 2022, an extra parcel was added to the monitoring network, in which a target level of 20 cm below surface was prescribed, using subsurface drains installed every 4 m. In this report, we show some results for this parcel as well, although this was not the main focus of the modelling.

6.2. Measurements

Manual groundwater level measurements used for model calibration were available from 2016 onwards. From 2020 and 2021 onwards (depending on the measurement), several continuous measurements were available. In addition, measurements of e.g. soil properties were used for the setup of the model. This data was obtained prior to the measurement period considered.

Soil description

Several borehole descriptions of the first 2 meters have been made across the field. The general soil buildup is given by an earthified top soil, of which the first ~30 cm are characterized as a clayey peat layer. This layer has the highest density and mineral content, due to the ongoing oxidation of the top peat layer, yet the organic matter content is still high with 30-35%. Due to the relatively high bulk density (0.6 g cm^{-3}), the carbon stock in this layer is significant. Moving down in the soil, the peat layer gradually becomes less degraded and bulk densities decrease to 0.15 g cm^{-3}. The peat itself consists mostly of woodland peat, in which tree trunks are common. This is alternated with some sedge peat, and occasionally some clayey layers. The aquifer starts at a depth of 6 to 7 m, and consists of a thick layer of sands.

Measurements of the soil water retention curve were available from three soil horizons in the RF, MP and HW plots. These were compared to the standard soil water retention dataset (Staringreeks; Heinen 2020). It was decided to use these common datasets as the locally determined parameters

This project has received funding from the European Union's Horizon 2020 research and innovation programme under grant agreement N° 862695

showed some variation but were within the same range as the commonly used parameter sets for this type of soil.

The saturated hydraulic conductivity has been measured by slug tests in the RF and MP plots, at 6 locations per plot. The mean hydraulic conductivity was 0.08 and 0.11 m d^{-1} for the reference and rewetted plot, respectively.

In addition to the aforementioned parameters, also measurements of pH, total carbon content and total nitrogen content were available for several depths. These measurements were used to parameterize the SWAP-ANIMO model and are shown in Figure 6.3.

Hydrology

The local hydrology is strongly determined by the ditches and, in case of the rewetted fields, the drains. Some exchange with the underlying aquifer occurs, but on a yearly-averaged basis this flux is near-neutral (Hendriks & van den Akker, 2012). There is no influence of any river systems.

The ditches surrounding the parcel have a rather constant water level of approximately 55 cm below field surface (Figure 6.2) for the RF and MP plots, and 20 cm below field surface for the HW plot. During extremely wet periods, open water levels may rise occasionally. With a parcel width of approximately 65 m, the ditches act as the primary drainage pathway, and during the summer, also some infiltration of water into the parcel occurs.

A secondary drainage pathway was installed in the rewetted fields (MP and HW) by means of drains, which were installed at a depth of 70 cm below soil surface and separated by 6 (MP) or 4 (HW) m. The level in the drains was controlled using a reservoir, of which the level could be set anywhere between 60 cm below field surface and slightly above field surface level. This way, the pressure inside the drains was regulated. A third drainage pathway was drainage through a trench in the middle of the parcel. Also surface runoff frequently occurs.

Measurements of the ditch water level, the level in the reservoir, and the average of the groundwater levels in the RF and MP fields are shown in Figure 6.2. Phreatic groundwater levels were monitored bi-weekly in 9 (RF) to 18 (MP) measuring wells located throughout the fields. Continuous measurements (logged every hour) on three locations in the fenced-off plot in the RF and MP fields were available from summer 2020 onwards. Automated measurements were adjusted to field-averaged values by a linear correction. Continuous measurements were also available for the HW field, starting in 2021. Based on the manual measurements, the mean groundwater level between 2016 and 2023 was 31 cm below field surface for the rewetted field (MP), compared to 36 cm below field surface for the reference field, which is an increase of only 5 cm. However, Figure 6.2 clearly shows that especially low groundwater levels, occurring in the warm summer season, were avoided in the rewetted field by raising the water level in the reservoir.

Continuous measurements of the aquifer head were available from 2022 onward and were measured in the HW field. The aquifer head showed a seasonal fluctuation, with an average head of 60 cm below soil surface and an amplitude of approximately 10 cm. We assumed the aquifer head does not differ between the fields, and shows the same general behaviour. However, as the field surface level of the RF and MP fields is approximately 10 cm lower, we assume a head of 50 cm below soil surface for these fields.

This project has received funding from the European Union's Horizon 2020 research and innovation programme under grant agreement N° 862695

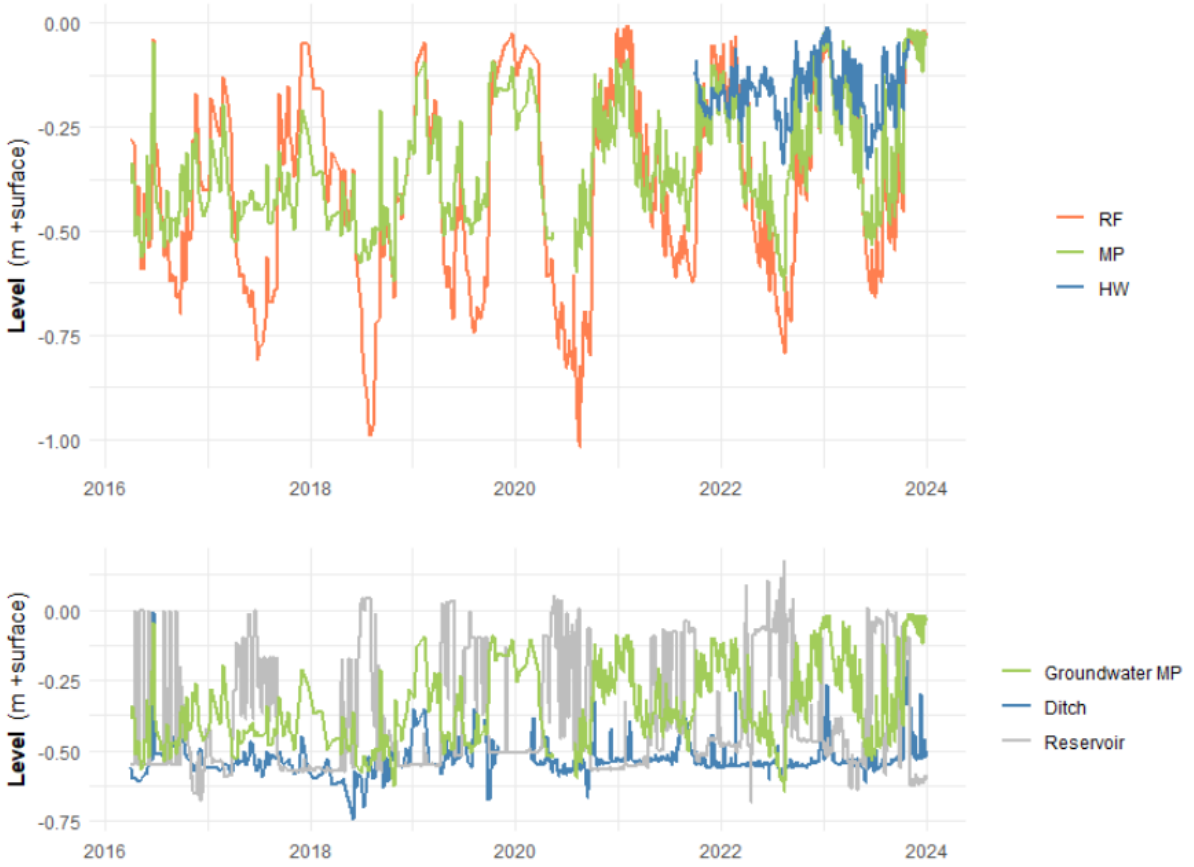

Figure 6.2 (A) Measured groundwater levels on the three parcels. From 2020 onwards, measurement frequency increased from bi-weekly to hourly. (B) Measured ditch water level of the ditches surrounding the RF and MP parcels and the measured level of the reservoir which is connected to the drains in the MP field. Also shown is the groundwater level fo the MP parcel.

NEE and meteorology

NEE (net ecosystem exchange) was measured from 2021 onwards with three automated chambers (AC) on the fenced-off plots in the RF and MP fields. These AC had a surface area of approximately 0.25 m^2, and closed every half an hour for approximately 3 minutes, during which changes in the CO_2 concentration in the chamber headspace were monitored. Chambers were rotated on in total 9 spots, such that each spot was occupied for approximately 1/3rd of the time to limit the effect of the chambers on e.g. grass growth or the water balance of that particular spot.

The flux data was partitioned and gapfilled based on the Lloyd-Taylor approach, combined with a light response curve, as outlined in Aben et al. (2024) for this site. All relevant meteorological conditions were measured on the RF field from 2020 onwards. From 2022 onwards, four AC were installed on the HW plot as well, which were slightly different from the type used in the other fields (Aben et al. 2024).

Field management

The site consists of intensively used grassland. The field is used for both grazing (cows) and mowing, but the fenced-off plots are only mowed. Mowing occurs typically once a month during the growing season, with 5-7 cuts per year starting in May. Yield was determined both within the AC and on the main part of the parcels (i.e. outside of the fenced-off plots).

This project has received funding from the European Union's Horizon 2020 research and innovation programme under grant agreement N° 862695

The fields are fertilized with a combination of manure and mineral fertilizer (200 – 250 kg N ha^{-1} yr^{-1}). Since 2020, the fenced-off plots are only fertilized with mineral fertilizer. However, remnants of manure may have affected the measured NEE in the plots, as soil carbon contents tend to decrease asymptotically from an equilibrium situation with manure application to a situation without manure application when application is terminated (e.g. Indraratne et al., 2009).

6.3. Simulation setup

SWAP model setup

A SWAP model simulation was set up based on the described data. We considered a soil column extending to 2 m below the soil surface. This column ends within the peat layer and misses approximately 4 m of this layer. As the bottom boundary condition is uncertain and we do not consider the formation of methane, this does not affect the simulation results.

Rainfall data was available from the KNMI location Zegveld, one km away from the field site. Other meteorological data was available from the site in De Bilt, situated approximately 20 km from the field site. This data was used for model simulations. Model initialization was based on the recorded weather from 1960 onwards.

The simulation period considered for this site spans from 2016-2023, of which especially the latter three years were of special interest due to the increased measurement availability. The starting date of 2016 was chosen as the subsurface drainage systems were installed in that year. Calibration of the model was based on measurements in the period January 2021 to December 2023. The model was first calibrated on the RF field, after which a calibration of the drainage resistance for the drains was performed for the MP and HW fields, leaving the other parameters as determined for the RF field.

Grass growth, gross primary production (GPP) and plant respiration were modelled in SWAP using the WOFOST-based grass module. With respect to the standard parameterization, we applied only one parameter adjustment based on a calibration with the 'measured' GPP, which was the relative management factor. This was set to 0.9 for RF, 0.88 for MP and 0.82 for HW. We did consider oxygen stress due to wet conditions, in contrast to the site Vejrumbro. The root zone thickness was estimated at 30 cm, with the majority of the roots in the upper 10 cm. We used prescribed mowing dates in SWAP following the actual mowing events whenever this information was available.

The description of the soil is given in Table 6.1. Based on a comparison with the measured soil water retention curves, the most appropriate top soil parameterization is B16 (0-35 cm-sl), followed by a subsoil O17 (35-200 cm-sl) for the more pristine peat layer below. We did not differentiate the description of the soil between the different treatments.

Table 6.1 Soil profile description as used in the SWAP-ANIMO model. Parameters listed include (in order of appearance) the residual water content ϑr, saturated water content ϑs, shape parameters (α, n, λ) and fitted saturated hydraulic conductivity based on the evaporation method, multiplied by 10 to include the effects of small macropores.

Depth	Staring nr.	Formal description	θ_r	θ_s	α	n	λ	Ksat
cm-sl	-	-	$cm^3\ cm^{-3}$	$cm^3\ cm^{-3}$	cm^{-1}	-	-	$cm\ d^{-1}$
0-35	B17	Peaty clay	0.0	0.719	0.019	1.14	0.0001	44.8
35-200	O17	Eutrophic peat	0.01	0.849	0.012	1.27	-1.25	34.0

This project has received funding from the European Union's Horizon 2020 research and innovation programme under grant agreement N° 862695

Hydrological boundary conditions on the sides and bottom of the SWAP column were described by two or three drainage systems (sides) and an aquifer head (bottom). Several combinations of drainage system - and bottom flux parameters were explored, based on the information described in section 6.2.

The bottom boundary condition was given by a fluctuating aquifer head at the bottom of the SWAP column based on a sine signal, with a mean of 50 cm below soil surface (60 cm for HW) and an amplitude of 10 cm. The maximum head was reached at the start of February each year. Based on calibration, a resistance of 1500 days was applied (excluding flow resistance in the soil column itself), which is also in agreement with values generally found in this area (Hendriks & van den Akker, 2012).

The drainage systems were defined by three levels: the first level represents the ditches, the second level represents the drains (if applicable) and the third level represents a shallow superficial drainage system towards the trenches, which accounts for some shallow interflow processes. Surface runoff may occur as well. The characteristics of the drainage systems are given in Table 6.2. Water levels were prescribed using the observations given in Figure 6.2 for the period available, and interpolated linearly if applicable. For the ditch, a constant water level of 55 cm below soil surface was assumed. For the reservoir, the levels were based on the modelled groundwater level in the RF field, using the following criteria, which reflect the current operation of the reservoir level (Figure 6.2):

- For MP: if the modelled groundwater level was deeper than 40 cm below soil surface, the reservoir was set to field surface. If the modelled groundwater level was shallower, the reservoir was set to 60 cm below soil surface.
- For HW: if the modelled groundwater level was deeper than 18 cm below soil surface, the reservoir was set to 20 cm above field surface. If the modelled groundwater level was shallower, the reservoir was set to 30 cm below soil surface.

Table 6.2 Drainage system characteristics used in modelling of the Zegveld site. The drainage resistance differs between the two sites due to the lower distance between the drains in the field with a target level of 20 cm (HW).

	Drainage resistance (d)	Infiltration resistance (d)	Depth (cm-sl)	Spacing (m)
Ditches	700	500	-90	63
Drains MP	400	300	-70	6
Drains HW	300	300	-70	4
Trench	50	-	-5	12

ANIMO model setup

An overview of the soil composition as measured and as used for model input is given in Figure 6.3. A gradual shift from degraded to more pristine peat is visible in dry bulk density and LOI. Despite a lower organic matter percentage in the top soil, the carbon content expressed as mass per volume is higher in the top soil compared to the subsoil due to its high density. The pH in the topsoil is somewhat lower compared to the subsoil. A pH below 6 has a limiting effect on the decomposition of organic material in the model, hence this is expected to play a role in Zegveld. The C/N ratio is slightly higher in the model after the initialization runs compared to the measurements. However, alternative measurements (Gross-Schmoelders et al. 2024) suggest somewhat higher C/N ratios for the Zegveld fields. Also, these higher C/N ratios are required to obtain a better fit between measured and modelled ammonia and nitrate concentrations in the pore water (results not shown).

An overview of the partitioning of the sources of organic matter at the start of the simulation period following the initialization runs is shown in Figure 6.4. Fresh organic material is present in the root zone, which is the resultant of added shoot and root material. Also humus, remaining from the

This project has received funding from the European Union's Horizon 2020 research and innovation programme under grant agreement N° 862695

decomposition of fresh organic material, is present. The amount of recently decayed organic material is substantially lower compared to the simulations in Vejrumbro, as grasses are harvested and removed from the soil, in contrast to the land management in Vejrumbro.

Figure 6.4 B also shows the soil respiration rate obtained after the initialization runs, excluding the influence of DOM. Also measurements of the soil respiration rate are shown. These measurements were performed in lab experiments in disturbed samples, and were obtained within several days after taking the samples. They were incubated at 20°C. As the baseline temperature in ANIMO is 10°C, they were translated to this temperature using a Q_{10} value which is also input to the ANIMO model. As the samples were disturbed, exposure of organic material was enhanced with respect to the field situation. As ANIMO requires respiration rates under field conditions, the model input should be lower compared to the measurements shown. The influence of temperature on the respiration rate was not measured in this study, but previous measurements in Zegveld (Hendriks, 1991) show an increasing value of Q_{10} with depth of 1.8 for the upper soil layer to 2.7 for a depth of 30 cm. Other measurements suggest further increasing values with depth (Vermeulen & Hendriks, 1996). An overview of the values used is provided in Table 6.3.

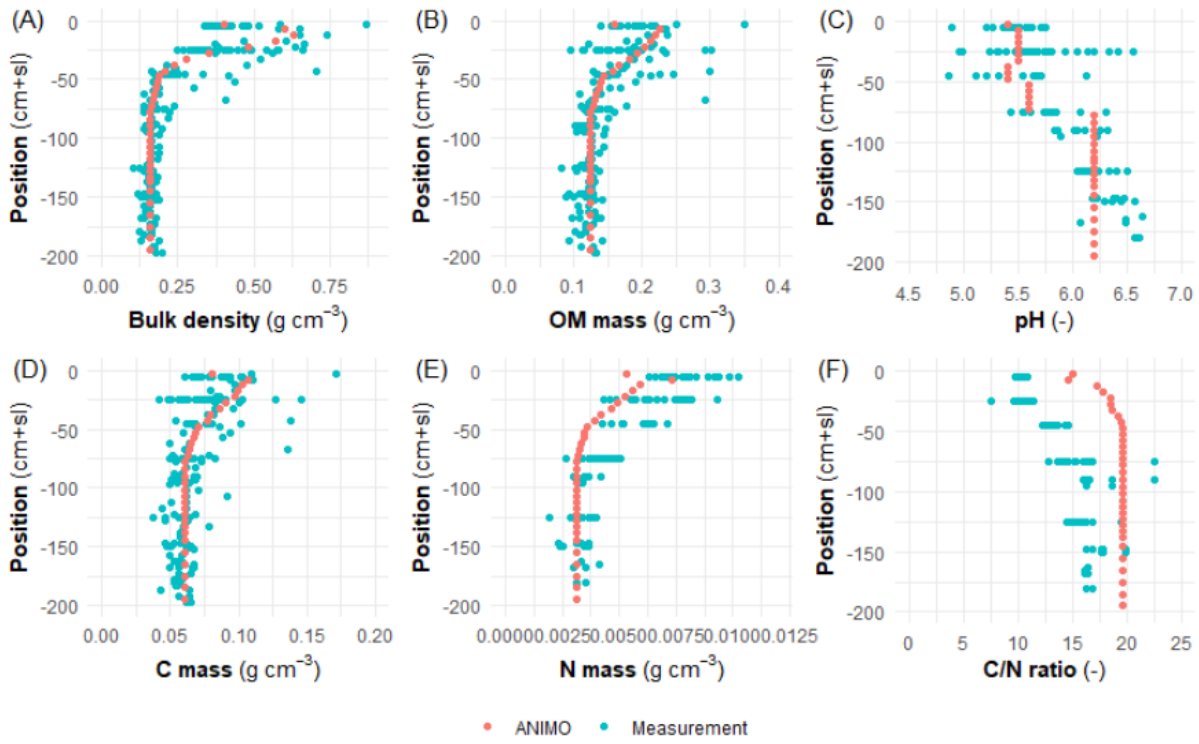

Figure 6.3 Measurements (blue) and model input after initialization runs (red) for Zegveld of dry bulk density (A), OM mass (B), pH (C), carbon mass (D), nitrogen mass (E) and C/N ratio (F), as function of depth. Measurements show the data from all three parcels combined

This project has received funding from the European Union's Horizon 2020 research and innovation programme under grant agreement N° 862695

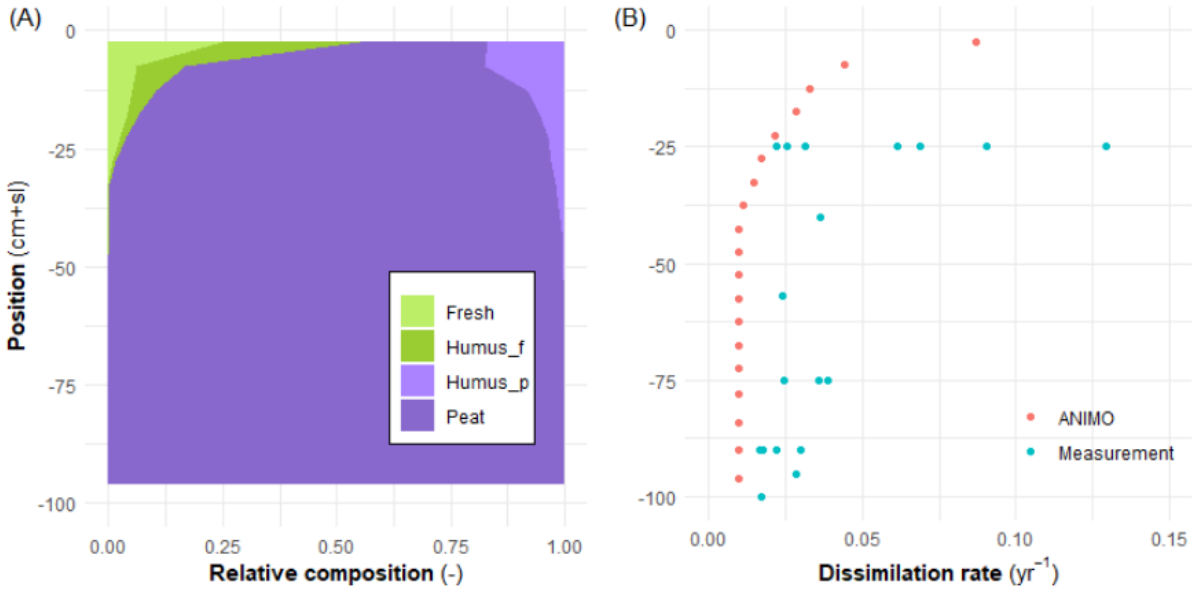

Figure 6.4 (A) Partitioning between fresh and peat (derived) materials at the start of the simulation in Zegveld, resulting from the initialization runs and (B) corresponding dissimilation rate (excluding DOM) at optimal conditions and 10 °C as function of depth in the soil.

Table 6.3 Overview of input parameters on the temperature sensitivity (Q_{10}) and gas diffusion parameters p_1 and p_2. The latter are distinguished per field, as the more deeply drained field have more developed macropores.

Depth	Q_{10}	p_1			p_2		
		RF	MP	HW	RF	MP	HW
0-5	2.3	0.5	0.1	0.1	1.25	1.25	1.25
5-20	2.6	0.5	0.1	0.1	1.25	1.4	1.4
20-35	3.1	0.4	0.08	0.06	1.3	1.8	1.6
35-75	3.5	0.5	0.5	0.5	2.5	2.5	2.5
75-200	3.4	0.5	0.5	0.5	2.5	2.5	2.5

This project has received funding from the European Union's Horizon 2020 research and innovation programme under grant agreement N° 862695

6.4.Scenario definitions

Recently, the Dutch meteorological insitute (KNMI) has published new climate scenarios for The Netherlands (van der Wiel et al., 2024). The shared socioeconomic pathways (SSPs) form the basis of the GHG concentrations underlying the climate scenarios.

In this study, we make use of the SSP1-2.6 and SSP5-8.5 pathways, which are referred to as the low (L) and high (H) emission scenarios, respectively. Based on outcomes of a number of climate models, a selection was made (van der Wiel et al., 2024) with models with a wetting trend (n) on the one hand, and a drying trend (d) on the other hand, resulting in the four future scenario combinations (Ld, Ln, Hd, Hn) considered in this study. The wetting trend expresses itself mainly in increased winter precipitation sums, combined with slightly decreasing summer precipitation sums, whereas for the drying trend the overal precipitation sums decrease, especially during summer.

Along with these climate scenario's, daily weather records were generated using the downscaled simulations of one climate model which were resampled to obtain the correct trends. Weather records were published for the 30 year climatic reference period (1990-2020) as well as for the future scenario combinations. Here, we make use of the 30-year outlook period centered around 2050 and the outlook period centered around 2100. For the low SSP scenario, generated weather records are only available for the period centered around 2100, as these were not significantly different from those around 2050. Therefore, the results of Ld and Ln are not differentiated between these two outlook periods.

For each period and combination for which weather data was generated, an 8-member ensemble was produced, such that 8 realizations were available. We split each member into three 10-year periods (therefore obtaining 24 10-year periods per scenario combination), for which we ran the SWAP-ANIMO model for each of the three fields individually, each time using the same initial conditions as defined by the prerun of the RF field. We do, therefore, not account for any changes in e.g. peat composition over the period considered. The SWAP-ANIMO model was run for the reference parcel as well as the two parcels with water infiltration systems, using parameter combinations obtained with the calibrated model of the current situation.

6.5. Base simulation results

Hydrology

Groundwater levels simulated by SWAP-ANIMO show the general trends as observed in the different parcels quite well (Figure 6.5), even though generally the RMSE and MAE is around 10 cm.

For the reference plot, the model tends to drain water from the field somewhat too fast when compared to the continuous measurement period, yet comparing to the period with manual measurements (which are more evenly distributed across the field), the model performs very well. In the extremely dry summer of 2018, minimum groundwater levels are somewhat underestimated by the model. In times of shallow groundwater conditions, the model shows a rather peaky behaviour in groundwater levels, which, according to the measurements, is not the case. However, as during these times the top soil is very wet anyway, this has limited consequences for further modelling with ANIMO.

In the parcel with subsurface irrigation drains with a target level of 50 cm below soil surface (MP), the measurements show that the level rarely drops below 60 cm, not even during the dry summer of 2018. The model captures this behaviour very well. Again, as with the reference field, we see a

This project has received funding from the European Union's Horizon 2020 research and innovation programme under grant agreement N° 862695

somewhat peaky behaviour during times of shallow groundwater levels. This is even more so for the HW parcel. Despite not having the actual data on operation of the reservoir for this field, it seems that it is well approximated using the methodology outlined in section 6.3.

An overview of the monthly modelled water balance terms is given in Figure 6.6. In the reference field, the net water supply over the three year period shown originates from precipitation (939 mm yr^{-1}) only. The majority of water is removed from the parcel via evapotranspiration (48%). Subsurface drainage to the ditch (10%) and trench (12%) and surface runoff towards the ditch (27%) account for most of the remaining water. Downward seepage accounts for 4%, which amounts to a small downward seepage rate of 0.1 mm d^{-1}. Considering daily fluxes, some infiltration of water occurs from the ditches into the parcels during periods of deep groundwater levels. This amounts to 23 mm yr^{-1}in the period 2021-2023. This is opposed by a drainage flux of 115 mm yr^{-1}.

In the MP field, the water balance is strongly affected by the presence of the drains. The net water supply over this three year period still only originates from rainfall. Yet, surface runoff removes less water from the parcel (22%), while drainage accounts for a larger percentage (25%), indicative of less occurrence of very shallow groundwater levels. The bottom flux is slightly increased, accounting for 5% of the net water removal due to the, on average, elevated groundwater levels. Again considering the daily fluxes, the ditch now no longer acts as a supply pathway during any part of the year (for the period 2021-2023). It now drains 121 mm yr^{-1}. The drains, however, also discharge 126 mm yr^{-1}, mainly during the winter season. Yet, they also infiltrate 102 mm yr^{-1} during the summer season, resulting in a net drainage rate of 24 mm yr^{-1}. This illustrates that they are quite efficient in maintaining a more constant groundwater level within the field. Yet, they do have implications for the surface water management: they require water supply in summer, and elevate water discharge amounts during winter.

In the HW parcel, the effect of the drains is even more pronounced, while also the higher ditchwater level plays a role. In contrast to the other parcels, net water supply over the three year period originates from rainfall and from the subsurface infiltration system. To be able to compare the percentages with the other parcels, we still compare the fluxes to the rainfall supply. For the HW field, surface runoff accounts for 37% of the rainwater removal, and evapotranspiration is slightly reduced (45%) due to a reduction in transpiration rates due to poorer grass growth. The combined drainage pathways account for only 6% of the net water removal, and the bottom flux is increased significantly, now contributing to 12% of the water removal, in correspondence with the lower head in the aquifer compared to the raised groundwater levels in the field. Considering drainage fluxes in more detail, the ditches now infiltrate 5 mm yr^{-1} and drain 51 mm yr^{-1}over the 2021-2023 period, which is much less than in the MP field due to the higher surface water levels. The drains only drain 60 mm yr^{-1} and infiltrate 212 mm yr^{-1}, such that they are indeed a net source of water in this parcel. However, drainage by the trench (163 mm yr^{-1}) makes that the combination of all defined drainage measures is still removal of water.

Concluding, the effectiveness of the subsurface infiltration drains strongly depends on the target level employed, as well as on the ditch water levels surrounding the parcel. It is likely that, with large-scale implementation of such systems, also the aquifer underlaying the parcels will be affected by the increased phreatic groundwater levels, resulting in less seepage losses.

This project has received funding from the European Union's Horizon 2020 research and innovation programme under grant agreement N° 862695

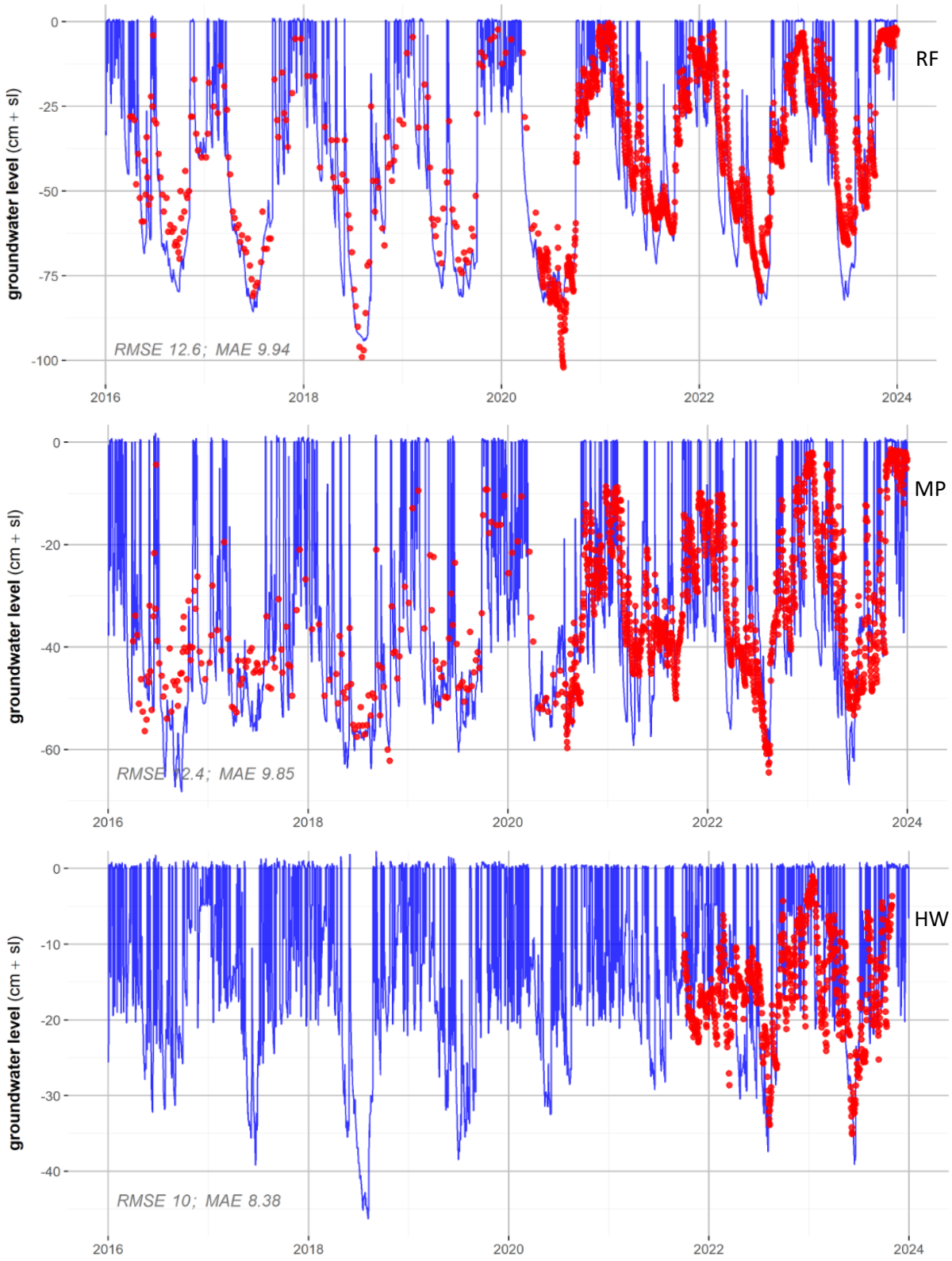

Figure 6.5 Measured (red dots) and modelled (blue line) phreatic groundwater levels in Zegveld, for the RF, MP and HW parcels, respectively. The root mean squared error (RMSE) and mean absolute error (MAE) of the simulations compared to the measurements is indicated in each plot.

This project has received funding from the European Union's Horizon 2020 research and innovation programme under grant agreement N° 862695

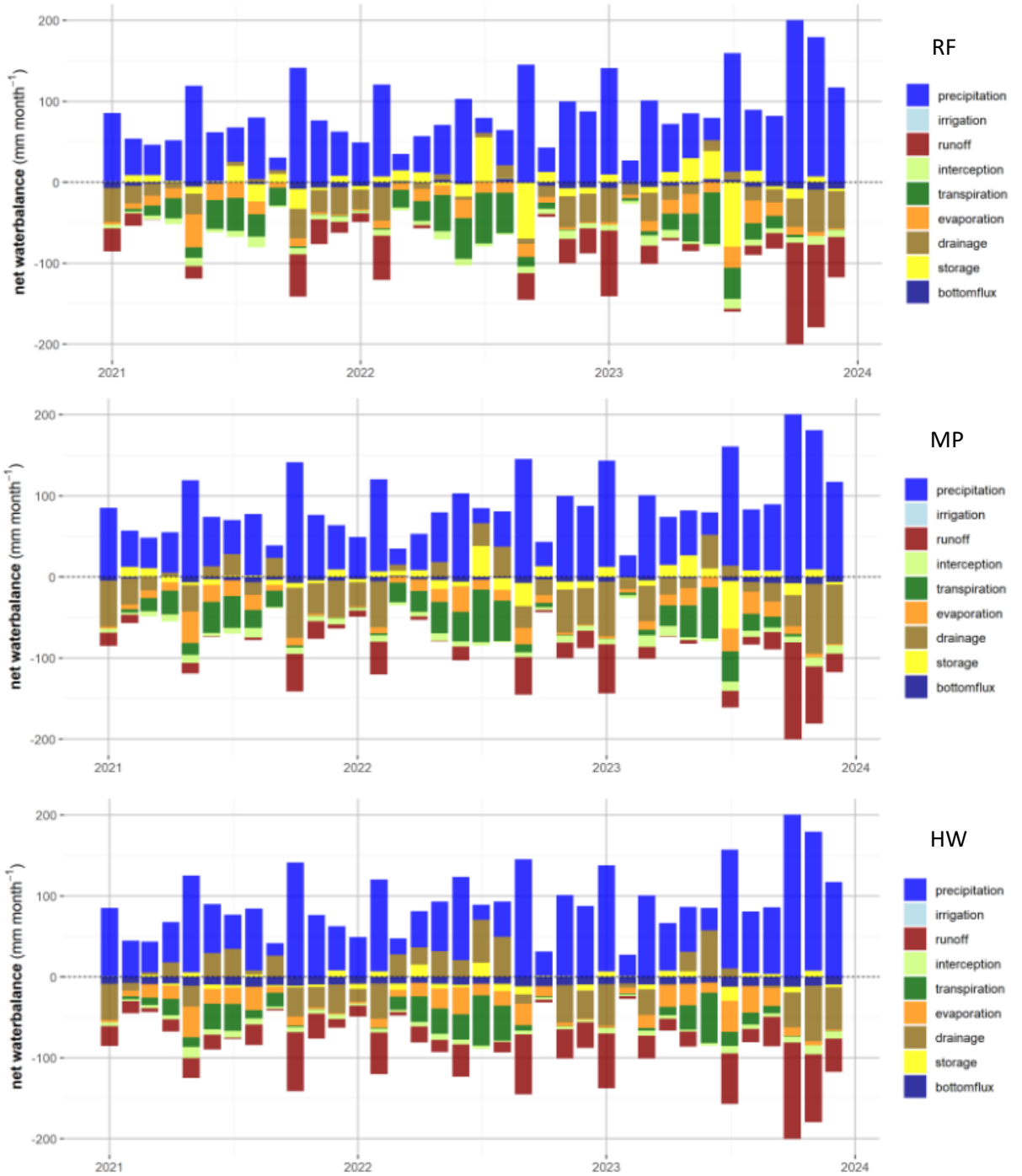

Figure 6.6 Modelled monthly water balance terms from 2021 to 2023 in Zegveld, showing fields RF, MP and HW, respectively. Positive terms describe water supply towards the soil and canopy, negative terms describe removal from the soil and canopy.

This project has received funding from the European Union's Horizon 2020 research and innovation programme under grant agreement N° 862695

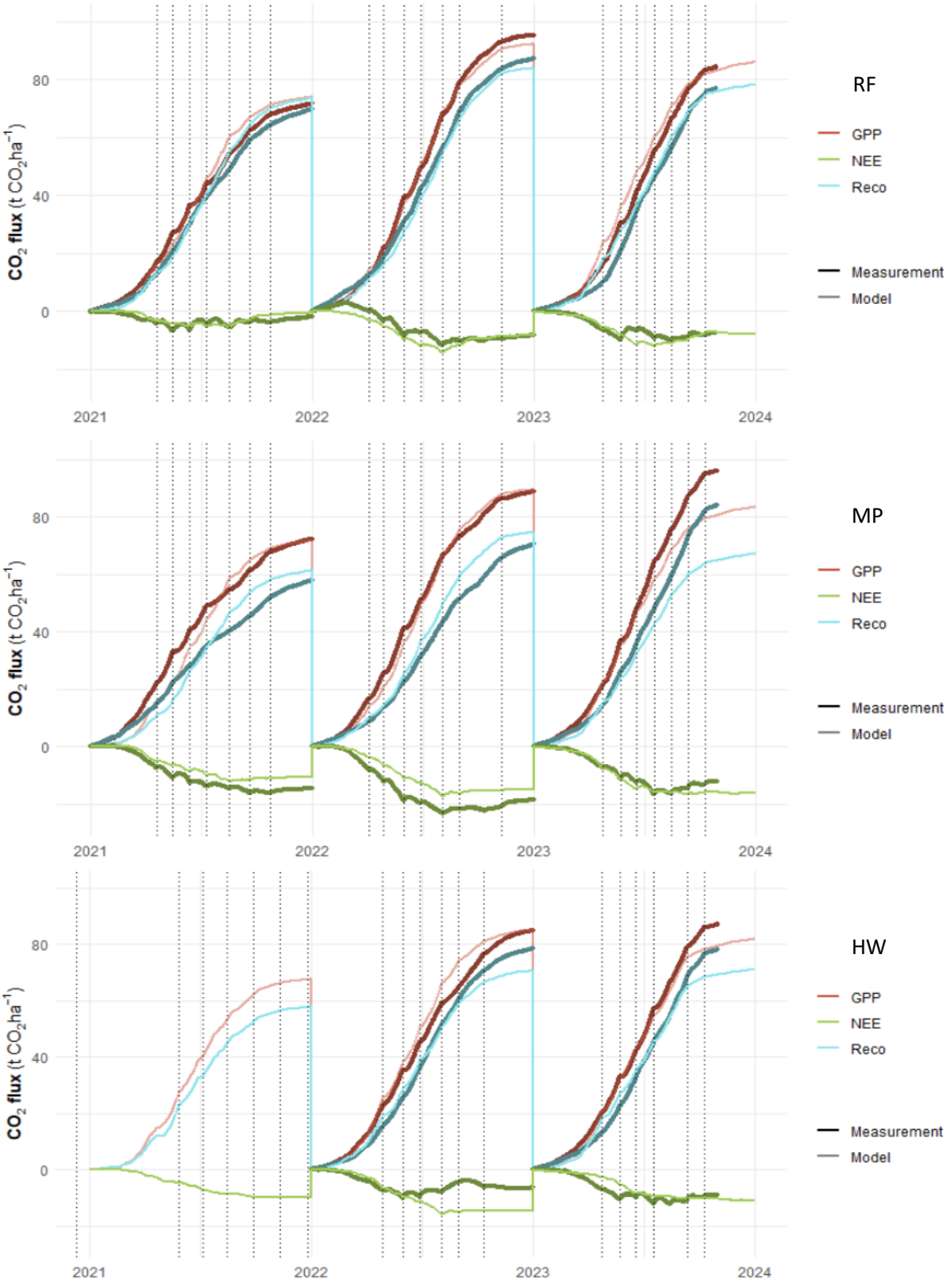

Figure 6.7 Cumulative measured (dark colors) and modelled (light colors) NEE, GPP and Reco for RF, MP and HW parcels, respectively. NEE was measured by AC and gapfilled, GPP and Reco 'measurements' were obtained by partitioning half-hourly gap-filled AC fluxes. Modelled lines were obtained with SWAP-ANIMO. The dotted vertical lines indicate harvest moments. Measurements end at the end of October, 2023. For HW, no measurements are available in 2021.

This project has received funding from the European Union's Horizon 2020 research and innovation programme under grant agreement N° 862695

CO_2 fluxes

The yearly cumulative modelled and measured net ecosystem exchange (NEE), gross primary production (GPP) and ecosystem respiration (Reco) are shown in Figure 6.7 for the three parcels. NEE is mostly negative (i.e. a net uptake of CO_2) for all years, and clearly is more negative for the MP parcel compared with the RF parcel. In the HW parcel, the measured NEE tends to be somewhat less negative compared to the MP field, which coincides with a reduced harvest amount. The largest net uptake occurs in spring and early summer, while the NEE is near neutral in the remainder of the year.

In general, seasonal patterns are well-captured by the model. Also the effects of harvest events are clearly distinguishable in both the model and measurements. Immediately following such an event, a net emission tends to occur which lasts for a few days, as a consequence of a lack of green leaf area and limited photosynthesis rate.

A few discrepancies between the model and measurements should be highlighted.

- The onset of growth following the winter period in 2021 seems to be later in the model compared to the measurements. Yet, in terms of the net flux (NEE), both the model and measurements suggest that this is around zero. Hence, this only influences cumulative GPP and Reco.
- In both 2021 and 2022, at some point in time the measurements suggest a reduction in both GPP and Reco occurs in the MP parcel during summer. This reduction is not modelled at all, and it is unclear what caused this reduction. A similar reduction in measured GPP is found in the HW parcel in 2022.
- In all three parcels, the measurements indicate that the onset of photosynthesis was late following the second cut in 2023. Grass height measurements indicate that grass was cut rather short at a height of 5 cm on average, rather than 7 cm on most of the other mowing moments, which may be the cause for this delay in onset.
- In 2023, the measurements suggest an exceptionally high photosynthesis - and respiration rate in the second half of summer in the MP and (to a lesser extent) HW parcel. This high photosynthesis is not reflected in an exceptionally high yield (Table 6.4) and therefore seems to be unlikely, especially for the MP parcel.
- NEE is modelled rather well for the RF parcel. For the MP parcel, modelled NEE is too high (i.e. not as negative as measured) in 2021 and 2022, whereas for the HW parcel, modelled NEE is too low in 2022.

A comparison of modelled and measured daily GPP and Reco rates in the RF parcel shows that no systematic bias exists (Figure 6.8), although substantial scatter is found. Similar results were obtained for the other parcels. We use Lin's Concordance Correlation Coefficient (CCC) as a measure to determine both the accuracy and precision of all the datapoints with respect to the 1:1 line. A perfect fit yields a value of 1, whereas no relation at all yields a value of 0, similar to Pearsons correlation coefficient. The obtained CCC for the modelled GPP and Reco are 0.764 and 0.734, respectively, for the RF parcel, 0.709 and 0.620 for the MP parcel and 0.743 and 0.670 for the HW parcel.

This project has received funding from the European Union's Horizon 2020 research and innovation programme under grant agreement N° 862695

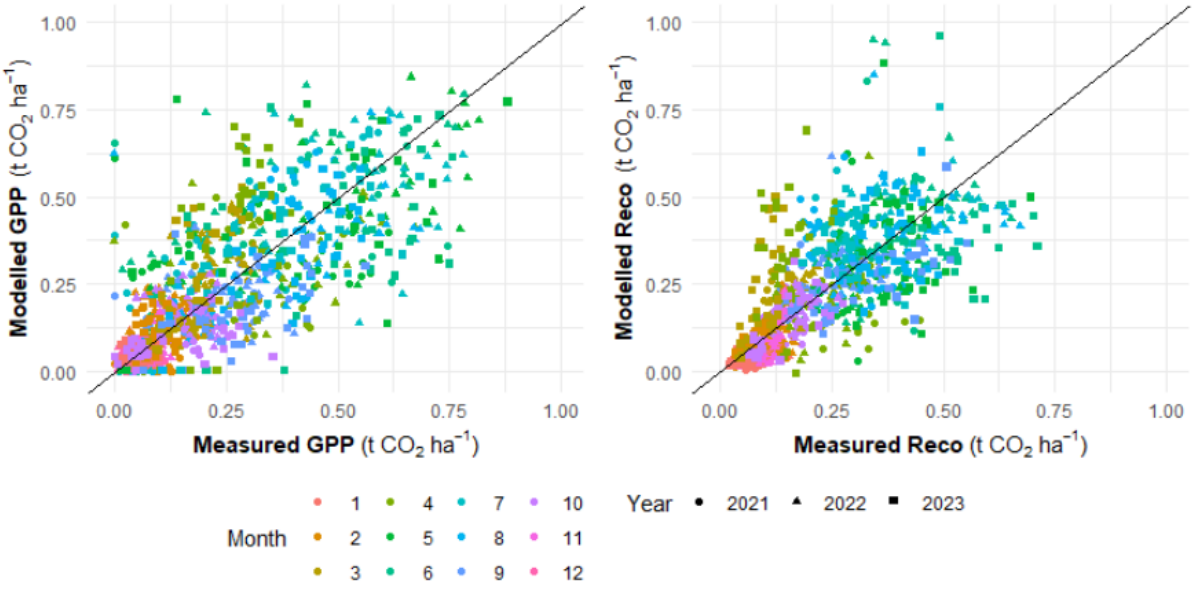

Figure 6.8 Relation between daily modelled and daily measured GPP (left side) and daily modelled and daily measured Reco (right side) for the reference parcel in Zegveld. Colors indicate the month of the year, symbol shapes denote the year. The line indicates a 1 :1 relation.

We obtained year budgets over the measured period from January 2021 to December 2023 (Table 6.4). The measured fluxes for the year 2023 were obtained using the period November 2022 to October 2023, as data for the last two months of 2023 was not available. Modelled budgets were obtained for each year individually.

The measured yield inside the chambers in 2021 in both the MP and RF parcels seems to be unrealistically high with about 19 t dry matter (DM) ha^{-1} yr^{-1}, especially when compared with the relatively low GPP in this year in both parcels. The measured yield would indicate that 45% of the estimated GPP was harvested, as compared to a fraction of only 0.2 to 0.3 for the other years and also obtained from the model results. Also, yield estimates obtained outside the chambers in the main part of the parcel (i.e. the part which was not fenced off) do not support these exceptionally high yields in 2021. This high yield also influences the measured NECB for this year, which exceeds the measured NECBs of the other years by 10 t CO_2 ha^{-1} (leading to a doubling of the NECB compared to the other years). Finally, the drying of grass was done at a different site in 2021 and the first two cuts in 2022 compared to the rest of the measurements, and there are indications that the dried grasses still contained some moisture. This would then result in higher estimates of the DM production. We therefore deem these measurements unlikely and consider the measured NECBs for this year to be too high.

Neglecting the yields in 2021, modelled yields tend to be somewhat higher than measured, despite the GPP being well-represented. This may result from several factors. First, the measured yield was obtained based on a relatively small sample area (i.e. the inner circle of the AC) for each chamber on only one of the three locations on which chambers rotated. As the presence of chambers likely influences grass growth through alterations on e.g. humidity, temperature, wind speed and soil moisture conditions, harvest of only one of the three locations may result in under – or overestimations of grass yields. As such, the harvest is likely not representative for the entire parcel. Furthermore, there was a quite large spread between the measured harvest for each individual chamber (i.e. amounting to a standard deviation of 2 – 3 t CO_2 ha^{-1} yr^{-1}). Second, we did not adapt any grass growth parameters other than the management factor. As such, we did not alter the

This project has received funding from the European Union's Horizon 2020 research and innovation programme under grant agreement N° 862695

partitioning of carbohydrates between plant components, which may actually be different for the specific site. Third, we did not consider any losses of grass during harvest.

Taking the above into consideration, the modelled and measured NECBs are generally well represented by the model. Interestingly, the modelled peat oxidation is, in all cases, slightly lower than the NECB. Apart from year-to-year imbalances in the NECB (i.e. pools which are not in equilibrium over a one-year period), also remnants of manure continue to contribute to the modelled ecosystem respiration, even after a few years (Figure 6.9).

*Table 6.4 Measured and modelled yearly average groundwater level (GWL; in cm+sl) and cumulative CO_2 flux terms (all in t CO_2 ha^{-1}; positive to the atmosphere) for the RF, MP and HW parcels in Zegveld. The period considered for 2023 lasts from November 2022 to October 2023. Harvest was calculated as dry matter yield * carbon fraction * 44/12, with an assumed fraction of 0.45. DOM considers net transport to surface water via runoff and drainage, excluding net transport via the bottom boundary of the model. DOM was not measured. The column 'peat' denotes the modelled decomposition of peat and its derived products, including the net transport via DOM. A '-' indicates the value was not measured. Measurements indicated with an asterisk (*) seem unrealistic.*

Year	Dataset	GWL	GPP	Reco	NEE	Yield	DOM	NECB	Peat
RF									
2021	Measured	-33.0	-71.6	69.9	-1.7	32.2*	-	30.5*	-
	Modelled	-31.9	-74.0	73.6	-0.4	21.0	+0.8	21.4	16.5
2022	Measured	-39.2	-95.2	87.1	-8.1	25.1	-	17.0	-
	Modelled	-40.1	-92.3	84.0	-8.3	30.1	+0.6	22.4	20.2
2023	Measured	-27.8	-87.7	81.6	-6.1	20.7	-	14.5	-
	Modelled	-28.9	-86.1	78.3	-7.8	23.1	+0.9	16.2	15.0
MP									
2021	Measured	-29.9	-72.2	57.9	-14.3	32.8*	-	18.5*	-
	Modelled	-31.0	-71.9	61.5	-10.4	21.2	+1.7	12.5	9.3
2022	Measured	-32.2	-88.7	70.4	-18.3	26.5	-	8.2	-
	Modelled	-31.1	-89.5	74.6	-14.9	26.5	+1.3	12.9	11.1
2023	Measured	-24.0	-99.5	90.2	-9.22	18.9	-	9.7	-
	Modelled	-27.2	-83.5	67.3	-16.2	24.3	+2.0	10.0	9.5
HW									
2021	Measured	-	-	-	-	-	-	-	-
	Modelled	-11.2	67.7	57.9	-9.9	14.9	+1.7	6.7	
2022	Measured	-15.0	84.8	78.5	-6.3	13.5	-	7.2	
	Modelled	-13.4	85.2	70.8	-14.5	20.8	+1.3	7.6	6.5
2023	Measured	-15.0	92.4	82.9	-9.5	15.1	-	5.7	
	Modelled	-10.4	81.9	71.1	-10.8	14.4	+1.7	5.3	4.4

This project has received funding from the European Union's Horizon 2020 research and innovation programme under grant agreement N° 862695

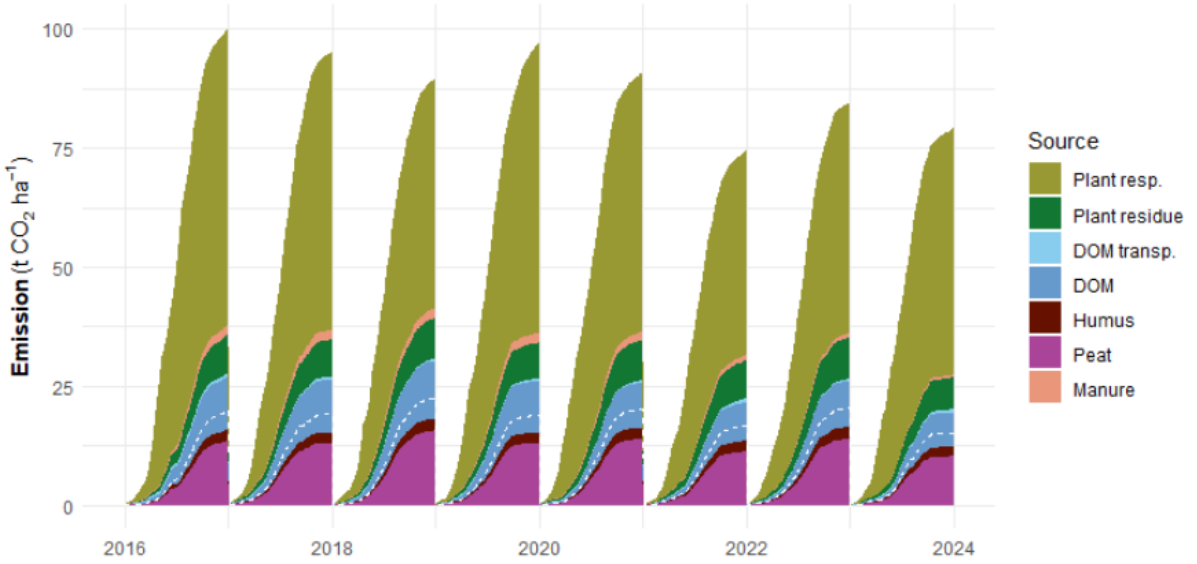

Figure 6.9 Contribution of the different terms to the yearly cumulative CO_2 emission from 2016 to the end of 2023 for the reference parcel in Zegveld, excluding emission due to harvest and uptake due to photosynthesis. The terms displayed involve plant respiration (direct plant respiration due to growth, maintenance and suboptimal conditions), plant residue (breakdown of recently died off plant material), dissolved organic matter (DOM) transport (net transport of DOM to surface water via runoff and drainage), DOM (breakdown of DOM within the soil), humus (breakdown of humus within the soil), manure and peat (breakdown of peat within the soil). The white dashed line indicates the sum of the direct and indirect contribution of peat to the CO_2 emission, which involves the entire term of peat, and a part of the humus, DOM and DOM transport terms.

An overview of the contributions of the different terms to the yearly cumulative CO_2 emission is given in Figure 6.9. The figure displays the terms involved in Reco plus the net loss of CO_2 due to transport to surface waters. Harvest is not shown. As with the other modelled sites, the largest contributor to the CO_2 emission is direct plant respiration, accounting for over 60% of the total emissions. The majority of the emissions originating from the soil itself is due to the breakdown of peat and peat-derived products. There are significantly less plant residues compared to the situation in Vejrumbro, as these residues are harvested. The majority of the plant residues in Figure 6.9 stems from the breakdown of roots. Breakdown of manure accounts for a few tons of CO_2 emission per year. Manure application stopped in 2020, leading to a gradually declining contribution of this source for the following years. Yet, in 2023, manure residues still contribute to the carbon budget.

Year to year variation in carbon sources contributing to the emission is especially large for the plant respiration term, which is directly related to the growth of grass. This, in turn, strongly depends on the growing conditions such as incoming solar radiation, soil moisture and temperature. Comparing the (extremely dry) year 2018 with 2019, it is clear that the total modelled ecosystem respiration (Reco) is higher in 2019 than 2018, yet the soil respiration is higher in 2018 compared to 2019.

This project has received funding from the European Union's Horizon 2020 research and innovation programme under grant agreement N° 862695

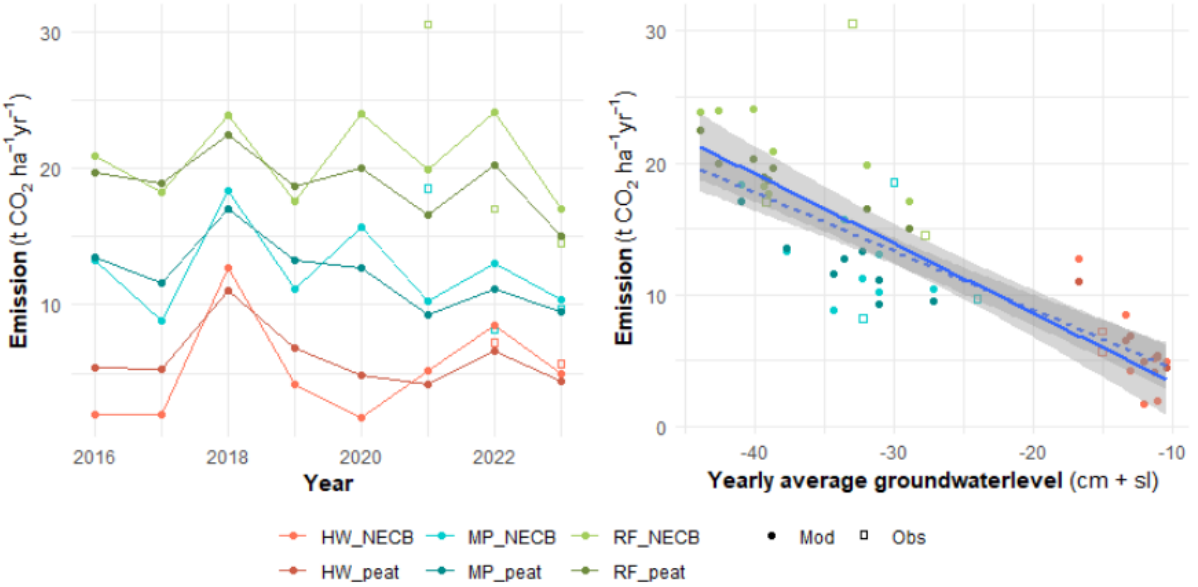

Figure 6.10 Yearly modelled NECB (light) and oxidation related to peat decomposition (dark) for the three parcels in Zegveld, as function of time (left panel) and as function of modelled groundwater level (right panel). Measurements of the NECB (excluding the contribution of DOM) are given by open squares. The lines in the right panel give a linear model fit to the data points for the NECB (solid line) and peat (dashed line) emissions, including uncertainty bounds in the model fit (grey shaded).

An overview of the modelled emissions is given in Figure 6.10, where emissions are plotted both as NECB and as oxidation of peat (and its derived products). Once again, we see a clear difference between the three parcels, with the highest emissions from the drained RF parcel, and the lowest emission from the parcel with a target groundwater level of 20 cm below soil surface. Do note that the measurements in the year 2021 clearly stand out from the other measurements and modelled data, as discussed. The modelled NECB shows a larger year-to-year variation compared to the modelled peat oxidation. This is a consequence of the nature of the different carbon pools. Where peat is not added to the soil and therefore this pools only reduces over time, the size of other pools (i.e. remnants of roots) is subject to changes in both in- and output of C. Combined with the higher decomposition rate of these pools, they show a larger fluctuation, and are not in equilibrium on a year-to-year basis. This illustrates the need to monitor the NECB for a few years, to capture the effects of these imbalances. It can also be seen that in the years 2020 – 2023, the NECB tends to exceed the modelled peat oxidation; a consequence of the contribution of manure to the NECB. For the HW parcel, the NECB tends to be somewhat lower than the modelled peat oxidation. This is related to the fact that we use the same initial conditions in 2016 for all three parcels, based on the reference situation. As the groundwater levels are suddenly very different from this initial situation, an imbalance exists in the different pools.

Plotting the emissions as function of the yearly average groundwater level (Figure 6.10 B) clearly shows decreasing CO_2 emissions with shallower groundwater levels. The linear model fits for this relation obtained for the modelled NECB and peat oxidation are not significantly different for the two metrics. The fits are given by

$$NECB = -0.53\, GWL_a - 1.9 \qquad (r^2 = 0.77)$$
$$R_{peat} = -0.44\, GWL_a - 0.02 \qquad (r^2 = 0.84).$$

For all Dutch NOBV sites (including Zegveld) in combination, also a relation was found (Aben et al. 2024) between the measured NECB using AC and the annual groundwater table depth, which was given by

This project has received funding from the European Union's Horizon 2020 research and innovation programme under grant agreement N° 862695

$$NECB = -0.31\, GWL_a + 0.2.$$

The relation based on model results is therefore somewhat steeper compared to the one based on measurements. Do note that these measurements stem from 2020 to 2023, with the majority of sites only contributing in 2022 and 2023 – which are relatively low in emission, at least for Zegveld (Figure 6.10).

6.6. Scenario simulation results

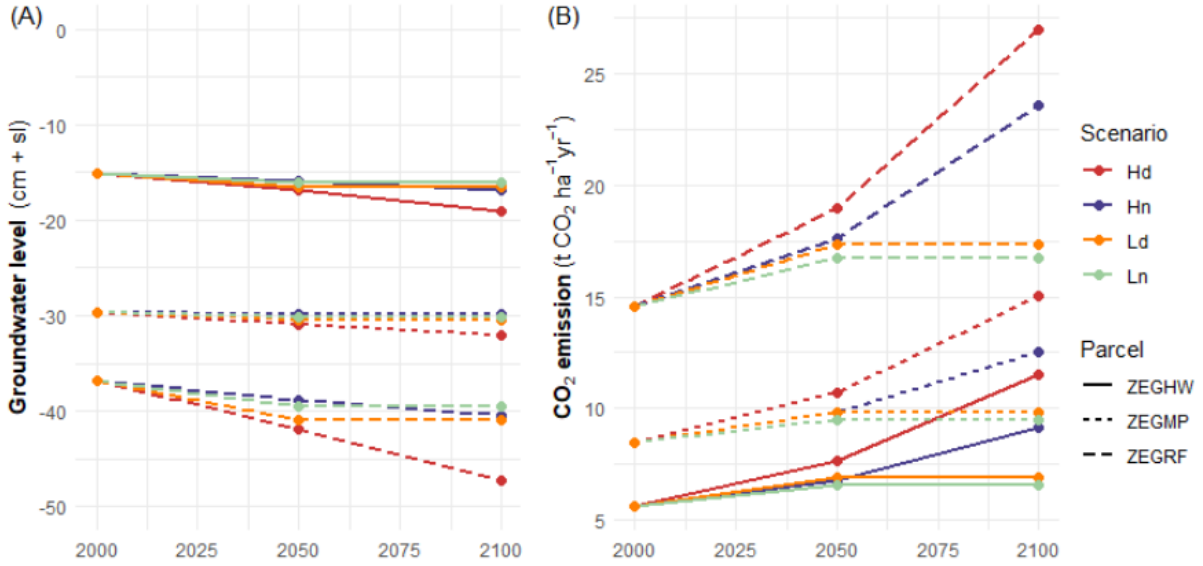

Figure 6.11 Average modelled groundwater level (A) and CO_2 emission related to peat oxidation (B) for the three parcels and four climate scenarios for each 30-year climatic period. The reference periods are identical for all climate scenarios, and also the climate does not change between 2050 and 2100 for the low global CO_2 emission scenarios.

The average modelled groundwater level and CO_2 emission for each combination of parcel and climate scenario is given in Figure 6.11. For the reference period, the average modelled emissions amount to 14.5, 8.4 and 5.6 t CO_2 ha^{-1} yr^{-1} for the RF, MP and HW parcel, respectively, which is in agreement with the more shallow yearly average groundwater table depth in the rewetted parcels.

Over time, the modelled groundwater levels show a decreasing trend for all climate scenarios. This trend is clearly the strongest for the high global emission scenario and drying trend, with decreasing summer precipitation and increasing evaporative demands. The lowering of the groundwater tables is less for the high global emission scenario and wetting trend compared to the low emission and drying trend scenario. Nonetheless, modelled CO_2 emissions from peat oxidation increase much more in the high global emission scenario compared to the low global emission scenario due to the increase in temperatures in this high emission scenario. Also, it should be noted that the lowering of the groundwater table is most pronounced in the RF parcel. The effect is less pronounced in the parcels with subsurface irrigation, as here an additional supply of water is available.

The modelled increase in peat oxidation would, in the most severe scenario, amount to 12.4 t CO_2 ha^{-1} yr^{-1} for the RF parcel by 2100, whereas this increase would be limited to 6.6 and 5.9 t CO_2 ha^{-1} yr^{-1} for the MP and HW parcels, respectively. This implies that rewetting not only helps in reducing emissions in the reference climate, but also helps to limit the increase in emissions due to climate change.

This project has received funding from the European Union's Horizon 2020 research and innovation programme under grant agreement N° 862695

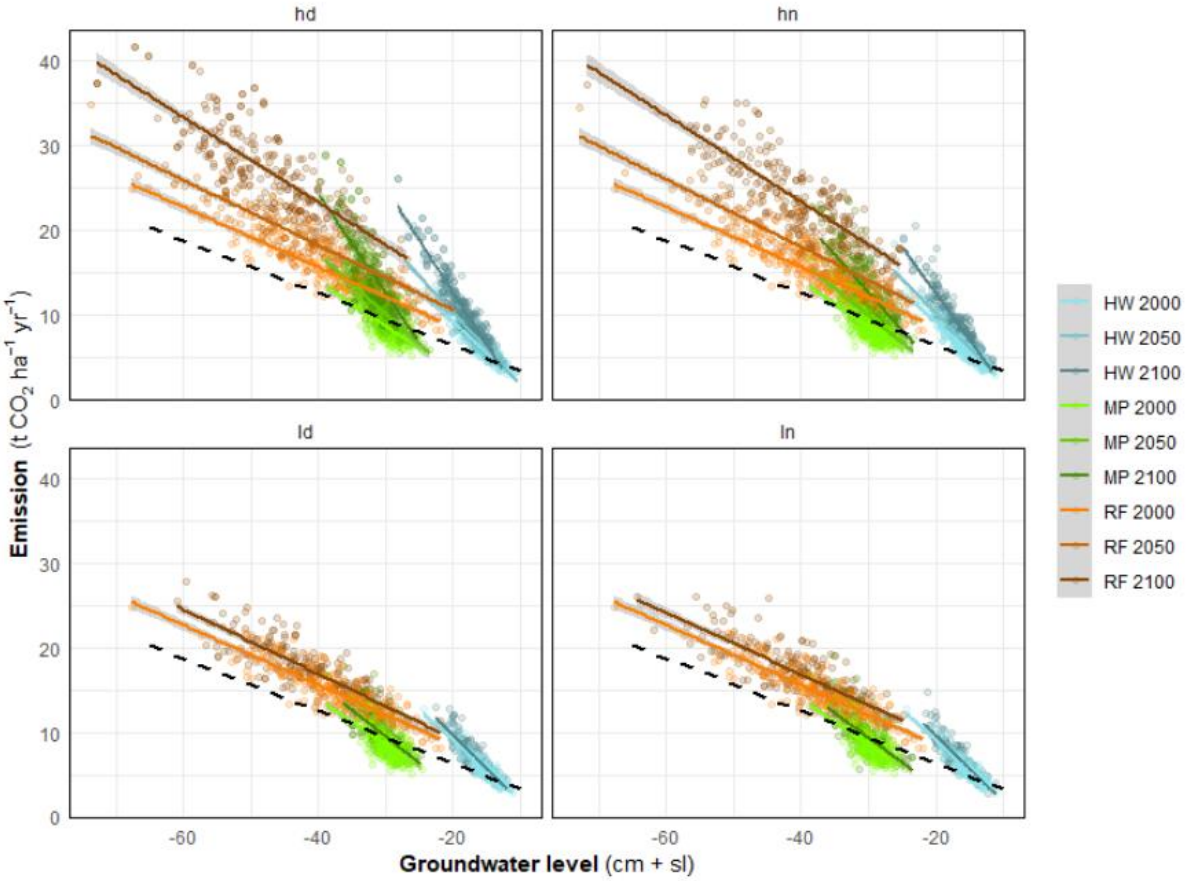

Figure 6.12 Overview of the modelled CO_2 emissions from peat oxidation and the modelled, yearly averaged groundwater level for four climate scenarios (panels), the three parcels (colors orange, green and blue for the reference (RF), the field with a target level of 50 cm-surface (MP) and the field with a target level of 20 cm-surface (HW), respectively) and outlook years (brightness of the color). Each dot represents one simulated year. The lines indicate linear model fits between CO_2 emissions and groundwater levels for the respective combination of parcel and simulation period. The dashed line indicates the relation between NECB and groundwater level obtained based on measurements on several Dutch peat meadows (including Zegveld) between 2020 and 2024 using automated chambers (Aben et al. 2024).

A more detailed overview of the simulations for each climate scenario is given in Figure 6.12, where each dot represents the simulation of one year. The reference results are identical for all scenarios, and for the simulations with a low global CO_2 emission scenario the outlook periods of 2050 and 2100 are identical as well. For the reference parcel, the linear relation between the emission and the groundwater level obtained from the model is very close to the relation found for Dutch peat meadows (Aben et al. 2024), which is indicated by the black dashed line, albeit with an upward shift. This shift corresponds to the results presented in Aben et al. (2024), with the emissions from the Zegveld site being slightly higher than the given relation, except for the MP parcel.

In all cases, the future climate scenarios result in an increase in CO_2 emission for any given groundwater table depth compared to the reference. This increase is much more pronounced in the scenarios with a high global CO_2 emission (Hd and Hn) compared to the low emission scenarios (Ld and Ln). The linear model fits in Figure 6.12 all show the tendency to become steeper under warming climates, which indicates that for a deeper groundwater level, the modelled emissions increase more compared to situations with a shallower groundwater level, which likely results from an increase in soil temperatures in a warming climate.

This project has received funding from the European Union's Horizon 2020 research and innovation programme under grant agreement N° 862695

Differences between the wetting and drying trend are less well observable from Figure 6.12. These two trends do not have a significant impact on the linear model fit for a given combination of parcel and simulation period, e.g. the linear model for the reference parcel in 2100 is not significantly different for scenarios Hd and Hn. Yet, the difference on the average emission from a parcel is evident (Figure 6.11).

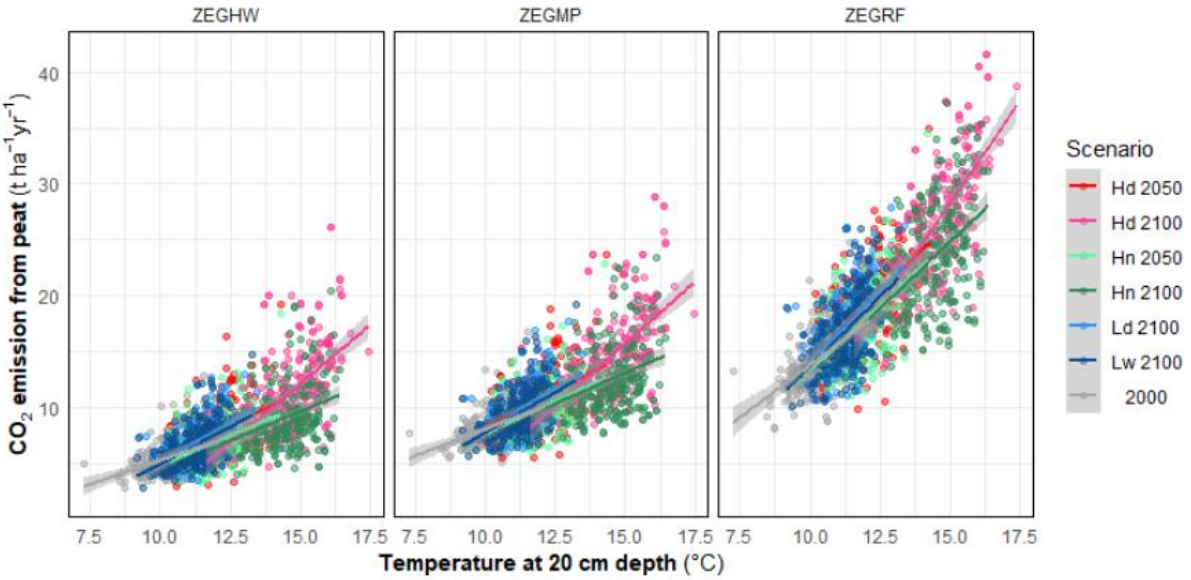

Figure 6.13 Modelled yearly CO_2 emission from peat oxidation as function of modelled soil temperature at 20 cm depth for the three parcels in Zegveld. Colors indicate the climate scenarios and outlook periods. Note that the reference period is identical for all scenarios, and there is no distinction in outlook years 2050 and 2100 for the low global CO_2 emission scenarios. Note the red line for the scenario Hd is largely obscured by the lines for Ld and Lw.

The influence of a temperature increase on the modelled CO_2 emissions is shown in Figure 6.13 for the three parcels. It is evident that, with increasing temperatures, the CO_2 emission increases. Yet, the relation between temperature and CO_2 emission is much steeper in the RF parcel compared to the other parcels. This likely stems from the correlation between yearly average groundwater levels and temperature: generally, higher temperatures coincide with deeper groundwater tables, which in itself also result in an increasing emission as more peat is exposed to aerobic decomposition. This may also explain the increasing steepness of the relation shown in Figure 6.12: as the range in groundwater levels decreases, the influence of temperature on this relation increases.

For the climate scenarios with a drying trend, there seems to be an exponentially increasing relationship between emission and temperature, whereas for the scenarios with a wetting trend, this relation is much less pronounced. This seems to be a consequence of the fact that the decrease in groundwater tables is less for the wetter scenarios compared to the drier scenarios, resulting in less exposed carbon.

Concluding, the effect of climate change on the emissions is two-fold. It affects the groundwater tables and temperature, and the correlation between the two makes it important to consider both aspects at the same time.

This project has received funding from the European Union's Horizon 2020 research and innovation programme under grant agreement N° 862695

7. Synthesis

In this section we combine the results of the three peatland sites which were shown in the preceding chapters, to highlight the effects of different properties of the sites on the modelled CO_2 fluxes.

The modelled peatland sites in three countries (Cressier, Switzerland; Vejrumbro, Denmark; Zegveld, The Netherlands) exhibit widely differing properties with regards to many aspects, which were shown for each site individually in the preceding chapters. It is noteworthy that, in all cases, the model was able to model the measured GPP, Reco and NECB quite well, even though the sites were substantially different in aspects ranging from land use and soil buildup to hydrological and meteorological conditions. Obviously, the model did require site specific calibrations, which were mainly related to crop growth parameters.

The buildup of the soil is rather different for the three sites (Figure 7.1), even though they all have undergone decades to centuries of degradation following drainage of the soil. The peat layer in Cressier is relatively thin and heavily degraded. Groundwater levels frequently drop to depths beyond the bottom of the peat layer, thus exposing the entire peat layer to oxygen. In Zegveld, the top layer is also heavily degraded due to frequent low groundwater levels, but the bottom of the peat layer is well below the lowest groundwater level and more or less pristine peat can be found at larger depths. In Vejrumbro, the peat is less dense and less degraded due to the shallower groundwater tables at this site. These differences are reflected in a relatively high soil bulk density in the entire peat profile of Cressier, whereas in the other sites a gradient from relatively high to low bulk densities can be found at larger depths in the soil. As a consequence, the available carbon in the top 50 cm is highest in Cressier and Zegveld, and substantially lower in Vejrumbro (Figure 7.1).

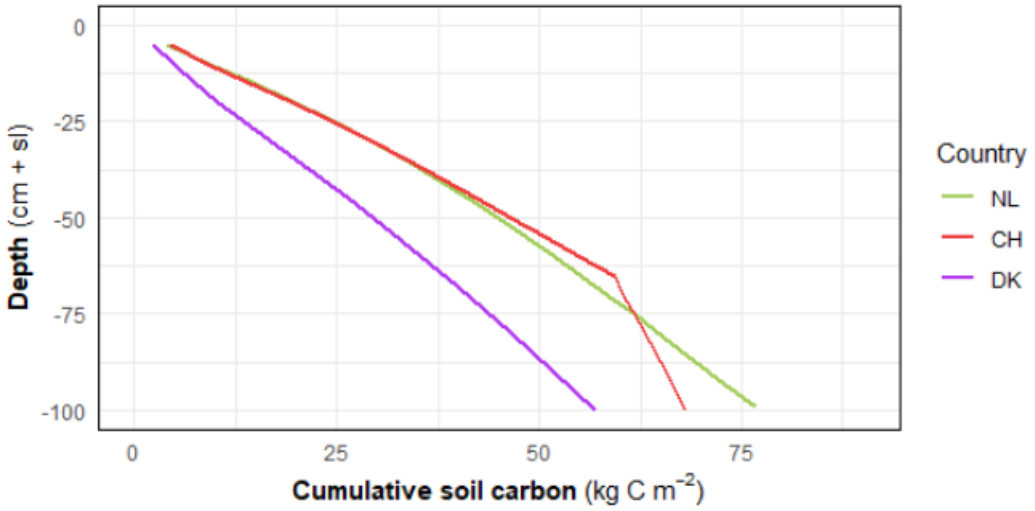

Figure 7.1 Cumulative soil carbon amount in the first 100 cm of soil at the Dutch Zegveld site (NL), the Swiss Cressier site (CH) and the Danish Vejrumbro site (DK).

The hydrological behaviour is also very dissimilar. In Vejrumbro, the deepest groundwater levels rarely exceed 40 cm below soil surface, whereas in the other two sites the groundwater levels may drop to 1 meter below soil surface in dry summers. In Cressier water is drained artificially when groundwater levels exceed a certain threshold. In Zegveld, the dense drainage network of ditches and drains (in the rewetted situations) result in a fast interaction with the surrounding surface waters, especially for the rewetted situations with subsurface drains. In Vejrumbro, exchange of water occurs primarily at the surface through precipitation, evapotranspiration and surface runoff.

This project has received funding from the European Union's Horizon 2020 research and innovation programme under grant agreement N° 862695

Also land management differs per site, even though they are all grasslands. In Zegveld, the site is intensively managed, with frequent fertilization and harvesting, resulting in a relatively high photosynthesis rate and input of organic matter into the soil. In Cressier, the site is not fertilized, yet it is mown three times a year. In Vejrumbro, the site is mown infrequently, and grasses are left to decay on the field. This results in most input of (decaying) plant material in the Vejrumbro and Zegveld sites, whereas in Cressier this input of fresh organic carbon is estimated to be less.

The measured and modelled gross CO_2 fluxes are highest in Zegveld (especially the reference field) owing to the high productivity of the grassland and relatively deep groundwater levels, and lowest in Vejrumbro due to the low productivity and high groundwater levels, but also due to a somewhat lower yearly averaged temperature. The net CO_2 fluxes of the reference fields of Zegveld and Cressier are comparable in magnitude. The rewetted fields in Zegveld exhibit a lower net CO_2 flux, and the lowest net flux is found in Vejrumbro.

Comparing the modelled soil temperatures at 20 cm depth (Figure 7.2 A) shows that for the reference period soil temperatures in Vejrumbro are 2 to 3 °C lower compared to the Zegveld and Cressier sites, which has a direct influence on (peat) oxidation rates due to the temperature dependency of oxidation processes. The effect of climate change on the modelled soil temperatures at 20 cm depth are well comparable for all sites, with a very similar increase in soil temperature for each of the atmospheric GHG emission scenarios, despite the choice of different climate models for the different sites. In all cases, soil temperatures tend to increase by as much as 4 to 5 °C in the highest global GHG scenario compared to the reference period.

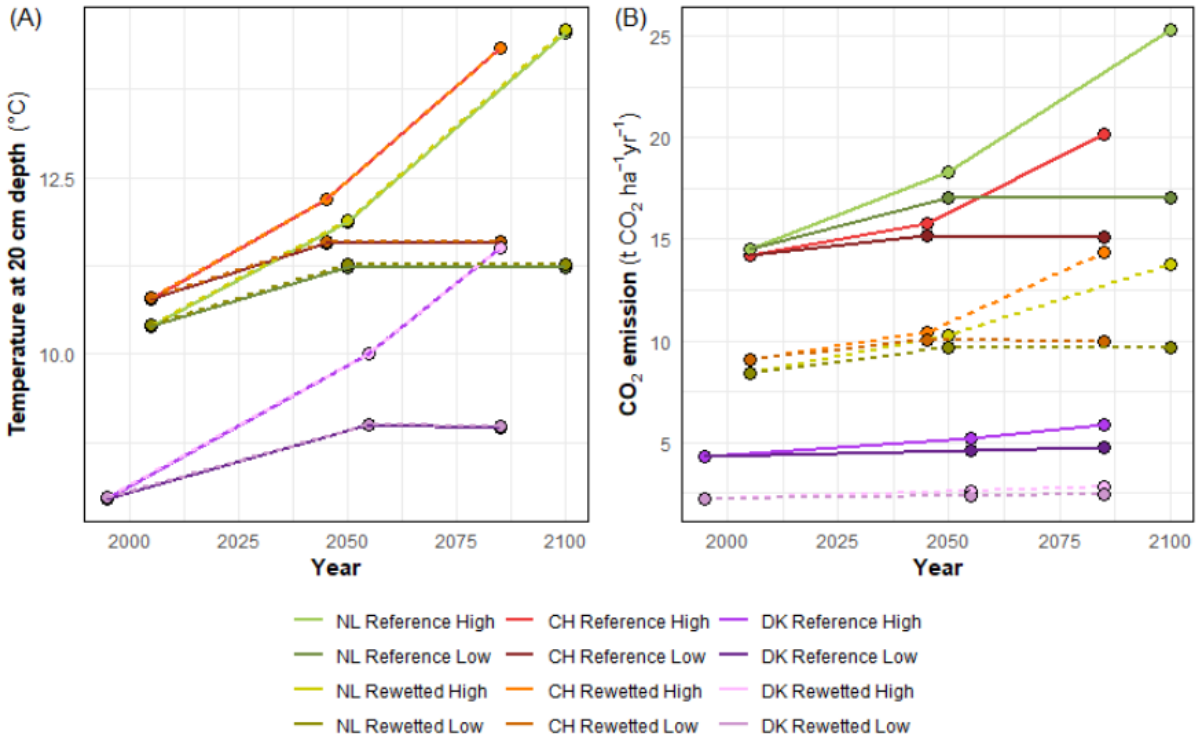

Figure 7.2 Average modelled soil temperatures at 20 cm depth (A) and average modelled CO_2 emission related to peat oxidation (B) for different periods in time for the Dutch Zegveld site (NL), the Swiss Cressier site (CH) and the Danish Vejrumbro site (DK), for both the reference and rewetted scenario. The rewetted line in Zegveld refers to the ZEGMP field. Each dot represents the average of a 30-year period, for the entire model ensemble, but differentiated between low and high global GHG emission scenarios.

This project has received funding from the European Union's Horizon 2020 research and innovation programme under grant agreement N° 862695

The increase in CO_2 emission rates due to peat oxidation, however, does deviate between the different sites (Figure 7.2 B). The increase is rather limited for the Vejrumbro site, is moderate for the Cressier site and is highest for the Zegveld site. This may be related to the temperature dependency of the oxidation rates, as represented by Q_{10} values. The values used for modelling the Zegveld and Vejrumbro sites are higher compared to the Q_{10} values used for the Cressier site (Figure 4.4). The Q_{10} values for the latter site were specifically measured on the modelled field, whereas for Zegveld the information was only available from older literature, and for Vejrumbro this information was lacking altogether.

In all sites, the effect of climate change is concentrated in the first half of the century when the SSP1-2.6 scenario is considered, which indicates that if global GHG emissions are reduced significantly, the effects of climate change on the oxidation of peat are limited. However, if the high global GHG emission scenario is followed (SSP5-8.5), peat oxidation is increasing over time due to both increasing temperatures and decreasing groundwater levels (the latter only for Zegveld and Cressier). The degradation of peat would then, in itself, also add to the global GHG emission, indicating the existence of a positive feedback loop.

The implementation of rewetting measures of peatlands can, in principle, contribute to a decrease in CO_2 emissions from the peatlands (Figure 7.2 B). However, in the high global GHG emission scenario the CO_2 emission reduction may be countered by an increase in oxidation due to elevated soil temperatures, depending on the site and the degree of rewetting. As such, to preserve peatlands as much as possible a strong degree of rewetting and reduction in global GHG emissions are required.

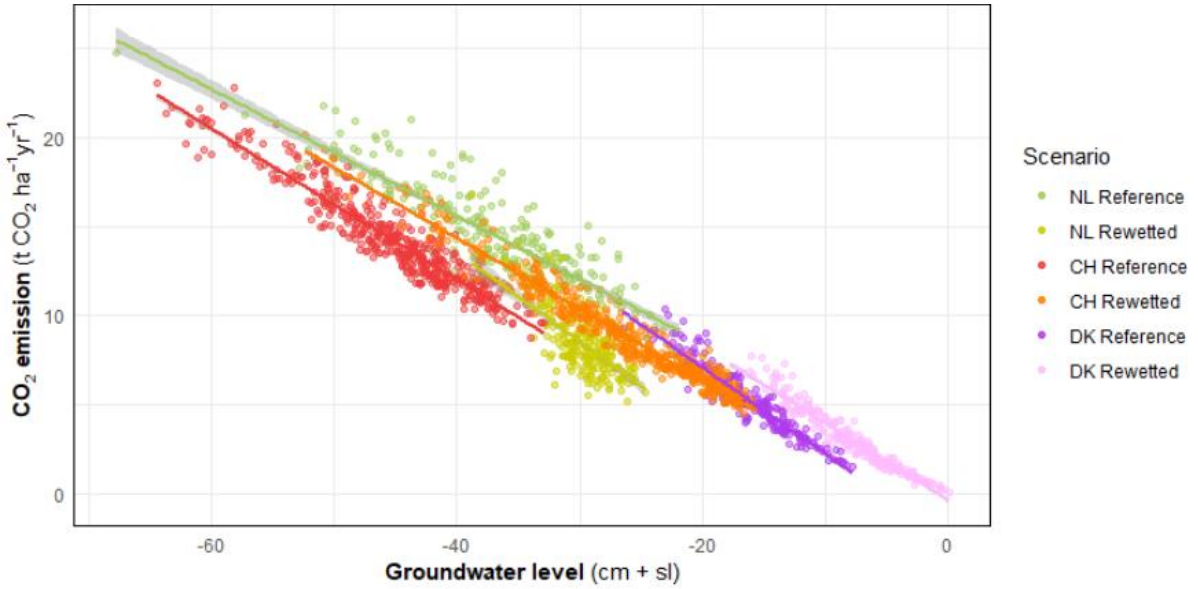

Figure 7.3 Relation between yearly modelled CO_2 emission related to peat oxidation and yearly averaged modelled groundwater level for the reference and rewetted (Zegveld: ZEGMP) fields in the reference period (between 1980-2020, exact range differs per site). Lines denote a linear model fit, each dot represents a modelled year.

A relation between modelled groundwater level and modelled CO_2 emission for the reference period is shown in Figure 7.3 for each site. In general, the angle of the relation is remarkably similar for each of the sites, although the absolute values at a given groundwater level may differ somewhat between sites due to e.g. the differences in soil composition. An interesting observation is that for Cressier, the emission at a given groundwater level is higher in the rewetted case compared to the reference case, whereas in Zegveld the emission in the reference field exceeds the emission in the rewetted field for a given groundwater level. The first (regarding Cressier) may be attributed to the

This project has received funding from the European Union's Horizon 2020 research and innovation programme under grant agreement N° 862695

correlation between groundwater level and soil temperatures: generally, at a given site and with a given water level management, higher soil temperatures (which themselves lead to a higher peat oxidation rate) coincide with deeper groundwater levels. For a given water level (i.e. 40 cm-sl), the temperature in the reference case would therefore be lower compared to the temperature in the rewetted case for that same water level, such that also the oxidation rate at that given water level is lower in the reference compared to the rewetted situation (see also Figure 4.13 and the corresponding text). The second (regarding Zegveld) may be explained by the nature of the rewetting measure. As in Zegveld both subsurface drainage of water and subsurface irrigation of water occur, the groundwater level fluctuations are limited compared to the reference situation. This results in deeper groundwater levels in winter, and shallower groundwater levels in summer. As relatively shallow groundwater levels tend to occur in winter (when temperatures are low) and relatively deep groundwater levels tend to occur in summer (when temperatures are high), the average groundwater level of the rewetted field may be similar in the reference and rewetted field, yet the oxidation of peat may be reduced. This is in contrast to the Cressier and Vejrumbro sites, where rewetting is achieved by limiting drainage, and not by actively promoting infiltration of water. Therefore, using the average yearly groundwater as a metric to estimate CO_2 emissions may not be adequate.

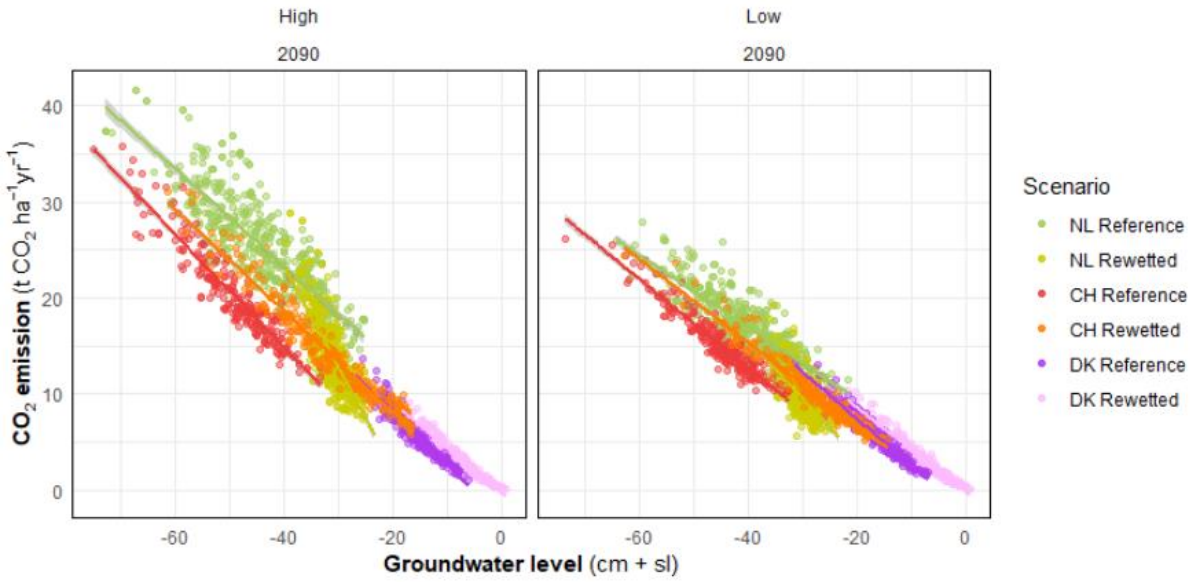

Figure 7.4 Relation between yearly modelled CO_2 emission related to peat oxidation and yearly averaged modelled groundwater level for the reference and rewetted (Zegveld: ZEGMP) fields in the last model period (between 2070-2115, exact range differs per site) for the high (left) and low (right) global GHG emission scenarios. Lines denote a linear model fit, each dot represents a modelled year.

The relation between groundwater level and CO_2 emission is not static in time, but may change over the course of years due to changes in temperature and hydrological conditions (Figure 7.4). With ongoing changes in climate leading to both higher temperatures and lower groundwater levels (in Cressier and Zegveld), the steepness of the relation tends to increase. As an example, at a groundwater level of 60 cm below soil surface, one may expect a CO_2 emission of 20 t CO_2 ha^{-1} yr^{-1} for the reference case in Cressier, which increases to 22 t CO_2 ha^{-1} yr^{-1} in the low global GHG emission scenario and even 26 t CO_2 ha^{-1} yr^{-1} in the high emission scenario.

This project has received funding from the European Union's Horizon 2020 research and innovation programme under grant agreement N° 862695

8. Conclusion

In this report we presented the application of the SWAP-ANIMO model to three distinctly different peatland sites in Europe. The model was used to analyse the development of the groundwater levels and CO_2 fluxes over time, and was found to be able to reproduce the measurements in each site to a large degree. The model was then applied to explore the effects of a reference case and a rewetting measure in both a reference period and in future climate scenarios in the mid- and end of this century, distinguishing between a low and high global greenhouse gas emission scenario.

The effects of climate change were most pronounced for the high global emission scenario at the end of the century, leading to decreasing groundwater levels in two of the three sites and increasing peat oxidation in all sites. The implementation of rewetting measures of peatlands can be used to raise groundwater levels and to lower CO_2 emissions. However, in the high global greenhouse gas (GHG) emission scenario the CO_2 emission reduction may be countered by an increase in oxidation due to elevated soil temperatures, depending on the site and the degree of rewetting. As such, to preserve peatlands as much as possible a strong degree of rewetting and reduction in global GHG emissions are required.

Acknowledgement

This work was realized with the framework of the EU funded project INSURE (Indicators for successful carbon sequestration and greenhouse gas mitigation by rewetting cultivated peat soils). INSURE is part of the EJP SOIL project which has received funding from the European Union's Horizon 2020 research and innovation programme under grant agreement N° 862695. Data collection in Zegveld was part of the Netherlands Research Programme on Greenhouse Gas Dynamics of Peatlands and Organic Soils (NOBV), which was launched in 2019 by the Dutch ministry of Agriculture, Nature management and Food quality (LNV) as part of the Climate Agreement and was co-funded by the Kennis Basis programma 34: Circulair and Climate Neutral Society Project KB-34-005-001 (Peat areas in new circular and climate positive production systems).

List of references

Aben, R.C.H., van de Craats, D., Boonman, J., Peeters, S.H., Vriend, B., Boonman, C.C.F., van der Velde, Y., Erkens, G., & van den Berg, M. (2024). CO_2 emissions of drained coastal peatlands in the Netherlands and potential emission reduction by water infiltration systems. *Biogeosciences, 21, 4099-4118*. https://doi.org/10.5194/bg-21-4099-2024.

Van den Akker, J.J.H., Massop, H., Gerritsen, P., Gerritsen, F., & van Houwelingen, K.M. (2021). Evaluation of 50 years subsidence monitoring of a peat meadow parcel to compare several methods to determine CO2-emissions. *Eurosoil 2021, Geneva.* https://edepot.wur.nl/562725.

Bader, C., Müller, M., Schulin, R., & Leifeld, J. (2017). Amount and stability of recent and aged plant residues in degrading peatland soils. *Soil Biology and Biochemistry, 109, 167-175.* https://www.sciencedirect.com/science/article/abs/pii/S0038071716303753.

Bader, C., Müller, M., Schulin, R., & Leifeld, J. (2018). Peat decomposability in managed organic soils in relation to land use, organic matter composition and temperature. *Biogeosciences, 15(3), 703-719.* https://bg.copernicus.org/articles/15/703/2018/.

Boogaard, H.L., de Wit, A.J.W., te Roller, J.A., & van Diepen, C.A. (2014). User's guide for the WOFOST Control Centre 2.1 and WOFOST 7.1.7 crop growth simulation model. *Wageningen, Alterra, Report Wageningen University & Research Centre. 133 pp.*

Chapin, F S., Woodwell, G M., Randerson, J T., Rastetter, E B., Lovett, . M., Baldocchi, D.D., Clark, D.A., Harmon, M.E., Schimel, D.S., Valentini, R., Wirth, C., Aber, J.D., Cole, J.J., Goulden, M.L., Harden, J. W., Heimann, M., Howarth, R.W., Matson, P.A., McGuire, A.D., … Schulze, E.D. (2006). Reconciling carbon-cycle concepts, terminology, and methods. *Ecosystems, 9(7), 1041–1050.* https://doi.org/10.1007/S10021-005-0105-7/FIGURES/2.

CH2018 (2018), CH2018 – Climate Scenarios for Switzerland, Technical Report, National Centre for Climate Services, Zurich, *ISBN: 978-3-9525031-4-0.*

CH2018 Project Team (2018): CH2018 - Climate Scenarios for Switzerland. National Centre for Climate Services. https://doi.org/10.18751/Climate/Scenarios/CH2018/1.0.

DMI (2024a). Methods used in Klimaatlas, the Danish Climate Atlas. DMI Report 24-11. *ISBN 978-87-7478-753-2.* https://www.dmi.dk/fileadmin/Rapporter/2024/DMI_rapport_24_11.pdf.

DMI (2024b). DMI Klimaatlas v2024a - Fremskrivninger af det danske klima (Projections of climate indicators in Denmark) [Data set]. Zenodo. https://doi.org/10.5281/zenodo.11402836.

Droppers, B., Supit, I., Leemans, R., Van Vliet, M.T.H., & Ludwig, F. (2022). Limits to management adaptation for the Indus' irrigated agriculture. *Agricultural and Forest Meteorology, 321, 108971.* https://doi.org/10.1016/j.agrformet.2022.108971.

Erkens, G., van der Meulen, M.J., & Middelkoop, H. (2016). Double trouble: subsidence and CO2 respiration due to 1,000 years of Dutch coastal peatlands cultivation. *Hydrogeol J 24, 551–568.* https://doi.org/10.1007/s10040-016-1380-4.

This project has received funding from the European Union's Horizon 2020 research and innovation programme under grant agreement N° 862695

Evans, C.D., Peacock, M., Baird, A.J., Artz, R.R.E., Burden, A., Callaghan, N., ... & Morrison, R. (2021). Overriding water table control on managed peatland greenhouse gas emissions. *Nature, 593(7860), 548-552.* https://doi.org/10.1038/s41586-021-03523-1.

FOEN (2024). Federal Office for the Environment – Hydrological data and forecasts. https://www.hydrodaten.admin.ch/en/seen-und-fluesse/stations/2154. Accessed May 2024.

Van Genuchten, M.T. (1980). A closed form equation for predicting the hydraulic conductivity of unsaturated soils. *Soil Science Society of America Journal, 44, 892-898.* https://doi.org/10.2136/sssaj1980.03615995004400050002x.

Groenendijk, P., Renaud, L.V., & Roelsma, J. (2005). Prediction of nitrogen and phosphorus leaching to groundwater and surface waters; Process descriptions of the ANIMO4.0 model. *Wageningen, Wageningen Environmental Research, Report 983.* https://edepot.wur.nl/35121.

Gross-Schmoelders et al. (2024). Soil organic matter stabilization increases with molecular diversity. *In prep.*

Heinen, M., G. Bakker, & J.H.M. Wösten (2020). Waterretentie- en doorlatendheidskarakteristieken van boven- en ondergronden in Nederland: de Staringreeks – Update 2018. *Wageningen, Wageningen Environmental Research, Rapport 2978.* https://doi.org/10.18174/512761.

Heinen, M., Mulder, M., van Dam, J., Bartholomeus, R., van Lier, Q.D.J., de Wit, J., de Wit, & Hack-ten Broeke, M. (2024). SWAP 50 years: Advances in modelling soil-water-atmosphere-plant interactions. *Agricultural Water Management, 298, 108883.* https://doi.org/10.1016/j.agwat.2024.108883.

Hendriks, R.F.A. (1991). Afbraak en mineralisatie van veen; literatuuronderzoek. *Wageningen, DLO-Staring Centrum. Rapport 199.* https://edepot.wur.nl/304337.

Hendriks, R.F.A., & van den Akker, J.J.H. (2012). Effecten van onderwaterdrains op de waterkwaliteit in veenweiden: modelberekeningen met SWAP-ANIMO voor veenweide-eenheden naar veranderingen van de fosfor-, stikstof- en sulfaatbelasting van het oppervlaktewater bij toepassing van onderwaterdrains in het westelijke veenweidegebied. *Wageningen, Alterra, Alterra-rapport 2354.* https://edepot.wur.nl/240125.

Hendriks et al. (2024). Modification of the ANIMO 4.1 code for enhancing GHG-simulations and their interpretations in peatland soils. *In prep.*

Hopple, A.M., Wilson, R.M., Kolton, M., Zalman, C.A., Chanton, J.P., Kostka, J., Hanson, P.J., Keller, J.K., & Bridgham, S.D. (2020). Massive peatland carbon banks vulnerable to rising temperatures. *Nature communications, 11(1), 2373.* https://doi.org/10.1038/s41467-020-16311-8.

Indraratne, S.P., Hao, X., Chang, C., & Godlinski, F. (2009). Rate of soil recovery following termination of long-term cattle manure applications. *Geoderma, 150(3-4), 415-423.* https://doi.org/10.1016/j.geoderma.2009.03.002.

Kroes, J.G., van Dam, J.C., Bartholomeus, R.P., Groenendijk, P., Heinen, M., Hendriks, R.F.A., Mulder, H.M., Supit, I., & van Walsum, P.E.V. (2017). SWAP version 4; Theory description and user manual. *Wageningen, Wageningen Environmental Research, Report 2780.*

This project has received funding from the European Union's Horizon 2020 research and innovation programme under grant agreement N° 862695

https://doi.org/10.18174/416321.

Kroes, J.G., & Supit, I. (2011). Impact analysis of drought, water excess and salinity on grass production in the Netherlands using historical and future climate data. *Agric. Ecosyst. Environ. 144 (1), 370–381.* https://doi.org/10.1016/j.agee.2011.09.008.

Leifeld, J., & Menichetti, L. (2018). The underappreciated potential of peatlands in global climate change mitigation strategies. *Nature communications, 9(1), 1071.* https://doi.org/10.1038/s41467-018-03406-6.

Leifeld, J., Klein, K., & Wüst-Galley, C. (2020). Soil organic matter stoichiometry as indicator for peatland degradation. *Scientific reports, 10, 7634.* https://doi.org/10.1038/s41598-020-64275-y.

Malinowski, R., Höfle, B., Koenig, K., Groom, G., Schwanghart, W., & Heckrath, G. (2016). Local-scale flood mapping on vegetated floodplains from radiometrically calibrated airborne LiDAR data. *ISPRS Journal of Photogrammetry and Remote Sensing, 119, 267-279.* https://doi.org/10.1016/j.isprsjprs.2016.06.009.

Mashhadi, S.R., Grombacher, D., Zak, D., Lærke, P.E., Andersen, H.E., Hoffmann, C.C., & Petersen, R.J. (2024). Borehole nuclear magnetic resonance as a promising 3D mapping tool in peatland studies. *Geoderma, 443, 116814.* https://doi.org/10.1016/j.geoderma.2024.116814.

Mualem, Y. (1976) A new model for predicting the hydraulic conductivity of unsaturated porous media. *Water Resources Research, 12(3), 513-522.* https://doi.org/10.1029/WR012i003p00513.

Nielsen, C.K., Stødkilde, L., Jørgensen, U., & Lærke, P.E. (2021). Effects of harvest and fertilization frequency on protein yield and extractability from flood-tolerant perennial grasses cultivated on a fen peatland. *Frontiers in Environmental Science, 9, 619258.* https://doi.org/10.3389/fenvs.2021.619258.

Nielsen, C. K., Elsgaard, L., Jørgensen, U., & Lærke, P.E. (2023). Soil greenhouse gas emissions from drained and rewetted agricultural bare peat mesocosms are linked to geochemistry. *Science of the Total Environment, 896, 165083*. https://doi.org/10.1016/j.scitotenv.2023.165083.

Nielsen, C.K., Liu, W., Koppelgaard, M., & Lærke, P.E. (2024). To Harvest or not to Harvest: Management Intensity did not Affect Greenhouse Gas Balances of Phalaris Arundinacea Paludiculture. *Wetlands 44, 79.* https://doi.org/10.1007/s13157-024-01830-7.

Olsen, A.M.E. 2005. Viborg Amt, sydøst delen af amtet, Potentialekort for det primære grundvandsmagasin. Viborg Amt.

Paul, S., Ammann, C., Alewell, C., & Leifeld, J. (2021). Carbon budget response of an agriculturally used fen to different soil moisture conditions. *Agricultural and Forest Meteorology, 300, 108319.* https://doi.org/10.1016/j.agrformet.2021.108319.

Peat, W. E. (1970). Relationships between photosynthesis and light intensity in the tomato. *Annals of Botany, 34(2), 319-328.* https://doi.org/10.1093/oxfordjournals.aob.a084372.

This project has received funding from the European Union's Horizon 2020 research and innovation programme under grant agreement N° 862695

Pullens, J.W., Rodriguez, A.F., & Lærke, P.E. (2024). Carbon Dynamics in a Passively Rewetted Fen Peatland: A Two-Year Study. *EGU General Assembly 2024, Vienna, Austria.* https://doi.org/10.5194/egusphere-egu24-12469.

Spitters, C.J.T., Toussaint, H.A.J.M., & Goudriaan, J. (1986). Separating the diffuse and direct component of global radiation and its implications for modeling canopy photosynthesis Part I. Components of incoming radiation. *Agricultural and Forest Meteorology, 38(1-3), 217-229.* https://doi.org/10.1016/0168-1923(86)90060-2.

Spitters, C.J.T. (1986). Separating the diffuse and direct component of global radiation and its implications for modeling canopy photosynthesis Part II. Calculation of canopy photosynthesis. *Agricultural and Forest meteorology, 38(1-3), 231-242.* https://doi.org/10.1016/0168-1923(86)90061-4.

Vermeulen, J., Hendriks, R.F.A. (1996). Bepaling van afbraaksnelheden van organische stof in laagveen; ademhalingsmetingen aan ongestoorde veenmonsters in het laboratorium. *Wageningen, DLO-Staring Centrum. Rapport 288.* https://edepot.wur.nl/303325.

van der Wiel, K., Beersma, J., van den Brink, H., Krikken, F., Selten, F., Severijns, C., et al. (2024). KNMI'23 climate scenarios for the Netherlands: Storyline scenarios of regional climate change. *Earth's Future, 12, e2023EF003983.* https://doi.org/10.1029/2023EF003983.

Wutzler, T., Lucas-Moffat, A., Migliavacca, M., Knauer, J., Sickel, K., Šigut, L., Menzer, O., & Reichstein, M. (2018). Basic and extensible post-processing of eddy covariance flux data with REddyProc. *Biogeosciences, 15(16), 5015-5030.* https://doi.org/10.5194/bg-15-5015-2018.

Wythers, K.R., Reich, P.B., Tjoelker, M.G., & Bolstad, P.B. (2005). Foliar respiration acclimation to temperature and temperature variable Q10 alter ecosystem carbon balance. *Global Change Biology, 11(3), 435-449.* https://doi.org/10.1111/j.1365-2486.2005.00922.x.

This project has received funding from the European Union's Horizon 2020 research and innovation programme under grant agreement N° 862695

Appendix I – Overview of climate model combinations

Table 0.1 Climate models used for the simulation of the Swiss (Cressier, CH) and Danish (Vejrumbro, DK) sites. The selection of the Swiss models is based on the availability of the required RCP scenarios and parameters. Data was obtained from the DAILY-LOCAL dataset for Neuchatel (CH2018, 2018). The selection of the Danish sites is based on the availability of the required RCP scenarios and the selection for Cressier. Three additional models were selected to obtain the same total of 8 models as for Cressier. Data was obtained on a 11 km resolution grid from DMI (2024b).

GCM	RCM	Resolution CH	Resolution DK
ICHEC-EC-EARTH	DMI-HIRHAM5	11	11
ICHEC-EC-EARTH	KNMI-RACMO22E		11
ICHEC-EC-EARTH	SMHI-RCA4	11	
ICHEC-EC-EARTH	SMHI-RCA4	44	11
MOHC-HadGEM2-ES	SMHI-RCA4	44	11
MOHC-HadGEM2-ES	KNMI-RACMO22E	44	11
MIROC-MIROC5	CLMCOM CCLM4		11
MIROC-MIROC5	SMHI-RCA4	44	
MPI-M-MPI-ESM-LR	KNMI-RACMO22E		11
MPI-M-MPI-ESM-LR	SMHI-RCA4	44	
NCC-NorESM1-M	SMHI-RCA4	44	11

This project has received funding from the European Union's Horizon 2020 research and innovation programme under grant agreement N° 862695